Fractionalization and Interaction in Topological Superconductors and Insulators

Sharmistha Sahoo

Cuttack, Odisha, India

Integrated M.Sc. ,

National Institute of Science Education and Research,

Bhubaneswar, Odisha, India, 2012

A Dissertation presented to

the Graduate Faculty of the University of Virginia

in Candidacy for the Degree of

Doctor of Philosophy

Department of Physics

University of Virginia

May, 2018

Acknowledgement

My deepest gratitude goes to my advisor Jeffrey Teo for his guidance and support. My knowledge on the physics of topological phases comes directly from our discussion over the years. He was always patient with me and was very approachable when I was stuck in research with any problem or idea.

I would like to thank Gia-Wei Chern who has been a great mentor to me over the years. Discussions with him brought many interesting topics into my attention and helped me to put my own research in a broader perspective.

I am grateful to Israel Klich and Paul Fendley, for their lectures in advanced condensed matter courses at University of Virginia(UVa) provided me with the requisite background to carry out research in later years. Conversation with both of them always inspired me. I am also thankful to Roger Melko and his team at University of Waterloo who hosted me for a semester which gave me the opportunity to learn about the entanglement entropies and other interesting topics.

I appreciate Israel Klich, Seunghun Lee, Gia-Wei Chern and Thomas Mark for putting their time and effort to review my research/ theses and giving me their feedback which were really important to me.

My sincere thanks goes to the physics department at UVa, who have been really supportive in my journey as a PhD student. I very much enjoyed discussing physics with other graduate students in the physics department, especially Alex Sirota, Syed Raza, Meng Hua, Zhao Zhang, Yifei Shi and Jing Luo. I thank all my friends in the department and in the university, because of whom I had a great time in Charlottesville. I have been fortunate to have made friends like Abha Rajan and Nguyen Ton, who have always been there for me.

At last, but most importantly, I could not have completed this thesis without my family's support. I am always thankful to them especially to Ajinkya Kamat who has been a constant source of encouragement.

Declaration

This thesis is adapted from the following publications

- Sharmistha Sahoo, Zhao Zhang, Jeffrey Teo, *Coupled wire model of Symmetric Majorana surfaces of topological superconductors*, Phys Rev B, Vol. 94, 165142 (2016).
- Sharmistha Sahoo, Alexander Sirota, Gil Young Cho, Jeffrey C. Y. Teo, *Surfaces and Slabs of Fractional Topological Insulator Heterostructures*, Phys Rev B, Vol. 96, 161108 (2017).

Thesis has been reviewed and approved by the following committee

- Jeffrey Teo,
  Assistant Professor, Physics department
- Israel Klich,
  Associate Professor, Physics department
- Gia-Wei Chern,
  Assistant Professor, Physics department
- Thomas Mark,
  Associate Professor, Mathematics department

Abstract

We present a study of novel topological order in three dimensional (3+1D) topological superconductors and fractional topological insulators. Such topological order occurs when the surface is gapped due to the presence of many-body interactions that respect the time-reversal symmetry.

3+1D time reversal symmetric topological superconductors are characterized by gapless (massless) Majorana fermions on its surface. They are robust against any time reversal symmetric single-body perturbation weaker than the bulk energy gap. We mimic this gapless surface by coupled wire models in two spatial dimensions. We show modified models with additional time-reversal symmetric many-body interaction, that gives energy gaps to all low energy degrees of freedom. We used the embedding trick using Wess-Zumino-Witten conformal field theory to find such interacting model Hamiltonian. We show the gapped models generically carry non-trivial topological order and support *anyons*. Using these anyons and their condensation process, we show the topological order has a 32-fold periodicity.

Fractional topological insulators (FTI) are electronic topological phases in 3+1D enriched by the time reversal and charge $U(1)$ conservation symmetries. We focus on the simplest series of fermionic FTI, whose bulk quasiparticles consist of deconfined *partons*. Theses partons carry fractional electric charges in integral units of $e^* = e/(2n+1)$ and couple to a discrete $\mathbb{Z}_{2n+1}$ gauge theory. We propose massive symmetry preserving or breaking FTI surface states. Combining the long-ranged entangled bulk with these topological surface states, we deduce the novel topological order of quasi-$(2 + 1)$ dimensional FTI slabs as well as their corresponding edge conformal field theories.

Contents

List of Figures

List of Tables

Chapter 1

Introduction

Condensed matter physics explores microscopic and macroscopic properties of matter. In the past few decades researchers have discovered interesting properties at low-temperature. An important discovery dates back to 1980 when Klitzing discovered that with application of a strong magnetic field the values of the Hall resistance in two-dimensional silicon samples were quantized [1], which was also later seen in semi-conductor quantum wells. A theoretical understanding requires us to consider electrons filling the quantized Landau levels, hence becoming localized in the two-dimensional plane except at the edge of the sample. Soon it was realized that magnetic field is not necessary to have a "protected" edge response. "Topological insulators" with time-reversal symmetry were proposed to have quantized conductance at the boundary and were later discovered in insulators like Bismuth Telluride, Bismuth Antimony [2, 3]. The properties of these systems seem to be robust against local perturbations and has possibilities for numerous novel applications. In addition to quantum mechanics, we borrow concepts from topology - a branch of mathematics - to understand these states. In this chapter, I will give a brief introduction to topological phases and the methods used to analyze them in the rest of this thesis.

1.1 Background

1.1.1 Classification of topological insulators and superconductors

The symmetry protected topological (SPT) phases are quantum phases of matter whose properties are robust as long as certain symmetries of the system are preserved. Here we will discuss SPT phases with fermionic degrees of freedom. Examples of such phases include topological insulator(TI) s and superconductor (TSC)s. They can be described using a band-Hamiltonian written in terms of free fermionic degrees of freedom. Although the bulk is gapped, the band structure for a finite system has states corresponding to the boundary that are gapless. These boundary states are robust against local perturbations, meaning even if we make small changes to the system, the boundary state remains gapless. However, if we break the defining symmetry then the boundary state is gapped and the SPT phase becomes "topologically trivial".

My aim in this section is to explain briefly what it means to consider a particular class of TSC/ TI. Before doing that let's understand them using a few simple examples. Throughout this thesis I will alternatively use $n+1$ D or n D to mean n-spatial dimensions and one temporal dimension. In 1D, well-known examples include Su-Schrieffer-Heeger (SSH) model [4] and p-wave superconductor [5], both modeled using free (non-interacting) fermions. The SSH model is an example of the TI. It describes a 1D chain of atoms, originally proposed to model poly-acetelyn. Let's say the electron hopping integral between the consecutive atoms alternates between v and w. Considering an enlarged unit-cell that has A and B atoms, the Hamiltonian can be written as

$$\mathcal{H}_{SSH} = \sum_{i=1}^{N} v c^{\dagger}_{A,i} c_{B,i} + w c^{\dagger}_{B,i} c_{A,i+1} + h.c. \tag{1.1}$$

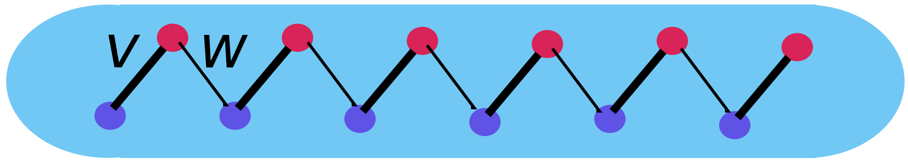

Figure 1.1: A poly-acetelyn molecule with alternating bond-strength

Assuming a periodic boundary condition, momentum k is defined to be $\frac{2\pi n}{N}$ for $n \in \mathbb{Z}_N$ (integer modulo N) called as the Brillouin zone (BZ). In the Fourier basis, $c_{A(B),k} = \frac{1}{\sqrt{N}} \sum_{j=1} c_{A(B),k} e^{-ijk}$ (1.1) becomes

$$\mathcal{H}_{SSH} = \sum_{k \in BZ} \sum_{\{\alpha,\beta\}=A,B} t c^{\dagger}_{\alpha}(k) h_{\alpha,\beta}(k) c_{\beta}(k) \tag{1.2}$$

where

$$h_{\alpha,\beta}(k) = \sigma_x \left[(v + w\cos(k)\right] + \sigma_y \left[w \sin(k)\right] \tag{1.3}$$

Here $\sigma_{x,y}$ are 2×2 Pauli matrices that act on A, B. Diagonalizing the Bloch hamiltonian $h_{\alpha,\beta}(k)$ gives $E_{\pm}(k)$ shown in figure 1.2, where eigenstates are given by $|u_{\pm}\rangle(k)$. The energy spectrum is gapless when strength of the hopping integral is equal in both bonds, i.e.$v = w$, but otherwise it has a finite gap even in the thermodynamic limit. That is why this is a model for an insulator when $v \neq w$. For a finite length chain (as in the figure 1.1), when $v < w$ the chain is completely dimerized, i.e. the electrons are localized in A and B atoms of the same unit-cell. When $v > w$, this chain is dimerized except the dangling bonds at the end. The atoms connected to these bonds have zero energy. These zero energy states are protected in the sense that as long as $v > w$ these states can not be removed. In other words, for $v < w$ the SSH chain is a "topologically trivial" insulator and for $v > w$ it is a "topologically non-trivial" insulator. The Berry's phase, defined for a closed path C as $-i \oint_C \langle u_n(k)|\frac{\partial u_n(k)}{\partial k}\rangle$, also distinguishes between these states. From the Hamiltonian (1.3), which is of the form $H = \mathbf{d} \cdot \boldsymbol{\sigma}$, where only d_x and d_y are non-zero, Berry's phase is calculated using the solid angle subtended by $\mathbf{d}$. When k goes from 0 to 2π, i.e. for a closed path in the 1D BZ, $\mathbf{d}$ traces a circle in the d_x-d_y plane as shown in figure (1.2). When the origin is inside the circle, the solid angle subtended by $\mathbf{d}$ (Berry's phase) is π. This distinguishes the TI from a trivial insulator and is called a "topological invariant". The topological property also has a correspondence with the symmetry of the system. The system has a sub-lattice or chiral symmetry, i.e. even if we switch A and B atoms, the model remains invariant. In momentum space $\{h_{\alpha,\beta}(k), \sigma_z\} = 0$, so this symmetry maps the positive energy eigen states to the negative energy eigenstates.. Any 1D system with such a chiral symmetry has same topological properties.

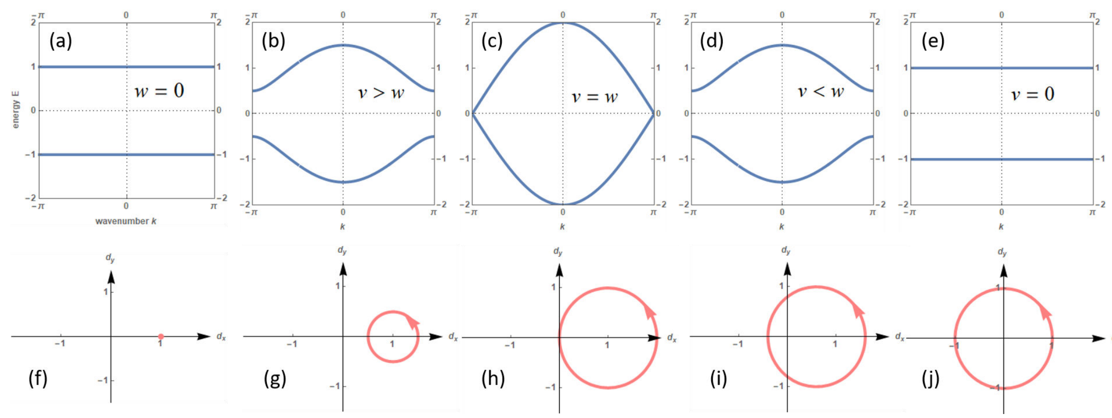

Figure 1.2: In top electron band dispersion for the SSH model with different values of hopping strength v and w. In bottom plots in d_x-d_y plane indicating whether the Berry's phase is 0 or π. For $v < w$ the chain is gapped and the Berry's phase is π as the circle encloses the origin making it a "topologically non-trivial" insulator.

In the Hamiltonian for a superconductor, in addition to the electron hopping term, we also have electron density-density interaction term. The interaction term is of two-body type, but we consider the mean-field approximation proposed by Bardeen, Cooper and Schrieffer (BCS), to make the Hamiltonian single-body type or in other words non-interacting. The mean field Hamiltonian for a p-wave superconductor in

1D is

$$\frac{1}{2}\sum_k \begin{pmatrix} c_k^\dagger & c_{-k} \end{pmatrix} \begin{pmatrix} k^2/2m-\mu & \Delta k \\ \Delta^* k & k^2/2m+\mu \end{pmatrix} \begin{pmatrix} c_k \\ c_{-k}^\dagger \end{pmatrix} \tag{1.4}$$

It is easy to check the system is gapped for $\mu < 0$ and $\mu > 0$, but these two cases belong to different phases. The p-wave superconductor is in topological phase for $\mu > 0$. The Hamiltonian has particle-hole symmetry that transforms an electron with positive momentum c_k to a hole with negative momentum, $c^\dagger(-k)$. If we write the Hamiltonian (1.4) in $\mathbf{d}.\boldsymbol{\sigma}$ form the trace of $\mathbf{d}$ vector will distinguish a topological phase. This agrees with the $\mathbb{Z}_2$ classification of a topological superconductor with only particle-hole symmetry. Refer [6] for a rigorous way to understand topological classification for 1D fermionic SPT phases with additional time-reversal (TR) symmetry.

The important point here is that the classification of a TSC or TI is determined by the symmetry of it's Hamiltonian. These symmetries can be discrete anti-unitary symmetries like particle-hole, time-reversal (TR), and chiral with operators $\mathcal{T}$,$\mathcal{C}$ and Π or unitary charge conservation $U(1)$ symmetry. Numerous research works have been devoted to finding complete classification of SPT phases with various symmetries, in different dimensions [7, 8, 9, 10].

A brief discussion of the 3D TSC serves both as an example of a SPT phase in higher dimension as well as prepares the reader for the next chapter. Superconductors in BCS mean field limit have Bloch Hamiltonian H_{BdG}, which is a function of crystal momentum $\mathbf{k}$. A general form of the Hamiltonian is

$$H_{\text{BdG}} = \begin{pmatrix} \varepsilon(\mathbf{k}) & \Delta(\mathbf{k}) \\ \Delta^*(\mathbf{k}) & -\varepsilon(\mathbf{k}) \end{pmatrix} \tag{1.5}$$

where the matrix is 4×4 when written in the Nambu spinor basis $(c_{\mathbf{k}\uparrow}c_{\mathbf{k}\downarrow}c^\dagger_{-\mathbf{k}\downarrow}-c^\dagger_{-\mathbf{k}\uparrow})$. H_{BdG} can be written in terms of Pauli matrices τ_i and σ_j for particle-hole and spin basis respectively. $\varepsilon(\mathbf{k})$ is the energy dispersion and $\Delta(\mathbf{k})$ is the pairing function for the superconductor.

H_{BdG} already has the particle-hole symmetry ($\mathcal{C}$) that transforms $c_{k\sigma} \to c^{\dagger}_{-k-\sigma}$. Certain superconductors can have additional time-reversal ($\mathcal{T}$) and chiral (Π) symmetries. In the presence of the TR symmetry the pairing potential has odd parity (spin triplet type). An example of such a pairing potential is $\Delta = \mathbf{k}.\boldsymbol{\sigma}(i\sigma_y)$ [11]. One can check that the following is true for this pairing

$$(\tau_0 \otimes i\sigma_y)H_{\text{BdG}}(\mathbf{k})(-\tau_0 \otimes i\sigma_y) = H_{\text{BdG}}(-\mathbf{k}) \tag{1.6}$$

$$(\tau_x \otimes \sigma_o)H_{\text{BdG}}(\mathbf{k})(\tau \otimes \sigma_0) = -H_{\text{BdG}}(-\mathbf{k}) \tag{1.7}$$

Here $\mathcal{T} = i\sigma_y \otimes \tau_o\mathcal{K}$ is the TR symmetry and $\mathcal{C} = \sigma_0 \otimes \tau_x\mathcal{K}$ is the particle-hole symmetry where $\mathcal{K}$ is the complex conjugation operator. We can also define an additional chiral symmetry $\Pi = i\mathcal{C}\mathcal{T}$ that anti-commutes with the Hamiltonian. The symmetries satisfy $-\mathcal{T}^2 = \mathcal{C}^2 = +1$. Superconductors with such symmetries are classified as DIII TSC. A classification table for TI and TSC can be found in [11, 12]. In 3D class DIII has further $\mathbb{Z}$ classification, which means we can define a bulk topological invariant that takes integer values. The *winding number* w, defined in the 3D BZ is shown to be the topological invariant in this case [11].

$$w = \frac{1}{24\pi^2}\int_{3DBZ} d^3k\epsilon^{\mu\nu\rho}\text{Tr}[q^{-1}\partial_\mu q q^{-1}\partial_\nu q q^{-1}\partial_\rho q] \tag{1.8}$$

Here $q(k)$ is Hamiltonian H_{BdG} under basis transformation which maps the 3D BZ to the space of matrices restricted by the symmetries.

Any class DIII TSC is topologically trivial if its band structure has $w = 0$. The winding number in the bulk corresponds to the number of gapless Majorana cones on the surface. This makes sense because on one side of the surface we have a gapped bulk with $w = N$ and the other side is vaccum that has $w = 0$. If we move from one side to the other adiabatically, then the gap will close N times along our path, in other words we will encounter N mid gap states at the boundary between two sides. So, the topological class of a TSC can be obtained by counting the surface Majorana cone.

1.1.2 Fractional topological insulators

Topological insulators (TI) [13, 14, 15] are time-reversal (TR) and charge ($U(1)$) symmetric electronic insulator. In the last section, it was explained how TI in 1D can be modeled using a band Hamiltonian for electrons. It can be different topological phases depending on the value of its topological invariant. In 3+1 D, TI is classified using a $\mathbb{Z}_2$ invariant. A TR symmetric topological field theory[16] for this $\mathbb{Z}_2$ TI is

$$\mathcal{S}_{(3+1)D} = \frac{\theta e^2}{8\pi^2} \int d^3x dt \epsilon^{\mu\nu\sigma\tau} \partial_\mu A_\nu \partial_\sigma A_\tau \tag{1.9}$$

where θ is the axion angle variable that takes π (mod 2π) value. Eqn 1.9 is just the axion electro-magnetic field theory with $\epsilon^{\mu\nu\sigma\tau}\partial_\mu A_\nu \partial_\sigma A_\tau = 2\mathbf{E}\cdot\mathbf{B}$. Because $\mathbf{E}\cdot\mathbf{B}$ is odd under TR symmetry, in general eqn 1.9 breaks TR symmetry. With a closed manifold the action integral evaluates to $m\theta$ where $m \in \mathbb{Z}$. The $\mathbb{Z}_2$ topological invariant is given by $e^{i\mathcal{S}_{(3+1)D}}$ which is $(-1)^m$ for $\theta = \pi$. This topological field theory also predicts a half-integer quantized Hall conductance on a boundary surface when TR is broken. The value of the Hall conductance on the surface is determined by the axion angle.

Fractional topological insulators (FTI) are also TR symmetric electronic phases but can not be explained using a single-body Hamiltonian picture because of interaction between electrons. However, a topological field theory for a simple case of FTI has been formulated [17]. The idea here was to decompose an electron into odd $2n+1$ fractionally charged fermionic *partons* that are de-confined and have their own dynamics. The partons are coupled with $SU(2n+1)$ gauge fields such that the electron is physical i.e. gauge invariant. When these partons form a topological insulator, a new electronic phase for the electrons emerges which we call FTI. When the axion angle, θ for the topological insulator formed by partons is π, for electrons effectively $\theta_{FTI} = \frac{\pi}{2n+1}$. This does not break the TR symmetry because the partons couple to the external electro-magnetic field with charge $e/2n+1$.

The surface of FTI is gapped when the TR symmetry is broken on the surface. For example, a perpendicular magnetic field on the surface would show $\frac{1}{2(2n+1)}\frac{e^2}{h}$ Hall conductance compared to $\frac{1}{2}\frac{e^2}{h}$ in case of TI. With magnetic field, the Dirac partons on the surface form landau levels just like electrons on TI surface. The 1D interface between opposite TR breaking surfaces on FTI has $\frac{1}{(2n+1)}\frac{e^2}{h}$ differential electrical conductance. In the past few years, much work has been done to find gapped surfaces for TI that do not break the TR symmetry. Such surfaces show TR symmetric topological order. One of the main results in this thesis is to show how using these partons we can also have TR symmetric topological order on FTI.

1.1.3 Topological order

Topological states are classified using *topological order*(TO) and *topological invariants*. Non-interacting topological superconductor and insulator phases have trivial TO , but we can define topological invariants that explains their robust properties as discussed in sec (1.1.1). Examples of the phases that have TO are the fractional quantum Hall insulators. The *Laughlin* state at filling $\nu = 1/3$ and the *Pfaffian* state at $\nu = 5/2$ were experimentally studied and have shown quasi-particles with fractional charge and spin. Existence of such quasi-particles correspond to TO in the system. Following are some key properties that defines the TO in $2+1$ D systems.

- **Ground state degeneracy**: It counts the number of independent ground states $|\psi\rangle$, obtained by solving the eigen-value problem $H|\psi\rangle = \varepsilon_{gd}|\psi\rangle$. It depends on the topology of the manifold. For example, a *topologically ordered* state like $\nu = 1/3$ Fractional quantum Hall state on a manifold has 3^g ground state degeneracy, where g is the genus of the manifold [18]. Non-interacting topological superconductor and insulator phases on any manifold have no ground state degeneracy. In this sense they have trivial TO . Such distinction also occurs in the quantum entanglement properties and fractional statistics.

- **Quantum entanglement**: It describes how a quantum state is entangled between different parts of the system. For example, bi-partition a system into part A and part B and can compute the entanglement entropy defined as $S_A = -\mathrm{Tr}[\rho_A log\,(\rho_A)]$ where $\rho_A = Tr_B|\psi\rangle\langle\psi|$. Entanglement entropy usually scales with the area of A with a few exceptions. For a phase with TO there is a constant term in addition to the area law scaling term, often referred to as *topological entanglement entropy*[19].

- **Fractional charge and spin**: A phase with TO has quasi-particle and quasi-vortex excitations with fractionalized charge and/or spin (statistics). Quasi-particles are collective excitations that occurs in the emergent low energy description of a system. In 2+1 D such quasi-particle excitations are called "anyons" which are de-confined in the sense that there is no energy cost to change their position. However, when they changes their position the phase of the wave function changes and this is the only relevant thing to keep track of. Their wave function gain a non-trivial phase under exchange of two such anyons even while they are separated by large distances[20, 21]. When two such anyons are brought together they can fuse to give another anyon. A particular TO is specified by a set of anyons along with their braiding (exchange) and fusion rules. Such a set (or "category") of anyons is often associated with a symmetry group and the anyons can be thought of as irreducible representations of the the symmetry group. Properties of these anyons are discussed below and will

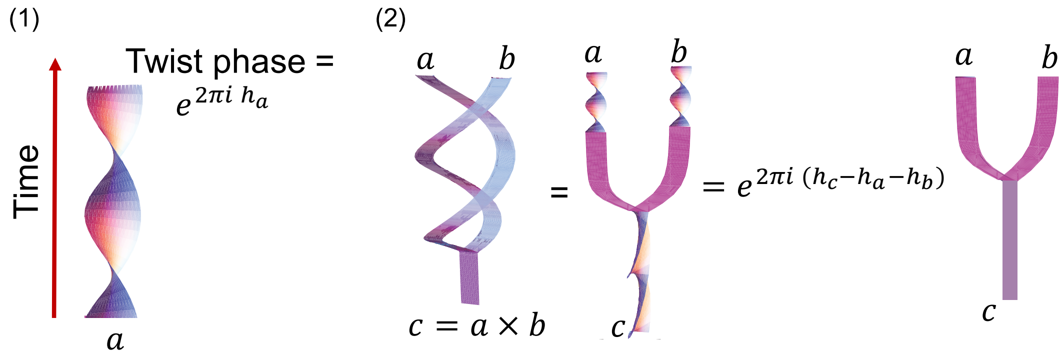

Figure 1.3: (1) Ribbon diagram showing topological spin of an anyon from the 2π twist. (2) Monodromy phase or the double exchange phase from ribbon twist phase.

be referred to frequently in later part of the thesis.

The topological spin, h_a: This defines the phase $e^{2\pi i h_a}$ incurred by the anyon, a, when it is rotated by 2π. So the world line of an anyon is like a ribbon as shown in figure 1.3. This is also the exchange phase of a and $\overline{a}$, where $\overline{a}$ is the unique "anti-particle " of a such that they fuse to vaccuum i.e. $\mathbb{1}$.

Fusion rules:

$$a_i \times a_j = \sum_k N_k^{ij} a_k \tag{1.10}$$

These rules tell us what possible anyons can form when a_i and a_j are brought together or fused. This is similar to the Clebsh-Gordon rules that tell how the tensor product of two representations can be written as direct sum of irreducible representations. In this thesis, N_k^{ij} is always taken to be 1 or 0. If the anyons are *abelian*, they fuse to give only one possible anyon. However, if anyons are *non-abelian* they have multiple fusion possibilities. Because of this, a pair of non-abelian anyons forms a Hilbert space with dimension greater than one. The quantum dimension of each anyon, d_a, indicates whether it is abelian or non-abelian.

Monodromy, M_c^{ab}: This is the phase gained when a circles around b. This is same as the phase gained when these two anyons exchange twice, and it also depends on the fusion channel of the two anyons. Figure 1.3 summarizes the ribbon identity, $M_c^{ab} = e^{2\pi i(h_{a\times b}-h_a-h_b)}$, using which we can calculate monodromy from the topological spins. A related quantity is the *braiding matrix* defined as

$$\mathcal{S}_{a,b} = \frac{1}{\mathcal{D}}\sum_c d_c N_{ab}^c M_c^{ab} \tag{1.11}$$

Finding new topological order that can realize anyons with interesting properties is useful. One can find a new TO by *gluing* and *fractionalizing* known TOs. *Gluing* involves *anyon condensation* [22] in a pair of TO s, which is similar to the bose condensation process. The anyons in the condensed phase are of the form a_1a_2 where, a_1 and a_2 belong to the two TO s respectively. We condense a set of bosons that are mutually local with respect to each other i.e. they have trivial mutual monodromy phases. This defines the new vacuum and a new TO . All the anyons that have nontrivial mutual monodromy phases w.r.t. any boson in the condensate are confined or not allowed in the new TO . The reverse of *anyon condensation* is *fractionalization* where the condensed phase fractionalizes to two topologically ordered phases. For example, condensing two Ising TO s each of which has Ising anyons with same topological spin gives us a trivial TO with just neutral fermions (since Ising TO is neutral). This also means, a fermion theory can be fractionalized to a pair of Ising TOs.

Although we discussed only $2+1$D TO , fractional charge and spin excitations also occurs in $3+1$D. It is true that the world lines of two pure point-like excitations can not braid due to presence of an extra dimension compared to $2+1$D, but in $3+1$D the world line of a point particle around a vortex line (that can be dynamic too) can not shrink to a point. Such vortex can occur as the flux of an internal gauge-field.

The quasi-particles and quasi-vortices set the TO in $3+1$D.

1.1.3.1 Topological field theory

One of the issues with topological states is that many states with TO don't always have a microscopic lattice model descriptions. Instead we can understand these topological states using a low-energy gauge theory description. The effective Chern-Simon's action [23] for abelian quasi-particles in 2+1D is given by

$$\mathcal{S}_{CS}[A] = \int d^3x \, \left[\frac{1}{4\pi}\epsilon^{\mu\nu\rho}\alpha^I_\mu K_{IJ}\partial_\nu \alpha^J_\rho - \frac{1}{2\pi}t_I\epsilon^{\mu\nu\rho}A_\mu\partial_\nu\alpha^I_\nu\right] \tag{1.12}$$

, where α^I_μ corresponds to N emergent $U(1)$ gauge fields for $I = 1\cdots N$ and A_μ is the external electro-magnetic gauge field. K_{IJ} corresponds to various Chern-Simon's coupling, which we call the K- matrix. Under the gauge transformation $\alpha^I_\mu \to \alpha^I_\mu - d_\mu\xi^I$ the theory should be invariant. This is the case when the system is defined on a manifold with no-boundary. For example, when $K = m$ is an integer, which is the case for abelian quantum Hall systems, $\alpha_\mu = \theta_\mu/L_\mu$ is the solution to the equation of motion. Here θ_μ is an angular variable that changes in multiples of 2π under the gauge transformation. The action in (1.12) becomes

$$S = \frac{im}{2\pi}\int d\tau\theta_y\frac{d\theta_x}{d\tau} \tag{1.13}$$

where τ is time. This is just a $p\dot{q}$ type kinetic term for θ fields and can be quantized by the relation, $\left[\hat{\theta}_x, \hat{\theta}_y\right] = \frac{2\pi i}{m}$. Note that if we define gauge invariant *Wilson loop operators* $W_i = e^{i\theta_x}$ along the two cycles of a torus, we can find the ground state degeneracy on the torus just using these commutation relations.

In the presence of a boundary, $\mathcal{S}_{CS}$ is not invariant under the gauge transformation because we get additional boundary terms. So, we need extra degrees of freedom at the boundary to cancel this term. Using the same example as before with integer

$K = m$, if we choose $\alpha_i = \partial_i \phi$ the action 1.12 gives an extra term at the boundary

$$\delta \mathcal{S}_{\text{bdry}} = -\frac{m}{4\pi} \int dx d\tau \partial_\tau \phi \partial_x \phi. \tag{1.14}$$

For $m = 1$ this is exactly the action for free chiral massless bosons. A general boundary action allowed by the gauge symmetries is

$$\mathcal{S}_{\text{bdry}} = -\frac{1}{4\pi} \int dx d\tau [K_{IJ} \partial_\tau \phi^I \partial_x \phi^J - V_{IJ} \partial_x \phi^I \partial_x \phi^J]. \tag{1.15}$$

This is the theory of left moving chiral Bosons and, particularly in the example of $K = m$, this is the $U(1)$ Kac-Moody theory at level m. This boundary gapless theory is a 1+1 D conformal field theory that will be described in detail later. In some cases, the boundary excitations from the gauge theory turn out to be non-chiral and become gapped within the allowed gauge symmetries. This is why not all systems with non-trivial TO have gapless boundary modes. These boundary modes are very useful in detecting the TO .

So far, I have not discussed how to visualize the quasi-particles within the Chern-Simons gauge theory. Interesting thing about the Chern-Simon's action is that its stress energy tensor vanishes, which means the Hamiltonian also vanishes. So this action is purely topological. To the action 1.12 with $K = m$, if we add a term $\int d^3 x \alpha_\mu j^\mu$ that couples the gauge fields to its currents, the equation of motion changes to

$$\frac{e^2}{2\pi\hbar} \epsilon^{\nu\lambda\mu} \partial_\nu \alpha_\lambda = j^\mu \tag{1.16}$$

Considering a static charge particle e, i.e. $j^0 = e\delta^2(x - x_0)$, we find upon integration the flux attached to this charge is $\frac{\hbar}{me}$. This is the origin of the fractional statistics because of the Aharnov-Bohm like phase gained by the charged particles when they circle around the flux [20] .

Just from the K-matrix K_{IJ} and the charge vector t_I, we can get information about the TO . For example, the ground state degeneracy is $|detK|$. The differential electrical conductance along the boundary (Hall conductance in 2+1D) is computed by integrating out the gauge fields a_μ's to get $\sigma = \nu \frac{\mathrm{e}^2}{\mathrm{h}} = \mathbf{t} \cdot K^{-1} \cdot \mathbf{t} \frac{\mathrm{e}^2}{\mathrm{h}}$. We designate different anyons which are sources for different currents by a vector so that they form a lattice. The topological spin of an anyon with lattice vector $\mathbf{a}$ is given by $\frac{1}{2}\mathbf{a}^T \cdot K^{-1} \cdot \mathbf{a}$. Similarly the monodromy, M_c^{ab} is given by $e^{2\pi i(\mathbf{a}\cdot(K)^{-1}\cdot\mathbf{b})}$.

Non-abelian anyons are understood using a non-abelian gauge theory other wise known as Wess-Zumino action[24]. Witten in [25] obtained the boundary conformal field for this gauge theory called as the Wess-Zumino-Witten CFT . Many examples of these will be discussed later. The purpose of this section was to show how the boundary of a topologically ordered state has gapless low energy modes. Such gapless field theories are the conformal field theories that will be discussed in details now.

1.1.4 Conformal field theory and bosonization

In $1 + 1$ D, a number of condensed matter systems can be described by relativistic field theories. This is because at low energy many systems show linear dispersions and hence have Lorentz invariance with the velocity of light replaced by the Fermi velocity, v_F. In imaginary time, Lorentz invariance becomes spatial-rotation invariance. A field theory with rotation, scale, and translation invariance is called *Conformal field theory* (CFT). Such a theory explains physics at the fixed point of a renormalization group transformation, otherwise known as a second order phase transition point. CFT also appears at the boundary of many topologically ordered systems, precisely at the interface between a $2 + 1$D topologically ordered phase and a trivial phase. There is a one-to-one correspondence between the primary operators of the boundary CFT and the quasi-particles (or anyons) in the topologically ordered phase. We use

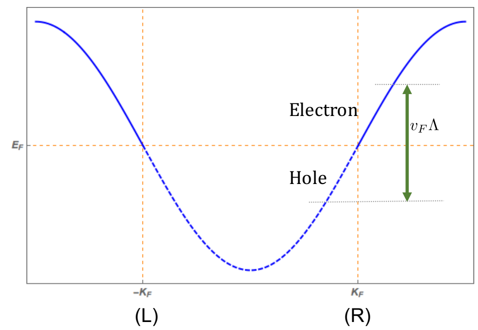

Figure 1.4: Band dispersion for free electron in 1D illustrating left and right Fermi points and the linear dispersion near these points.

this correspondence profusely in this thesis for finding TOs in $2+1$ D, since dealing with 1+1 D makes our problem easier and solvable. Conformal transformation maps space-time to itself, and in 1+1 D such transformations only have form $z \rightarrow \frac{az+b}{cz+d}$, such that $ad - bc = 1$. Here $z = i(v_F t - x)$ and $\overline{z} = i(v_F t + x)$ are coordinates in the complex plane. Any transformation in the two-dimensional complex plane is locally conformal. A local operator $\mathcal{O}(z, \overline{z})$ is called primary operator if it scales under a conformal transformation like $\mathcal{O}'(\alpha z, \overline{\alpha z}) = \alpha^{-h}\overline{\alpha}^{-\overline{h}}\mathcal{O}(z, \overline{z})$. The constants h and $\overline{h}$ are fundamental properties of the primary operator or the primary field called the conformal dimension. The operator product expansion (OPE) of an operator approximates the product of the operator at two nearby points by a sum of operators at either of those points. This is an important tool in CFT that makes bosonization work. CFT is also characterized by a number c, called the *central charge*, which is a measure of the number of degrees of freedom in the model considered. For example, $c = 1$ corresponds to a free boson and also to a complex or Dirac fermion. A complex free fermion theory can be equivalently written in terms of a free boson. Majorana fermions correspond to $c = 1/2$, so that when we add c for two Majorana fermions we get $c = 1$ for a complex fermion. The central charge for a set of N independent Majorana fermions can simply be added to give the net central charge to be $N/2$.

Let's consider a free electron ignoring its spin (a Dirac fermion) in 1+1 D. The

Hamiltonian near the Fermi energy as shown in fig(1.4) takes the following form

$$H_F = \int dk \frac{v_F}{2\pi} \left[\alpha^\dagger(k)\alpha(k) + \beta^\dagger(k)\beta(k)\right], \tag{1.17}$$

where α and β are electron annihilation operators at $+k_F$ and $-k_F$ respectively. The integration over k bounded by the momentum cut-off, Λ. We can define continuum fermion fields $c(x)$ and $\bar{c}$ valid only with this range of momenta i.e near the right Fermi point and the left Fermi point respectively. The time dependent fermion fields expanded in terms of α and β are

$$c(z) = \int_{k>0} \tfrac{dk}{2\pi} \left[e^{-kz}\alpha(k) + e^{kz}\beta^\dagger(k)\right] \tag{1.18}$$

$$\bar{c}(\bar{z}) = \int_{k<0} \tfrac{dk}{2\pi} \left[e^{k\bar{z}}\alpha(k) + e^{-k\bar{z}}\beta^\dagger(k)\right] \tag{1.19}$$

The field $\psi(z)$ is a super position of right moving electrons at $+k$ and left moving holes at $-k$. The low energy Hamiltonian written in terms of fermion fields is

$$H_F = -iv_F \int dx \left[c^\dagger \partial_x c - \bar{c}^\dagger \partial_x \bar{c}\right] \tag{1.20}$$

This is just the Dirac Hamiltonian as we expect. The negative sign in front of the second term is because $\bar{c}$ is a left moving chiral field. If the Hamiltonian has only c or $\bar{c}$ term, then the fermion moves only in one direction i.e the theory is chiral.

$$\begin{aligned}
\langle c(z)c(z')\rangle &= \int_{k>0} \frac{dk}{2\pi} \int_{k'>0} \frac{dk'}{2\pi} \langle 0|\alpha(k)\beta^{k'}|0\rangle e^{-kz+k'z'} \\
&= \int_{k>0} \frac{dk}{2\pi} e^{-k(z-z')} \\
&= \frac{1}{2\pi} \frac{1}{(z-z')}
\end{aligned}$$

Free boson in 1+1 D has the following Hamiltonian

$$\frac{v}{2}\int dx\,\left[\Pi^2+(\partial_x\phi)^2\right] \tag{1.21}$$

where the conjugate momentum field $\Pi=\frac{1}{v}\partial_t\phi$ such that $[\phi(x),\Pi(x)]=i\delta(x-x')$. The time dependent field can be written in terms of left and right moving fields, $\varphi(x,t)=\phi(x-vt)+\overline{\phi}(x+vt)$. The mode expansion for an infinite $1+1$ D bosonic system is

$$\phi(z)=\int_{k>0}\frac{dk}{2\pi}\frac{1}{\sqrt{2k}}[b_k e^{-kz}+b^\dagger(k)e^{kz}] \tag{1.22}$$

$$\overline{\phi}(z)=\int_{k>0}\frac{dk}{2\pi}\frac{1}{\sqrt{2k}}[\overline{b}_k e^{-k\overline{z}}+\overline{b}^\dagger(k)e^{-k\overline{z}}] \tag{1.23}$$

where b_k and $\overline{b}_k$ $(=b(-k))$ are bosonic creation operators that satisfy $[b_k,b^\dagger_{k'}]=2\pi\delta(k-k')$. There is a *dual* bosonic field, $\vartheta(x,t)$ defined by the relation $\partial_x\vartheta(x,t)=-\Pi=-\frac{1}{v}\,\partial_t\varphi(x,t)$, such that we can show the equal-time commutation relation is $[\varphi(x),\vartheta(x')]=-i\mathrm{sgn}(x-x')$ where . This means $i\vartheta(x')\equiv e^{\int_{-\infty}^{x'}dy\Pi(y)}$ shifts $\varphi(x)$ by 1 if $x>x'$. In next few paragraphs I will explain how any fermion operators including the Hamiltonian can be written in terms of bosonic fields. The electron density $n(x)$, a bilinear in electron field operators, has bose statistics. Let's say $\varphi(x)=\lambda\int_x^\infty dy\;n(y)$, which means adding a charged particle at $x'>x$ changes $n(x')$ and hence increases ϕ by λ. This seems like the shift operator we saw before, so the fermion creation operator can be written using this shift operator multiplied with any function of φ. The bosonization prescriptions for right and left moving fermions respectively are

$$\psi^\dagger(z)\sim:e^{i\alpha\phi}:,\quad \overline{\psi}^\dagger(\overline{z})\sim:e^{-i\alpha\overline{\phi}}: \tag{1.24}$$

where α is a constant which we will fix soon. : : means the operators are normal ordered since the exponent should have density dependence. The bosonization definition becomes more involved by including *Klein factors* when multiple species of fermions are considered, because the fermion anti-commutation relations are only true for same species. Let's first consider only one species of fermions. A normal ordered operator of the form $:e^{i\alpha\phi(z)}:$ is called a vertex operator. Using the Baker-Campbell-Hausdorff formula we have

$$:e^{i\alpha\phi(z)}::e^{i\beta\phi(z')}:=:e^{i\alpha\phi(z)+i\beta\phi(z')}:e^{-\alpha\beta\langle 0|\phi(z)\phi(z')|0\rangle} \tag{1.25}$$

$\langle\phi(z)\phi(z')\rangle$ is known as the Green's function and also called the OPE for free bosonic fields in CFT . It can be calculated using the mode expansion eqn 1.22 for bosonic fields. Note the expansion eqn 1.22 is not completely accurate, because it doesn't have the proper zero mode contribution. For details refer [26, 27, 23]. In the large length limit, $\langle\phi(z)\phi(z')\rangle \to -\frac{1}{4\pi}\ln(z-z')$. Hence, Green's function or OPE for fermion operators is

$$\langle\psi(z)\psi^\dagger(z')\rangle = \langle :e^{i\alpha\phi(z)}::e^{i\alpha\phi(z')}:\rangle = \langle :e^{i\alpha(\phi(z)+\phi(z'))}:\rangle(z-z')^{-\alpha^2/4\pi} \tag{1.26}$$

$\langle :e^{i\alpha(\phi(z)+\phi(z'))}:\rangle = 1$ because of normal ordering. Comparing with the fermion OPE (1.21) we choose the normalization such that $\psi^\dagger(z) = \frac{1}{\sqrt{2\pi}}:e^{i\sqrt{4\pi}\phi}:$.

Normal ordering a fermionic operator is same as using a *point splitting* prescription [28], for example $:\psi(z)^\dagger\psi(z):=\lim_{\epsilon\to 0}(\psi(z+\epsilon)^\dagger\psi(z)-\langle\psi(z+\epsilon)^\dagger\psi(z)\rangle)$. Let's now bosonize the fermionic Hamiltonian in eqn(1.20). The first term is

$$\psi(x)^\dagger\partial_x\psi(x) = -i\lim_{\epsilon\to 0}\psi(z+\epsilon)^\dagger\partial_z\psi(z) - \langle\psi(z+\epsilon)^\dagger\partial_z\psi(z)\rangle \tag{1.27}$$

First we expand $\psi(z')^\dagger\partial_z\psi(z) = \partial_z\psi(z')^\dagger\psi(z)$ in powers of $\epsilon = z' - z$

$$\partial_z \frac{1}{2\pi}\left[e^{i\sqrt{4\pi}\phi(z+\epsilon)}e^{-i\sqrt{4\pi}\phi(z)}\right] \tag{1.28}$$

$$=\partial_z \frac{1}{2\pi}\left[e^{i\sqrt{4\pi}(\phi(z+\epsilon)-\phi(z))}\frac{1}{\epsilon}\right] \tag{1.29}$$

$$=\partial_z\left[\frac{1}{2\pi(z-z')} + \frac{i}{\sqrt{\pi}}\partial_z\phi + i\frac{(z'-z)}{2\sqrt{\pi}}\partial_z^2\phi - (z'-z)(\partial_z\phi)^2\right] \tag{1.30}$$

After taking the derivative and plugging in eqn 1.27, the holomorphic part of the Hamiltonian becomes $-v\int dx\ [\frac{i}{2\sqrt{\pi}} : \partial_z^2\phi : + : (\partial_z\phi)^2 :] = -v\int dx \ \ : (\partial_x\phi)^2 :$ as the integral of the term linear in ϕ becomes 0. After similar treatment of the anti-holomorphic part

$$-v\int dx \ \ : (\partial_x\phi)^2 : + : (\partial_x\overline{\phi})^2 := -v/2\int_{dx}(\partial_x\varphi)^2 + (\partial_x\vartheta)^2 \tag{1.31}$$

This is exactly the Hamiltonian for a free boson.

The power of bosonization lies in expressing the interaction between fermions in terms of either free boson Hamiltonian or as sine-Gordon type potential terms. For a density-density coupling or interaction between the left and tight moving fermions we have following term

$$\gamma\int dx\ \psi_L^\dagger(x)\ \psi_L(x)\psi_R^\dagger(x)\psi_L(x) = \frac{\gamma}{(2\pi)^2}\int dx\ [(\partial_x\varphi)^2 - (\partial_x\vartheta)^2]. \tag{1.32}$$

Note that only the coefficients in the free boson Hamiltonian gets renormalized due to this interaction.

For multiple species of fermions that transform under a non-abelian symmetry group the conserved currents can be defined using the generators of the Lie group. This is called as the non-abelian bosonization process which gives us a bosonic theory with the same global symmetries as the fermionic theory. For example, there is $SU(2)$ spin rotation symmetry in addition to the $U(1)$ charge conservation symmetry if we consider spin-ful fermions. Using the chiral fields $\psi_{R,\sigma}$ and $\psi_{L,\sigma}$, the conserved $SU(2)$ currents are defined as $J^a_{R/L}(x) = \frac{1}{2}\psi^\dagger_{R/L,\sigma}(x)\tau^a_{\sigma,\sigma'}\psi_{R/L,\sigma'}$ which satisfy the $SU(2)$ Kac-Moody algebra with level $k = 1$. The bosonized action for the free spinful Dirac fermion becomes $S = \int d^2x \frac{1}{2}(\partial_\mu \phi)^2 + S^{k=1}_{WZW}[g]$. Here $S^{k=1}_{WZW}$ is the Wess-Zumino-Witten action for the WZW CFT .

$$
\begin{aligned}
S^{k=1}_{WZW} &= \frac{1}{4\lambda^2}\int d^2x \mathrm{Tr}(\partial_\mu g \partial^\mu g^{-1}) && (1.33)\\
&+ \frac{k}{24\pi}\int d^3y \epsilon^{\mu\nu\rho}\mathrm{Tr}\left(\overline{g}^{-1}\partial_\mu \overline{g}\overline{g}^{-1}\partial_\nu \overline{g}\overline{g}^{-1}\partial_\rho \overline{g}\right) && (1.34)
\end{aligned}
$$

where λ and k are constants related by $\lambda^2 = \frac{4\pi}{k}$. k is called the level of the WZW model also corresponds to level in the Lie algebra. In later chapter we will encounter WZW CFT for $SO(N)$ Lie group. The details for this is discussed in the appendix A.

1.2 Outline of the thesis

The 3+1D TR symmetric TSC was believed to have a gapless Majorana surface state as long as the TR symmetry is not broken. This was recently refuted by the proposal of a TR symmetric gapped surface with TO for this TSC [29]. Even the $\mathbb{Z}$ classification of TSC – or class DIII band theories according to the Altland-Zirnbauer classification [7] – relies heavily on the single-body BCS description of the electronic structure. The symmetric TO occurs when we go beyond the mean field BdG Hamiltonian in eqn(1.5) and include fermion interaction. The fact that the surface Majorana modes of *any* TSC can be gapped without breaking symmetries does not mean the TSC is topologically trivial. There would generically be a residual TO , that allows non-trivial anyonic excitations to live on the surface unless N is a multiple of 16. This reduces the $\mathbb{Z}$ classification of TSC to $\mathbb{Z}_{16}$[29, 30, 31, 32, 33, 34, 35]. An explicit microscopic gapping interaction that leads to such TO is constructed in this thesis.

Additionally, TO on this superconductor surface is analyzed with a different approach and shown to be consistent with the previous studies.

Similar story holds true for topological insulators [13, 14, 15, 16] in 3+1D. Many-body interactions allow the surface Dirac mode of a TI to acquire an energy gap without breaking time reversal or charge conservation symmetries. However, a non-trivial surface TO called the "$\mathcal{T}$-Pfaffian surface" would be left behind [36, 37, 38, 39].This indicates that the bulk insulator still carries a non-trivial $\mathbb{Z}_2$ symmetry protected topology (SPT) even in the many-body framework. Sec. 1.1.2 explained how FTI are formed for electrons when the constituent Dirac partons form a topological Insulator [16]. Similarly one expects that the FTI can have TR symmetric TO if partons on the surface are in the $\mathcal{T}$-Pfaffian topologically ordered state. This TO on the surface of the FTI, referred to here as the generalized $\mathcal{T}$-Pfaffian* surface, is proposed and explored in this thesis.

In chapter 2, we construct the "coupled wire model" for the non-interacting surface of class DIII TSC. We will introduce the single-body coupled Majorana wire model at the beginning of Sec. 2.1. A review of the $so(N)_1$ WZW CFT will be given in Sec. 2.1.1 and 2.1.2 as well as in appendices A, B and C.

Chapter 3 explores how inter-wire interaction gaps the surface and also discusses the TO of the resulting gapped surface. In Sec. 3.1, we will construct time reversal symmetric 4-fermion interactions that will open up an excitation energy gap. The discussion will be separated into the even and odd N cases in Sec. 3.1.1 and 3.1.2 respectively. In the even case, the gapping Hamiltonian will match the $O(r)$ Gross-Neveu model [40, 41, 42, 43] and we will show an energy gap in section 3.1.1.1 by (partially) bosonizing the problem. The gapping potential for the odd case will rely on a conformal embedding and relate to the Zamolodchikov and Fateev $\mathbb{Z}_6$ parafermion CFT [44, 45]. This will be discussed and reviewed in Sec. 3.1.2.1, 3.1.2.2 as well as in appendix D. The symmetric gapping interactions will correspond to non-trivial surface topological orders. This will be discussed in Sec. 3.2 where we will present the class of 32-fold periodic topological G_N states. In Sec. 3.3, we will describe alternative gapping interactions that would lead to even more possibilities.

Chapter 4 will be devoted to FTI where a parton construction in a slab geometry is used to explore three types of gapped surface states – ferromagnetic surfaces that break TR, superconducting surfaces that break charge $U(1)$ symmetry, and symmetric surfaces which generalize the $\mathcal{T}$-Pfaffian surface state of a conventional TI to $\mathcal{T}$-Pfaffian*. The TO for the FTI slab with these surfaces is discussed in Sec. 4.1, 4.2 and 4.3 respectively. In Sec. 4.4, we discuss, using an anyon condensation picture, the gluing of a pair of $\mathcal{T}$-Pfaffian* surfaces. In the last chapter I will conclude the thesis. Our main findings for both the TSC and FTI case are summarized along with some discussion on future possible explorations.

Chapter 2

Three dimensional (3D) topological superconductor (TSC)

The technique of modeling a quasi- 2D system from the arrays of 1D system was used in many publications from 1999-2002[46, 47, 48, 49, 50, 51] For example, in [48] and in [50] 1D wires with interacting fermion (Luttinger liquids) are coupled by the the forward scattering terms to form a sliding Luttinger liquid phase in two-dimension. Numerous gapped phases including the topological phases in two-dimensions can be built by considering back-scattering between one-dimensional wires[51]. The interaction effects are more controlled and better understood in such models. This theoretical technique has been frequently used in the study of fractional quantum Hall states[51, 52, 53, 54, 55], anyon models[56, 57], spin liquids[58, 59], (fractional) topological insulators[60, 61, 62, 63, 64, 65, 66] and superconductors[67, 68]. In addition to pure 2D phases, the coupled wire model can also be constructed for the surface of a three dimensional bulk [69]. We will build such a model for the 2D surface (boundary) of the 3D topological superconductor.

The coupled wire model for the integer quantum Hall state [52] is briefly discussed here. Consider a set of wires that carry electrons on the 2D stripe as shown in the

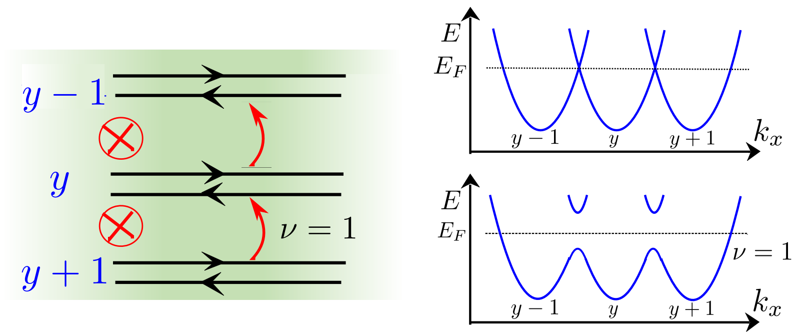

Figure 2.1: (Left) A coupled wire model description of the 2D quantum Hall insulator where the magnetic fields point into the plane. (Right) the energy dispersions for the wires before and after the coupling are shown respectively on top and bottom.

fig 2.1. Consider spinless electrons on the wires that are filled to the density, $n_e = \frac{k_F}{\pi a}$, a being the inter-wire distance. This is apparent from Luttinger's theorem that says the volume inside the Fermi surface is fixed by the total density of electrons inside the Fermi sphere. The presence of a magnetic field perpendicular to the plane of the stripe explains why electrons are effectively spinless. In the Landau gauge($\mathbf{A} = -By\hat{x}$) the electron dispersions along the momentum,k_x are shifted by $b = eaB/\hbar$. The filling fraction of the stripe is $\nu = \frac{\#\text{charge}}{\#\text{flux}} = 2k_F/b$. So, the left and right modes of adjacent wires exactly overlap at Fermi energy, E_F. If backscattering is turned on such that the left and right moving electron modes mix through the term $\int dx c_y^{L\dagger}(x) c_{y+1}^R(x)$, then we open a gap at E_F. Only the chiral (left or right) electron (Dirac) wires at the edge of the stipe remains gapless. This corresponds to the chiral Dirac mode at the edge of a quantum Hall insulator stripe with $\nu = 1$. The chiral electron wires on the stripe can be thought of as a chiral CFT for free Dirac fermions and the coupling a pair of wires is same as coupling a pair of CFT with opposite chirality. Later in this chapter we will consider a model built out of $SO(N)$ CFT .

2.1 Coupled wire construction of TSC surface

We consider a TR symmetric three dimensional topological superconductors that belongs to class DIII. As described in chapter(1) they host massless Majorana fermions on their surface that have gapless cone like spectra. The number of cones is a protected integer quantum number. In the simplest scenario, we have a single Majorana cone, which is the spectrum of a massless two-component real fermion $\mathcal{H}_{\pm} = iv\boldsymbol{\psi}^T\not{\partial}_{\pm}\boldsymbol{\psi}$, where $\not{\partial}_{\pm} = \partial_y\tau_x \pm \partial_x\tau_z$ and the Pauli matrices τ_x, τ_y, τ_z act on the surface real fermion, $\boldsymbol{\psi} = (\psi_R, \psi_L)$. Majorana fermions are hermitian $\psi_j^\dagger = \psi_j$ and obey the anti-commutation relation $\{\psi_j(\mathbf{r}), \psi_{j'}(\mathbf{r}')\} = 2\delta_{jj'}\delta(\mathbf{r}-\mathbf{r}')$. Time reversal switches the components $\mathcal{T}(\alpha_1\psi_L + \alpha_2\psi_R)\mathcal{T}^{-1} = \alpha_2^*\psi_L - \alpha_1^*\psi_R$ so that $\mathcal{T}^2 = -1$. The sign in the Hamiltonian $\mathcal{H}_{\pm}$ determines its *chirality.* So, in general the surface can have say N_R right chiral cones and N_L left chiral cones. Such a general Hamiltonian will take the following form

$$\mathcal{H}_c = \sum_{a=1}^{N_R} iv_a\boldsymbol{\psi}_a^T\not{\partial}_+\boldsymbol{\psi}_a + \sum_{b=1}^{N_L} iv_b\boldsymbol{\psi}_b^T\not{\partial}_-\boldsymbol{\psi}_b.. \tag{2.1}$$

Fermions $\boldsymbol{\psi}_a$ and $\boldsymbol{\psi}_b$ with opposite chiralities can annihilate each other by the time reversal symmetric mass term $im\boldsymbol{\psi}_a^T\tau_z\boldsymbol{\psi}_b$ Quadratic terms among fermions of the same chirality would however either break TR or only move the gapless Majorana cones away from zero momentum without destroying them. The net surface chirality $N = N_R - N_L$ is thus a robust topological signature that distinguishes and characterizes 3D bulk TSC. It cannot be altered by any time reversal symmetric two-body perturbations that are not strong enough to close the bulk excitation energy gap.

Let's describe these surface Majorana cones using an array of coupled fermion wires (see figure (2.2)). As we will see in the next chapter such description easily demonstrates how to get topologically ordered surface with gapped spectra from this original surface with gapless spectra. In other words, this coupled wire description

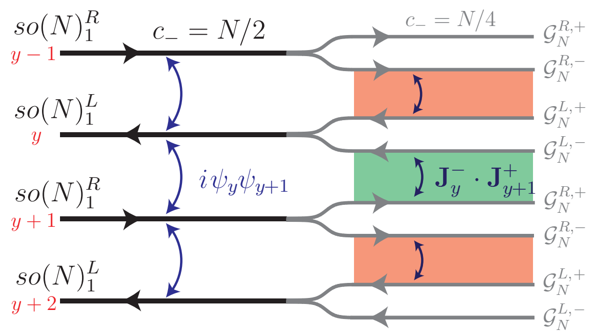

Figure 2.2: (Left) Coupled wire model (2.4) of N gapless surface Majorana cones. (Right) Fractionalization (3.4) and couple wires construction (3.8) of gapped anomalous and topological surface state.

helps us to construct explicit gapping terms. In figure (2.2) the horizontal wires are labeled according to their vertical position $y = \ldots, -2, -1, 0, 1, 2, \ldots$ and each carries N chiral (real) Majorana fermions $\boldsymbol{\psi}_y = (\psi_y^1, \ldots, \psi_y^N)$ which propagate only to the right (or left) if y is even (resp. odd). The number of flavors N here is going to be identified with the net chirality of the surface Majorana cone. Time reversal symmetry is non-local in this model as it relates fermions on adjacent wires that propagate in opposite directions,

$$\mathcal{T}\left(\sum_{a=1}^{N}\alpha_a\psi_y^a\right)\mathcal{T}^{-1} = (-1)^y\sum_{a=1}^{N}\alpha_a^*\psi_{y+1}^a. \tag{2.2}$$

Similar to the symmetry of an anti-ferrormagnet, here time reversal on the single-fermion Hilbert space squares to a primitive translation up to a sign, $\mathcal{T}^2 = -\hat{t}_y$, for $\hat{t}_y$ the vertical lattice translation $y \to y+2$ that relates nearest co-propagating wires. In the many-body Hilbert space,

$$\mathcal{T}^2 = (-1)^F\hat{t}_y \tag{2.3}$$

where $(-1)^F$ is the fermion parity operator whose sign depends on whether the fermion number is odd or even.

We mimic N copies of surface Majorana cones by the coupled wire Hamiltonian

$$\mathcal{H}_0 = \sum_{y=-\infty}^{\infty} iv_{\mathsf{x}}(-1)^y \boldsymbol{\psi}_y^T \partial_x \boldsymbol{\psi}_y + iv_{\mathsf{y}} \boldsymbol{\psi}_y^T \boldsymbol{\psi}_{y+1} \tag{2.4}$$

where the N-component Majorana fermion $\boldsymbol{\psi}$ disperses linearly (for small k_y) with velocities $v_{\mathsf{x}}, v_{\mathsf{y}}$ along the horizontal and vertical axes (see figure 2.3). By applying eqn((2.2)), we see $\mathcal{T}\mathcal{H}_0\mathcal{T}^{-1} = \mathcal{H}_0$ and the coupled wire model is therefore time reversal symmetric. Moreover, $\mathcal{H}_0$ has continuous translation symmetry along x and discrete translation along $y \to y+2$. The alternating sign in the first term of eqn((2.4)) specifies the propagating directions of the Majorans. Projecting to the $k_x = 0$ zero modes along the wires, the second term in (2.4) effectively becomes a 1D Kitaev Majorana chain[5] which has a linear spectrum for small k_y. More explicitly, by using the single-particle Nambu basis $\boldsymbol{\xi}_{\mathbf{k}}^a = (c_{\mathbf{k}}^a, {c_{-\mathbf{k}}^a}^\dagger)^T$ for $c_{\mathbf{k}}^a = \sum_{xy} e^{i(k_x x + k_y y)} c_y^a(x)$ the Fourier transform of the Dirac fermion $c_y^a(x) = (\psi_{2y-1}^a(x) + i\psi_{2y}^a(x))/2$, the coupled wire Hamiltonian in eqn((2.4)) can be expressed as $\mathcal{H}_0 = \sum_{a=1}^{N} \sum_{\mathbf{k}} \boldsymbol{\xi}_{\mathbf{k}}^{a\dagger} H_{\mathrm{BdG}}^0(\mathbf{k}) \boldsymbol{\xi}_{\mathbf{k}}^a$, where the BdG Hamiltonian is given by

$$H_{\mathrm{BdG}}^0(\mathbf{k}) = 2v_{\mathsf{x}} k_x \tau_x + v_{\mathsf{y}} \left[-\sin k_y \tau_y + (1 - \cos k_y)\tau_z \right] \tag{2.5}$$

for $-\infty < k_x < \infty$ and $-\pi \leq k_y \leq \pi$. Upon diagonalizing H_{BdG}^0, It shows a linear spectrum near zero energy and momentum as shown in figure 2.3 and in general we have N Majorana cones.

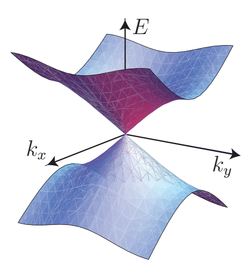

Figure 2.3: The energy spectrum of the coupled Majorana wire model (2.4)

Please note that if the time reversal operation in eqn((2.2)) was defined without the alternating sign $(-1)^y$, it would square to a different sign $\mathcal{T}^2 = +\hat{t}_y$ in the single-fermion Hilbert space and the vertical term in (2.4) would need to be modified into $\sum_y iv_{\mathrm{y}}(-1)^y \boldsymbol{\psi}_y^T \boldsymbol{\psi}_{y+1}$ in order to preserve the symmetry. This would correspond to an alternating Majorana chain in the y-direction, where the gapless Majorana cone would be positioned at $k_y = \pi$ instead of 0 and would still be protected by Kramers theorem as $T^2_{k_y=\pi} = e^{ik_y} = -1$. This scenario is actually equivalent and related to the original by a gauge transformation $(\psi_{4y}, \psi_{4y+1}, \psi_{4y+2}, \psi_{4y+1+3}) \to (\psi_{4y}, \psi_{4y+1}, -\psi_{4y+2}, -\psi_{4y+1+3})$, and therefore the sign of $\mathcal{T}^2$ is not important in this problem. Nevertheless, in the following discussions, we will stick with the previous convention defined in eqn((2.2)).

A chiral 1D system violates the fermion doubling[70] principle and can only be realized as an anomalous edge of a gapped 2D bulk[71, 72, 73]. The coupled Majorana wire model, (2.4) or figure 2.2, must therefore also be holographic and living on the surface of a 3D bulk superconductor. This can be modeled by a stack of alternating layers of spinless $p_x \pm ip_y$ superconductors (see figure 2.4(a)). The interwire backscattering in (2.4) can be generated by bulk interlayer electron tunneling and pairing that are not competing with the intra-layer $p + ip$ pairing. Time reversal (2.2) extends to the three dimensional bulk by relating fermions on adjacent layers. The coupled Majorana wire model can also live on the surface of a 3D class DIII topological superconductor where each chiral Majorana mode is bound between adjacent domains with opposite time reveral breaking phases $\phi = \pm\pi/2$ (see figure 2.4(b)).[74, 34] The discrete translation order along the y-axis perpendicular to the wire direction can be melted by proliferating dislocations (see figure 2.4(c)). With continuous translation symmetry restored, time reversal symmetry becomes local with $T^2 = -1$ and the coupled Majorana wire model in eqn(2.4) recovers the surface Majorana cone (2.1) in the continuum limit for small k_y.

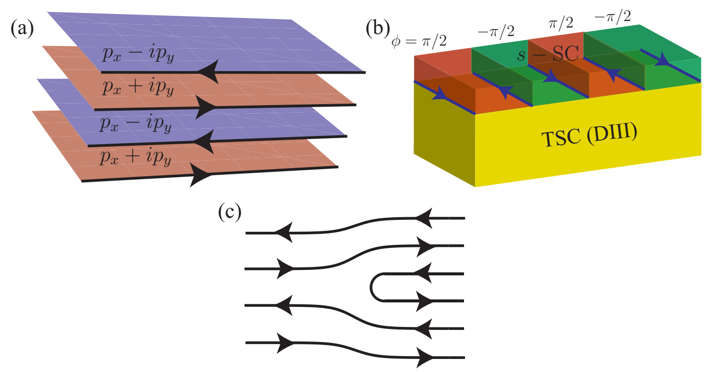

Figure 2.4: Coupled Majorana wire model on the surface of (a) a stack of alternating $p_x \pm ip_y$ superconductors, and (b) a class DIII topological superconductor (TSC) with alternating TR breaking surface domains. (c) A dislocation.

The non-local time reversal symmetry (2.2) actually provides a weaker topological protection to gapless surface Majorana's than a conventional local one. For instance in section 3.1, we will show that the $N = 2$ coupled Majorana wire model can be gapped by single-body backscattering terms without breaking time reversal, leaving behind a surface with trivial topological order. This reduced robustness stems from the half-translation component in the antiferrormagnetic time reversal. In the BdG description (2.5), the time reversal operator takes the momentum dependent form

$$T_{\mathbf{k}} = \left(\frac{1 + e^{ik_y}}{2} \tau_y + i \frac{1 - e^{ik_y}}{2} \tau_z \right) \mathcal{K} \tag{2.6}$$

for $\mathcal{K}$ the complex conjugation operator. It commutes with the BdG Hamiltonian $T_{\mathbf{k}} H^0_{\mathrm{BdG}}(\mathbf{k}) = H^0_{\mathrm{BdG}}(-\mathbf{k}) T_{\mathbf{k}}$ as well as the particle-hole (PH) $CT_{\mathbf{k}} = T_{-\mathbf{k}} C$, for $C = \tau_x \mathcal{K}$ the PH operator. In the continuum limit or for small k_y, $T \simeq \tau_y \mathcal{K}$ agrees with the conventional local time reversal operator and protects a zero energy Majorana Kramers' doublet. The BdG Hamiltonian has a chiral symmetry $\Pi_{\mathbf{k}} H^0_{\mathrm{BdG}}(\mathbf{k}) = -H^0_{\mathrm{BdG}}(\mathbf{k}) \Pi_{\mathbf{k}}$, for $\Pi_{\mathbf{k}} = iCT_{\mathbf{k}}$ the chiral operator. It can be used to assign the chirality of a Majorana cone by an integral winding number

$$n = \frac{1}{2\pi i} \oint_{\mathcal{C}_\varepsilon(\mathbf{k}_0)} \mathrm{Tr}\left[h(\mathbf{k})^{-1} \nabla_{\mathbf{k}} h(\mathbf{k})\right] \cdot d\mathbf{l} \tag{2.7}$$

locally around a loop $\mathcal{C}_\varepsilon(\mathbf{k}_0)$ ε away from the zero mode at $\mathbf{k}_0$. Here $h(\mathbf{k})$ is the elliptic operator

$$h(\mathbf{k}) = P^+_{\mathbf{k}} H^0_{\mathrm{BdG}}(\mathbf{k}) P^-_{\mathbf{k}} \tag{2.8}$$

for $P^\pm_{\mathbf{k}} = (P^\pm_{\mathbf{k}})^2$ the two *local* projectors diagonalizing the chiral operator $\Pi_{\mathbf{k}} = e^{-ik_y/2}(P^+_{\mathbf{k}} - P^-_{\mathbf{k}})$. However, as time reversal squares to $T_{\mathbf{k}} T_{-\mathbf{k}} = -e^{ik_y}$, which is the eigenvalue of the primitive translation $-\hat{t}_y$ at momentum $\mathbf{k}$, so does the *non-symmorphic* chiral operator $\Pi^2_{\mathbf{k}} = e^{-ik_y}$. The two chiral branches $\Pi_{\mathbf{k}} = \pm e^{-ik_y/2}$ switch across the Brillouin zone when $k_y \to k_y + 2\pi$. As a result, a *global* winding number can only be defined modulo 2. In the next section we will write the model Hamiltonian using CFT currents.

2.1.1 The $so(N)_1$ current algebra

We notice the couple Majorana wire model (2.4) has a $SO(N)$ symmetry that rotates the N-component Majorana fermion $\psi^a_y \to O^a_b \psi^b_y$. Consequently, there is a chiral $so(N)$ WZW theory[24, 25] or affine Kac-Moody algebra at level 1 along each wire. Here we review some relevant features of the $so(N)_1$ algebra, which are well-known and can be found in standard texts on conformal field theory (CFT)(1) such as Ref.[26].

The $so(N)_1$ currents have the free field representation

$$J^\beta(z) = \frac{i}{2} \boldsymbol{\psi}(z)^T t^\beta \boldsymbol{\psi}(z) = \frac{i}{2} \sum_{ab} \psi^a(z) t^\beta_{ab} \psi^b(z) \tag{2.9}$$

where the t^β's are antisymmetric $N \times N$ matrices that generate the $so(N)$ Lie algebra (see appendix A), $z = e^{\tau+ix}$ is the complex space-time parameter, and (2.9) is normal ordered. The coupled Majorana wire model carries currents that propagate in alternating directions (see figure 2.2) so that $J_y^\beta(z)$ are holomorphic for even y and $J_y^\beta(\overline{z})$ are anti-holomorphic for odd y. Focusing on an even wire, the OPE of the fields are

$$\psi^a(z)\psi^b(w) = \frac{\delta^{ab}}{z-w} + \dots. \tag{2.10}$$

The $so(N)_1$ currents obey the product expansion

$$J^\beta(z)J^\gamma(w) = \frac{\delta^{\beta\gamma}}{(z-w)^2} + \sum_\delta \frac{if_{\beta\gamma\delta}}{z-w}J^\delta(w) + \dots \tag{2.11}$$

where $f_{\beta\gamma\delta}$ are the structure constants of the $so(N)$ Lie algebra with $\left[t^\beta, t^\gamma\right] = \sum_\delta f_{\beta\gamma\delta}t^\delta$ (see appendix A). The Sugawara energy momentum tensor (along a single wire) is equivalent to the free fermion one[75]

$$T(z) = \frac{1}{2(N-1)}\mathbf{J}(z)\cdot\mathbf{J}(z) = -\frac{1}{2}\boldsymbol{\psi}(z)^T\partial_z\boldsymbol{\psi}(z) \tag{2.12}$$

for $\mathbf{J} = (J^\beta)$ the current vector and $\boldsymbol{\psi} = (\psi^1,\dots,\psi^N)$ the N-component real fermion. The energy momentum tensor defines a chiral Virasoro algebra and characterizes a chiral CFT. It satisfies the OPE

$$T(z)T(w) = \frac{c_-/2}{(z-w)^4} + \frac{2T(w)}{(z-w)^2} + \frac{\partial_w T(w)}{z-w} + \dots \tag{2.13}$$

where the chiral central charge $c_- = N/2$, loosely speaking, counts the conformal degrees of freedom on the Majorana wires and is proportional to the energy current[76, 77, 73, 78] and entanglement entropy[79, 80, 81] carried by the wire.

Excitations of the N-component Majorana wire transform according to the $SO(N)$

symmetry. They decompose into *primary fields* and their corresponding descendants. A primary field $\mathbf{V}_\lambda = (V^1, \ldots, V^d)$ is a simple excitation sector that irreducibly represents the $so(N)_1$ Kac-Moody algebra.

$$J^\beta(z)V^r(w) = -\sum_{s=1}^{d} \frac{(t^\beta_\lambda)_{rs}}{z-w} V^s(w) + \ldots \tag{2.14}$$

where λ labels some d-dimensional irreducible representation of $so(N)$ and t^β_λ is the $d \times d$ matrix representing the generator t^β of $so(N)$. For example it is straightforward to check by using the definition (2.9) and the OPE (2.10) that the Majorana fermion $\boldsymbol{\psi} = (\psi^1, \ldots, \psi^N)$ is primary with respect to the fundamental representation, i.e.

$$J^\beta(z)\psi^a(w) = -\sum_{b=1}^{N} \frac{t^\beta_{ab}}{z-w} \psi^b(w) + \ldots. \tag{2.15}$$

From (2.12), space-time translation of a primary field $\mathbf{V}_\lambda$ is governed by

$$T(z)\mathbf{V}_\lambda(w) = \frac{h_\lambda}{(z-w)^2}\mathbf{V}_\lambda(w) + \frac{\partial_w \mathbf{V}_\lambda(w)}{z-w} + \ldots \tag{2.16}$$

where the conformal (scaling) dimension is given by

$$h_\lambda = \frac{\mathcal{Q}_\lambda}{2(N-1)} \tag{2.17}$$

for $-\sum_\beta t^\beta_\lambda t^\beta_\lambda = \mathcal{Q}_\lambda \mathbb{1}_{d\times d}$ the quadratic Casimir operator. For instance $\mathcal{Q}_\psi$, the quadratic Casimir eigenvalue for the fundamental representation, is $N-1$ (see appendix A) and therefore the fermion $\boldsymbol{\psi}$ has conformal dimension $h_\psi = 1/2$. This agrees with the OPE (2.10) by dimension analysis.

There are extra primary fields other than the the trivial vacuum 1 and the fermion ψ. The spinor representations (see appendix A) σ, for N odd, or s_+ and s_-, for N even, also correspond to primary fields of $so(N)_1$. Their conformal dimensions can be read off from their quadratic Casimir values (A.7), and are

$$h_\sigma = \frac{N}{16}, \quad h_{s\pm} = \frac{N}{16}. \tag{2.18}$$

Unlike the infinite number of irreducible representations of a Lie algebra, the extended affine $so(N)_1$ algebra only has a truncated set of primary fields $\{1, \sigma, \psi\}$, for N odd, or $\{1, s_+, s_-, \psi\}$, for N even.

These $so(N)_1$ primary fields take more explicit operator forms after bosonization and can be found in appendix B and C.

2.1.2 Bosonizing even Majorana cones

In the case when $N = 2r$ is even, the N Majorana fermions on each wire can be paired into r Dirac fermions and *bosonized*[27, 23]

$$c_y^j = \frac{\psi_y^{2j-1} + i\psi_y^{2j}}{\sqrt{2}} \sim \frac{1}{\sqrt{l_0}} \exp\left(i\widetilde{\phi}_y^j\right) \tag{2.19}$$

where $\widetilde{\phi}_y^1, \ldots, \widetilde{\phi}_y^r$ are real bosons on the y^{th} wire, and the vertex operator in (2.19) is normal ordered (see chapter 1). The bosons obey the equal-time commutation relation

$$\begin{aligned}\left[\widetilde{\phi}_y^j(x), \widetilde{\phi}_{y'}^{j'}(x')\right] =& i\pi(-1)^{\max\{y,y'\}}\Big[\delta_{yy'}\delta^{jj'}\mathrm{sgn}(x'-x) \\ &+ \delta_{yy'}\mathrm{sgn}(j-j') + \mathrm{sgn}(y-y')\Big]\end{aligned} \tag{2.20}$$

where $\mathrm{sgn}(s) = s/|s| = \pm 1$ for $s \neq 0$ and $\mathrm{sgn}(0) = 0$. The first line of (2.20) is equivalent to the commutation relation between conjugate fields

$$\left[\widetilde{\phi}_y^j(x), \partial_{x'}\widetilde{\phi}_{y'}^{j'}(x')\right] = 2\pi i(-1)^y \delta_{yy'}\delta^{jj'}\delta(x-x') \tag{2.21}$$

and is set by the "$p\dot{q}$" term of the Lagrangian density

$$\mathcal{L}_0 = \frac{1}{2\pi}\sum_{y=-\infty}^{\infty}\sum_{j=1}^{r}(-1)^y\partial_x\widetilde{\phi}_y^j\partial_t\widetilde{\phi}_y^j. \tag{2.22}$$

The second line of (2.20) guarantees the correct anticommutation relations between Dirac fermions along distinct channels. The alternating signs $(-1)^y$ in (2.21) and (2.22) specify the propagating directions along each wire, R (or L) for y even (resp. odd). Eq.(2.20) is symmetric under time reversal (2.2), which sends

$$\mathcal{T}c_y^j\mathcal{T}^{-1} = (-1)^y c_y^{j\dagger}, \quad \mathcal{T}\widetilde{\phi}_y^i\mathcal{T}^{-1} = \widetilde{\phi}_{y+1}^i + \pi y. \tag{2.23}$$

We notice time reversal, in this convention, flips the fermion parity as it interchanges between the creation and annihilation operators.

The entire coupled Majorana wire Hamiltonian (2.4), when $N = 2r$ is even, can be turned into a model of coupled boson wires. The total Lagrangian density is a combination

$$\mathcal{L} = \mathcal{L}_0 - \mathcal{H} = \mathcal{L}_0 - \left(\mathcal{H}_\parallel + \mathcal{H}_\perp\right) \tag{2.24}$$

where the Hamiltonian density $\mathcal{H} = \mathcal{H}_\parallel + \mathcal{H}_\perp$ consists of the sliding Luttinger liquid[46, 47, 48, 49, 50] (SLL) component along each wire

$$\mathcal{H}_\parallel = V_{\mathsf{x}}\sum_{y=-\infty}^{\infty}\sum_{j=1}^{r}\partial_x\widetilde{\phi}_y^j\partial_x\widetilde{\phi}_y^j \tag{2.25}$$

and the backscattering component between wires

$$\mathcal{H}_\perp = -V_{\mathsf{y}}\sum_{y=-\infty}^{\infty}\sum_{j=1}^{r}(-1)^y\cos\left(2\vartheta_{y+1/2}^j\right) \tag{2.26}$$

$$2\vartheta_{y+1/2}^j = \widetilde{\phi}_y^j - \widetilde{\phi}_{y+1}^j. \tag{2.27}$$

The SLL Hamiltonian (2.25) contains the (normal ordered) kinetic term $i\boldsymbol{\psi}_y^T\partial_x\boldsymbol{\psi}_y = i(c_y^\dagger\partial_x c_y + c_y\partial_x c_y^\dagger)$ in (2.4) as well as possible forward scattering terms like the density-density coupling $(c_y^\dagger c_y)(c_y^\dagger c_y)$. The interwire backscattering Hamiltonian (2.26) is identical to the second term $i\boldsymbol{\psi}_y^T\boldsymbol{\psi}_{y+1} = i(c_y^\dagger c_{y+1} + c_y c_{y+1}^\dagger)$ in (2.4). This can be derived directly by applying the bosonization prescription (2.19). The alternating sign $(-1)^y$ in (2.26) is crucial to preserve time reversal symmetry (2.23), which relates $\mathcal{T}2\vartheta^j_{y+1/2}\mathcal{T}^{-1} = 2\vartheta^j_{y+3/2} - \pi$.

The r sine-Gordon terms in (2.26) between the same pair of adjacent wires mutually commute

$$\left[2\vartheta^j_{y+1/2}(x), 2\vartheta^{j'}_{y+1/2}(x')\right] = 0 \tag{2.28}$$

and share simultaneous eigenvalues. If there was a single pair of counter-propagating wires, these potentials would have pinned $\langle 2\vartheta^j_{y+1/2}(x)\rangle = (2n+y)\pi$ between the two wires. However, they compete with the sine-Gordon terms between the next pair of wires due to the non-commuting relation

$$\begin{aligned}&\left[2\vartheta^j_{y+1/2}(x), 2\vartheta^{j'}_{y+3/2}(x')\right]\\ =&2\pi i(-1)^y\left[\theta(j-j') + \delta^{jj'}\theta(x'-x)\right]\end{aligned} \tag{2.29}$$

where the unit step function $\theta(s) = 0$ when $s \leq 0$, or 1 when $s > 0$. In other words, the vertex operators $e^{i2\vartheta^j_{y+1/2}}$ produces fluctuations to adjacent pairs,

$$\begin{aligned}&e^{-i2\vartheta^j_{y+1/2}(x)}2\vartheta^j_{y+3/2}(x')e^{i2\vartheta^j_{y+1/2}(x)}\\ =&2\vartheta^j_{y+3/2}(x') + 2\pi(-1)^y\theta(x'-x).\end{aligned} \tag{2.30}$$

The uniform backscattering strength V_{y}, as protected by time reversal (2.2), exactly balances the competing potentials so that the Hamiltonian $\mathcal{H} = \mathcal{H}_\parallel + \mathcal{H}_\perp$ remains gapless.

Chapter 3

Interaction and Surface Topological Order

The previous chapter describes the gapless surface Majorana fermions of a 3D topological superconductor using a coupled wire model (2.4). It consists of an array of chiral wires, each of which carries N flavors of Majorana fermions co-propagating in alternating directions (see figure 2.2). Together with uniform backscattering interactions between adjacent wires, the model captures N surface Majorana cones with linear energy dispersion about zero energy and momentum (see figure 2.3). In this section we construct explicit fermion interactions that introduce an excitation energy gap to the surface Majorana cones while preserving time reversal symmetry. Generically, this leaves behind a fermionic surface topological order, which will not be discussed until the next section.

3.1 Many-body interaction in coupled wire model

We begin with the simplest case when there are $N = 2$ chiral Majorana channels along each wire and correspond to two surface Majorana cones. As eluded in section 2.1, due to the non-local nature of time reversal, the coupled wire model can be gapped by single-body backscattering terms without violating the symmetry. Although this cannot be applied to a conventional topological superconductor with local time reversal, this model demonstrates the idea of *fractionalization*, which can be generalized to the many-body interacting case and subsequently lead to surface topological order. The Hamiltonian $\mathcal{H} = \mathcal{H}_0 + \mathcal{H}_{\mathrm{bc}}$ consists of the original model (2.4) with two fermion flavors $\boldsymbol{\psi}_y = (\psi^1_y, \psi^2_y)$ and the inter-flavor backscattering

$$\mathcal{H}_{\mathrm{bc}} = iu \sum_{y=-\infty}^{\infty} \psi^1_y \psi^2_{y+1} \tag{3.1}$$

which is symmetric under the time reversal (2.2), $\mathcal{T} : \psi^a_y \to (-1)^y \psi^a_{y+1}$. The BdG Hamiltonian $H_{\mathrm{BdG}}(\mathbf{k}) = H^0_{\mathrm{BdG}}(\mathbf{k}) + H^{\mathrm{bc}}_{\mathrm{BdG}}(\mathbf{k})$ is the combination of (2.5) and

$$\begin{aligned} H^{\mathrm{bc}}_{\mathrm{BdG}}(\mathbf{k}) =& \frac{u}{2} \left[(1 - \cos k_y)\sigma_x\tau_z + (1 + \cos k_y)\sigma_y\tau_y \right. \\ & \left. - \sin k_y (\sigma_y\tau_z + \sigma_x\tau_y) \right] \end{aligned} \tag{3.2}$$

which is symmetric under $T_{\mathbf{k}}$ in (2.6). The energy spectrum depends on the relative strength between the two interwire couplings $iv_{\mathsf{y}}(\psi^1_y\psi^1_{y+1} + \psi^1_y\psi^1_{y+1})$ and $iu\psi^1_y\psi^2_{y+1}$ (see figure 3.1). When $u = 0$, the two Majorana cone coincide at zero momentum. A finite u separates the two until they have traveled across the Brillouin zone and annihilate each other at $k_y = \pi$ when $u > 2v_{\mathsf{y}}$. Once an energy gap has opened up, the BdG Hamitonian has a unit Chern invariant

$$\mathrm{Ch} = \frac{i}{2\pi} \int_{-\infty}^{\infty} dk_x \int_{-\pi}^{\pi} dk_y \mathrm{Tr}\left(\mathcal{F}_{\mathbf{k}}\right) = 1 \tag{3.3}$$

where $\mathrm{Tr}\left(\mathcal{F}_{\mathbf{k}}\right) = \mathrm{Tr}\left(\langle \partial_{k_y} u^a_{\mathbf{k}} | \partial_{k_x} u^b_{\mathbf{k}} \rangle - \langle \partial_{k_x} u^a_{\mathbf{k}} | \partial_{k_y} u^b_{\mathbf{k}} \rangle \right)$ is the Berry curvature constructed from the two occupied eigenstates $u^1_{\mathbf{k}}, u^2_{\mathbf{k}}$ below zero energy of $H_{\mathrm{BdG}}(\mathbf{k})$. The coupled Majorana wire model thus behaves like a chiral $p + ip$ topological superconductor[82, 72]. However the single-body Hamiltonian does not possesses a topological order in the sense that it does not support anyonic excitations. For instance the $\psi \to -\psi$ $\mathbb{Z}_2$ symmetry is global and π-vortices are not quantum excitations of the model but rather introduced as classical extrinsic defects.

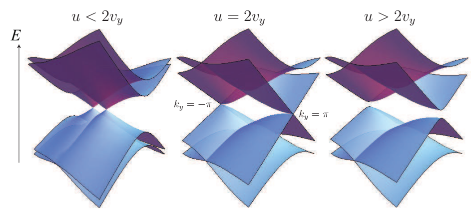

Figure 3.1: Energy spectrum of the $N = 2$ coupled Majorana wire model with inter-flavor mixing.

This example relies on a simple decomposition of the degrees of freedom along each wire, $N = 2 = 1 + 1$. The two Majorana fermions ψ_y^1, ψ_y^2 are backscattered independently to adjacent wires in opposite directions. Unlike the intra-flavor couplings $iv_{\mathsf{y}}(\psi_y^1\psi_{y+1}^1 + \psi_y^1\psi_{y+1}^1)$, inter-flavor terms $iu\psi_y^1\psi_{y+1}^2$ freeze independent degrees of freedom and they are not competing with each other. It is useful to notice that the decomposition breaks the $SO(2)_1$ symmetry described in section 2.1.1, and as a result the $so(2r)_1$ CFT along each wire splits into a pair of chiral Ising CFT's.

We can now generalize this idea to all N, but with many-body interwire interactions. From now on, unless specified otherwise, we turn off all single-body scattering terms. For instance, the vertical velocity now vanishes, $v_{\mathsf{y}} = 0$, in the kinetic part $\mathcal{H}_0$ of the coupled wire model (2.4). First we seek a decomposition of the $so(N)_1$ degrees of freedom along each wire (see section 2.1.1) into a pair of identical but independent sectors (also see figure 2.2)

$$so(N)_1 \supseteq \mathcal{G}_N^+ \times \mathcal{G}_N^- \tag{3.4}$$

where $\mathcal{G}_N^{\pm}$ are the Kac-Moody subalgebras

$$\mathcal{G}_N^{\pm} = \begin{cases} so(N/2)_1 & \text{for } N \text{ even} \\ so(3)_3 \times so\left(\frac{N-9}{2}\right)_1 & \text{for } N \text{ odd} \end{cases} \tag{3.5}$$

to be discussed below. This fractionalization has to be complete in the sense that the Sugawara energy-momentum tensor exactly splits into

$$T_{so(N)_1} = T_{\mathcal{G}_N^+} + T_{\mathcal{G}_N^-}. \tag{3.6}$$

In particular the central charge divides

$$c_-\left(so(N)_1\right) = 2c_-\left(\mathcal{G}_N\right) = c_-\left(\mathcal{G}_N^+\right) + c_-\left(\mathcal{G}_N^-\right) \tag{3.7}$$

and there are no degrees of freedom left behind. Using the subalgebra current operators $\mathbf{J}_{\mathcal{G}_N^{\pm}}$, which are quadratic in ψ's, we construct the four-fermion backscattering interaction

$$\begin{aligned} \mathcal{H}_{\text{int}} &= u \sum_{y=-\infty}^{\infty} \mathbf{J}^{y}_{\mathcal{G}_N^-} \cdot \mathbf{J}^{y+1}_{\mathcal{G}_N^+} \\ &= u \sum_{y'=-\infty}^{\infty} \mathbf{J}^{2y'-1}_{\mathcal{G}_N^{L,-}} \cdot \mathbf{J}^{2y'}_{\mathcal{G}_N^{R,+}} + \mathbf{J}^{2y'}_{\mathcal{G}_N^{R,-}} \cdot \mathbf{J}^{2y'+1}_{\mathcal{G}_N^{L,+}} \end{aligned} \tag{3.8}$$

for u positive, and R, L labels the propagating directions of the currents. This is pictorially presented in figure 2.2 and 3.2.

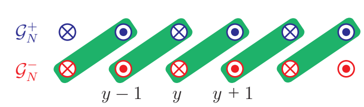

Figure 3.2: Interwire gapping terms (3.8) (green rectangular boxes) between chiral fractional $\mathcal{G}_N^{R,\pm}, \mathcal{G}_N^{L,\pm}$ sectors (resp. $\otimes, \odot$) in opposite direction.

In this section, we design the fractionalization (3.4) of $so(N)_1$ for all N and show that the backscattering interactions (3.8) open an excitation energy gap without breaking time reversal. In CFT context, (3.4) is also known as a conformal embedding[26, 83, 84, 85]. When $N = 2r$ is even, there is an obvious decomposition

$$so(2r)_1 \supseteq so(r)_1^+ \times so(r)_1^- \tag{3.9}$$

where the "+" sector contains $\psi^1, \ldots, \psi^r$ while the "−" one contains the rest $\psi^{r+1}, \ldots, \psi^{2r}$. In section 3.1.1, we review how the $\mathbf{J}_{so(r)_1^R} \cdot \mathbf{J}_{so(r)_1^L}$ interactions contribute an energy gap. This is a direct application of the well-studied $O(N)$ Gross-Neveu problem[40, 41, 42, 43] in 1D. In the discrete limit, this is related to the Haldane $O(3)$ antiferrormagnetic spin chain[86, 87], the Affleck - Kennedy - Lieb - Tasaki (AKLT) spin chains[88, 89] and the $SO(n)$ Heisenberg chain[90, 91, 92]. When N is odd, the splitting (3.4) is less trivial. We will make use of the level-rank duality[26, 93, 94]

$$so(n^2)_1 \supseteq so(n)_n \times so(n)_n \tag{3.10}$$

which comes from the fact that the tensor product $SO(n) \otimes SO(n)$ is a Lie subgroup in $SO(n^2)$. In particular, we will demonstrate the simplest case in section 3.1.2 when $n = 3$. The division of $so(9)_1$ can subsequently be generalized to $so(N)_1$ for all odd N effectively by writing $N = 9 + 2r$. This sets $\mathcal{G}_N^\pm = so(3)_3 \times so(r)_1$ in (3.4) and the corresponding interwire backscattering interactions (3.8).

3.1.1 Gapping even Majorana cones

We begin with the coupled Majorana wire model (2.4) (or figure 2.2) with $N = 2r$ chiral fermion channels per wire and corresponds to the same number of gapless Majorana cones. Similar to the previously shown $N = 2$ case, the gapless modes can be removed using simple single-body backscattering terms. We however are interested in finding gapping interactions that would support surface topological order as well.

In section 2.1.1 and appendices B, C, we described the $so(N)_1$ WZW theory, which along the y^{th} wire is generated by chiral current operators (2.9)

$$J_y^{(a,b)} = (-1)^y i\psi_y^a\psi_y^b. \tag{3.11}$$

We take the alternating sign convention $(-1)^y$ so that under time reversal, $\mathcal{T}J_y^{(a,b)}\mathcal{T}^{-1} = J_{y+1}^{(a,b)}$. We consider two subsets of generators, $so(r)_1^+$ containing $J^{(a,b)}$ for $1 \leq a < b \leq r$, and $so(r)_1^-$ containing $J^{(a,b)}$ for $r+1 \leq a < b \leq 2r$. As they act on independent fermion sectors, the two sets of operators commute or equivalently their operator product expansions (OPE) are trivial up to non-singular terms. Moreover the Sugawara energy-momentum tensor (2.12) for $so(N)_1$ completely splits into a sum between

$$T_{so(r)_1^+} = -\frac{1}{2}\sum_{a=1}^{r}\psi^a\partial\psi^a, \quad T_{so(r)_1^-} = -\frac{1}{2}\sum_{a=r+1}^{2r}\psi^a\partial\psi^a. \tag{3.12}$$

This ensures all degrees of freedom in $so(2r)_1$ are generated by tensor products between those in the $so(r)_1^\pm$ sectors. Precisely this means any $so(2r)_1$ primary field is a fusion channel of the OPE of certain primary field pair in $so(r)_1^+$ and $so(r)_1^-$. Thus as long as the gapping terms independently freeze both sectors, they remove all gapless degrees of freedom.

The backscattering interactions (3.8) couples the $so(r)_1^-$ sector on the y^{th} wire with the $so(r)_1^+$ sector on the $(y+1)^{\text{th}}$ one. They can explicitly written as

$$\mathcal{H}_{\text{int}} = u\sum_{y=-\infty}^{\infty}\sum_{1\leq a<b\leq r}\psi_y^{r+a}\psi_y^{r+b}\psi_{y+1}^a\psi_{y+1}^b. \tag{3.13}$$

Firstly, the interactions are time reversal symmetric as (3.13) is unchanged by $\psi_y^a \to (-1)^y\psi_{y+1}^a$. Secondly, it breaks the $O(2r)$ symmetry to $O(r)^+\times O(r)^-$. The symmetry breaking can be faciliated by forward scattering within wires that renormalizes the velocities differently between the $so(r)_1^{\pm}$ sectors. Eq.(3.13) is also a combination allowed by the chiral $O(r)$ symmetry

$$\psi_y^a \to \left(\mathcal{O}^{(-1)^y}\right)^a_b \psi_y^b, \quad \psi_y^{r+a} \to \left(\mathcal{O}^{(-1)^{y+1}}\right)^a_b \psi_y^{r+b}. \tag{3.14}$$

The chiral symmetry only allows cross couplings $\mathbf{J}^y_{so(r)_1^{\pm}} \cdot \mathbf{J}^{y+1}_{so(r)_1^{\mp}}$ between adjacent wires. Instead of (3.13), another possibility would be its mirror image with summands $\psi_y^a\psi_y^b\psi_{y+1}^{r+a}\psi_{y+1}^{r+b}$. This competes with the original, but as long as mirror symmetry is broken and their strength is asymmetric, an energy gap will open. In the following we will ignore the mirror image by assuming it is weaker.

Next we notice that the four-fermion interaction (3.13) is marginally relevant when velocity $v_{\times}$ is uniform. The dimensionless coupling strength u follows the renormalization group (RG) flow equation

$$\frac{du}{d\lambda} = +4\pi(r-2)u^2 \tag{3.15}$$

when length scale renormalizes by $l \to e^{\lambda} l$. This can be verified by applying the RG formula among marginal operators[95]

$$\frac{dg_l}{d\lambda} = -2\pi \sum_{mn} C_l^{mn} g_m g_n \tag{3.16}$$

where C_l^{mn} is the fusion coefficient of the OPE $\mathcal{O}_m\mathcal{O}_n = C_l^{mn}\mathcal{O}_l + \dots$ between operators in the perturbative action $\delta S = \int d\tau dx \sum_m g_m \mathcal{O}_m$. In the current case, the fusion coefficient $\mathcal{O}\mathcal{O} = -2(r-2)\mathcal{O} + \dots$ can be evaluated simply by applying the Wick's theorem of fermions, for $\mathcal{O} = -\sum_{y,a,b} \psi_y^{r+a}\psi_y^{r+b}\psi_{y+1}^a\psi_{y+1}^b$. The plus sign in (3.15) shows the interacting strength grows at weak coupling. To show that the backscattering (3.13) indeed opens up a gap, we first focus on a single coupled pair of counter-propagating $so(r)_1$ channels (see figure 3.2).

3.1.1.1 The $O(r)$ Gross-Neveu model

Here we concentrate on a particular set of backscattering terms in (3.13) at say an even y. We relabel $\psi_y^{r+a} = \psi_R^a$ and $\psi_{y+1}^a = \psi_L^a$, for $a = 1, \ldots, r$. The interaction between the y^{th} and $(y+1)^{\text{th}}$ wire is identical to that of the $O(r)$ Gross-Neveu (GN) model[40, 41, 42, 43]

$$\mathcal{H}_{\text{GN}} = -\frac{u}{2}\left(\boldsymbol{\psi}_R \cdot \boldsymbol{\psi}_L\right)^2 \tag{3.17}$$

where the minus sign is from the fermion exchange statistics $\psi_R^a\psi_R^b\psi_L^a\psi_L^b = -\psi_R^a\psi_L^a\psi_R^b\psi_L^b$. This GN model is known to have an excitation energy gap for $r > 2$.

For even $r = 2n > 2$, the Majorana fermions can be paired into Dirac ones and subsequently bosonized (see section 2.1.2), $c_{R/L}^j = (\psi_{R/L}^{2j-1} + i\psi_{R/L}^{2j})/\sqrt{2} \sim e^{i\widetilde{\phi}^j_{R/L}}$, for $j = 1, \ldots, n$. Using

$$\boldsymbol{\psi}_R \cdot \boldsymbol{\psi}_L = \sum_{j=1}^{n} c_R^j (c_L^j)^\dagger + (c_R^j)^\dagger c_L^j \sim \sum_{j=1}^{n} \cos\left(2\Theta^j\right) \tag{3.18}$$

for $2\Theta^j = \widetilde{\phi}_R^j - \widetilde{\phi}_L^j$ (also see (2.27)) are mutually commuting variables, the GN interation (3.17) takes the bosonized form

$$\begin{aligned}\mathcal{H}_{GN} &\sim u\sum_{j=1}^{n}\partial_x\widetilde{\phi}_R^j\partial_x\widetilde{\phi}_L^j - u\sum_{j_1\neq j_2}\sum_{\pm}\cos\left(2\Theta^{j_1} \pm 2\Theta^{j_2}\right)\\ &= u\sum_{j=1}^{n}\partial_x\widetilde{\phi}_R^j\partial_x\widetilde{\phi}_L^j - u\sum_{\boldsymbol{\alpha}\in\Delta}\cos\left(\boldsymbol{\alpha}\cdot 2\boldsymbol{\Theta}\right)\end{aligned} \tag{3.19}$$

where $2\boldsymbol{\Theta} = (2\Theta^1, \ldots, 2\Theta^n)$ and $\boldsymbol{\alpha}$ are roots of $so(2n)$ (see (A.8)). The first term renormalizes the velocity V_{x} in (2.25) as well as the Luttinger parameter. We assume $V_{\mathsf{x}} >> u$ so that the first term can be dropped. The remaining sine-Gordon terms are responsible for gapping out all low energy degrees of freedom. Firstly the angle parameters mutually commute and share simultaneous eigenvalues. The ground state minimizes the energy by uniformly pinning the ground state expectation value (GEV)

$$\left\langle 2\Theta^j(x)\right\rangle = \pi m_\psi^j, \quad m_\psi^j \in \mathbb{Z}. \tag{3.20}$$

We notice in passing that the following subset of sine-Gordon terms

$$\begin{aligned} -u\sum_{I=1}^{n}\cos\left(\boldsymbol{\alpha}_I\cdot 2\boldsymbol{\Theta}\right) &= -u\sum_{I=1}^{n}\cos\left[\sum_{J=1}^{n}K_{IJ}(\phi_R^J-\phi_L^J)\right] \\ &= -u\sum_{I=1}^{n}\cos\left(\mathbf{n}_I^T\mathbb{K}\boldsymbol{\Phi}\right) \end{aligned} \tag{3.21}$$

using the simple roots $\boldsymbol{\alpha}_I$ in (A.9), is already enough to remove all low energy degrees of freedom. Here K_{IJ} is the Cartan matrix (A.12) of $so(2n)$ that appears in the Lagrangian density

$$\mathcal{L}_0 = \frac{1}{2\pi}\partial_x\boldsymbol{\Phi}^T\mathbb{K}\partial_t\boldsymbol{\Phi} \tag{3.22}$$

for $\mathbb{K} = K\oplus(-K)$ and $\boldsymbol{\Phi} = (\boldsymbol{\phi}_R, \boldsymbol{\phi}_L)$, and ϕ is related to $\widetilde{\phi}$ by the basis transformation (B.13). For instance, the n vector coefficients $\mathbf{n}_J = (\mathbf{e}_J, \mathbf{e}_J)$ in (3.21) form a null basis

$$\mathbf{n}_I^T\mathbb{K}\mathbf{n}_J = 0 \tag{3.23}$$

and guarantee an energy gap according to Ref.[96]. The remaining GN terms in (3.19) are compatible with (3.21) as they share the same minima.

There are constraints on the GEV m_ψ^j in (3.20). In order to minimize $-\cos(\boldsymbol{\alpha}\cdot 2\boldsymbol{\Theta})$ in (3.19), $\langle\boldsymbol{\alpha}\cdot 2\boldsymbol{\Theta}\rangle$ must be an integer multiple of 2π. This restricts uniform parity among m_ψ^j so that the sign in the fermion backscattering amplitude

$$\begin{aligned} \langle\psi_R^a(x)\psi_L^a(x)\rangle &= \left\langle c_R^j(x)c_L^j(x)^\dagger\right\rangle \\ &\sim \left\langle e^{i2\Theta^j(x)}\right\rangle = (-1)^{m_\psi}. \end{aligned} \tag{3.24}$$

does not depend on fermion flavor j. This is not the only non-zero GEV as ψ is not the only primary field in $so(2n)_1$. The backscattering of spinor fields $V_{s_\pm} = e^{i\boldsymbol{\varepsilon}\cdot\tilde{\boldsymbol{\phi}}/2}$ (B.24) corresponds to the two GEV's

$$\left\langle V^R_{s_\pm}(x) V^L_{s_\pm}(x)^\dagger \right\rangle = \left\langle e^{i\boldsymbol{\varepsilon}\cdot\boldsymbol{\Theta}(x)} \right\rangle = e^{i\pi m_{s_\pm}/2} \tag{3.25}$$

where $\boldsymbol{\varepsilon} = (\varepsilon_1, \ldots, \varepsilon_n)$ for $\varepsilon_j = \pm 1$, and the overall sign $\prod_j \varepsilon_j$ is positive for the even spinor field s_+, or negative for s_-. Here the GEV (3.25) does not depend on the choice of $\boldsymbol{\varepsilon}$. This is because given $\boldsymbol{\varepsilon}$ and $\boldsymbol{\varepsilon}'$ with the same overall parity $\prod \varepsilon_j = \prod \varepsilon'_j$, $\boldsymbol{\varepsilon}\cdot\boldsymbol{\Theta}$ and $\boldsymbol{\varepsilon}'\cdot\boldsymbol{\Theta}$ differ by some combination of $\boldsymbol{\alpha}\cdot 2\boldsymbol{\Theta}$, which takes expectation value in $2\pi\mathbb{Z}$.

There are extra constraints between m_ψ and $m_{s_\pm}$ from the fusion rules of the primary fields of $so(2n)_1$ (see (B.25) and (B.26)). Firstly, $s_\pm \times \psi = s_\mp$ requires

$$m_{s_+} \equiv m_{s_-} + 2m_\psi \mod 4\mathbb{Z}. \tag{3.26}$$

Take the highest weights $\boldsymbol{\varepsilon}^0_+ = (1, \ldots, 1)$ and $\boldsymbol{\varepsilon}^0_- = (1, \ldots, -1)$ for instance. $\boldsymbol{\varepsilon}^0_+ \cdot \boldsymbol{\Theta} = \boldsymbol{\varepsilon}^0_- \cdot \boldsymbol{\Theta} + 2\Theta^n$ imples $m_{s_+}(\boldsymbol{\varepsilon}^0_+) = m_{s_-}(\boldsymbol{\varepsilon}^0_+) + 2m^n_\psi$. Lastly the fusion rules

$$s_\pm \times s_\pm \begin{cases} 1, & \text{for } n \text{ even} \\ \psi, & \text{for } n \text{ odd} \end{cases} \tag{3.27}$$

requires the GEV's to obey

$$\begin{cases} (-1)^{m_{s_\pm}} = 1 & \text{for } n \text{ even} \\ (-1)^{m_{s_\pm}} = (-1)^{m_\psi} & \text{for } n \text{ odd} \end{cases} \tag{3.28}$$

for similar reasons.

The GN model therefore has four ground states when $r = 2n > 2$. They are specified by the quantum numbers (i) $m_{s_+} = 0, 1, 2, 3$ modulo 4 when n is odd, or (ii) $m_{s_+} = 0, 2$ and $m_{s_-} = 0, 2$ modulo 4 when n is even. The rest are fixed by (3.26) and (3.28). Quasiparticle excitations are trapped between domain walls or kinks separating distinct ground states[42, 43, 97]. For example, the vertex operator $V^R_{s_+}(x_0) = e^{i\boldsymbol{\varepsilon}^0_+ \cdot \widetilde{\boldsymbol{\phi}}_R(x_0)/2}$ of an even spinor field creates a jump in the GEV (3.24)

$$\left\langle V^R_{s_+}(x_0)^\dagger e^{i2\Theta^j(x)} V^R_{s_+}(x_0) \right\rangle = (-1)^{m'_\psi + \theta(x_0 - x)} \tag{3.29}$$

because of the Baker-Hausdorff-Campbell formula and the commutation relation from (2.20)

$$\left[2\Theta^j(x), \boldsymbol{\varepsilon}^0_+ \cdot \widetilde{\boldsymbol{\phi}}_R(x_0)/2 \right] = i\pi \left(\theta(x_0 - x) - n + j - 1 \right) \tag{3.30}$$

for θ the unit step function $\theta(s) = 0$ when $s \leq 0$, or 1 when $s > 0$, and $m'_\psi = m_\psi + n - j + 1$. In general, the primary fields $V^R_{s_\pm} = e^{i\boldsymbol{\varepsilon} \cdot \widetilde{\boldsymbol{\phi}}_R}$ and $c^j_R = e^{i\widetilde{\phi}^j_R}$ corresponds to the domain walls of $m_{s_\pm}$:

$$\begin{aligned} \left\langle V^R_{s_\pm}(x_0)^\dagger e^{i\boldsymbol{\varepsilon}^0_\pm \cdot \boldsymbol{\Theta}(x)} V^R_{s_\pm}(x_0) \right\rangle &= e^{\frac{i\pi}{2}\left(m'_{s_\pm} + n\theta(x_0 - x)\right)} \\ \left\langle V^R_{s_\mp}(x_0)^\dagger e^{i\boldsymbol{\varepsilon}^0_\pm \cdot \boldsymbol{\Theta}(x)} V^R_{s_\mp}(x_0) \right\rangle &= e^{\frac{i\pi}{2}\left(m'_{s_\pm} + (n-2)\theta(x_0 - x)\right)} \\ \left\langle c^j_R(x_0)^\dagger e^{i\boldsymbol{\varepsilon}^0_\pm \cdot \boldsymbol{\Theta}(x)} c^j_R(x_0) \right\rangle &= e^{\frac{i\pi}{2}\left(m'_{s_\pm} + 2\theta(x_0 - x)\right)}. \end{aligned} \tag{3.31}$$

Now we move on to the odd $r = 2n + 1 > 1$ case. First we pair the first $2n$ Majorana fermions into n Dirac ones and bosonize them similar to the previous even r case. This leaves a single unpaired Majorana fermion $\psi^r_{R/L}$. Dropping terms that only renormalizes velocities, the GN model (3.17) takes the partially bosonized form

$$\begin{aligned}\mathcal{H}_{\text{GN}} \sim -u &\sum_{\boldsymbol{\alpha}\in\Delta_{so(2n)}} \cos\left(\boldsymbol{\alpha}\cdot 2\boldsymbol{\Theta}\right) \\ &- u\left[\sum_{j=1}^{n}\cos\left(2\Theta^{j}\right)\right] i\psi_R^r\psi_L^r \end{aligned} \tag{3.32}$$

where the first line is identical to the even r case (3.32) and is responsible for gapping out first $2n$ Majorana channels. Projecting onto the lowest energy states and taking the GEV $\langle\cos(2\Theta^j)\rangle = (-1)^{m_\psi}$, the interacting Hamiltonian becomes

$$\mathcal{H}_{\text{GN}} \sim -2n(n-1)u - nu(-1)^{m_\psi} i\psi_R^r\psi_L^r \tag{3.33}$$

which is identical to the continuum limit of the quantum Ising model with transverse field after a Jordan-Wigner transformation. The remaining Majorana channel $\psi_{R/L}^r$ is gapped by the single-body backscattering term. The sign of the mass gap $nu(-1)^{m_\psi}$ determines the phase of the Ising model. We take the convention so that a negative (or positive) mass with $m_\psi \equiv 1$ (resp. $m_\psi \equiv 0$) corresponds to the order (resp. disorder) phase.

Like the previous case, the fermion backscattering amplitude (3.24) is not the only ground state expectation value. From (C.5) appendix C, the Ising twist field of $so(2n+1)_1$ can be written as the product $V_\sigma = e^{i\boldsymbol{\varepsilon}\cdot\widetilde{\boldsymbol{\phi}}/2}\sigma^r$, where $\boldsymbol{\varepsilon} = (\varepsilon_1,\ldots,\varepsilon_n)$ for $\varepsilon_j = \pm 1$, and $\sigma_{R/L}^r = \sigma_{R/L}^{2n+1}$ is the twist field along the last Majorana channel. There are three possible GEV for the backscattering

$$\begin{aligned}\left\langle V_\sigma^R(x)V_\sigma^L(x)^\dagger\right\rangle &= \left\langle e^{i\boldsymbol{\varepsilon}\cdot\boldsymbol{\Theta}(x)}\sigma_R^r(x)\sigma_L^r(x)\right\rangle \\ &\sim \begin{cases} 0 & \text{for the disorder phase} \\ \pm 1 & \text{for the order phase}\end{cases}.\end{aligned} \tag{3.34}$$

Here we choose the convention so that $\sigma_R\sigma_L$ takes the role of the spin operator $\boldsymbol{\sigma}$ in the Ising model and its non-trivial GEV's in the order phase specify two ground states $|\uparrow\rangle$ and $|\downarrow\rangle$.

Again, quasiparticle excitations are trapped between domain walls separating distinct ground states[42, 43, 97]. For example a twist field V^R_σ (or V^L_σ) sits between the order to disorder phase boundary where the quantum number m_ψ flips from 1 to 0, or equivalently the fermion mass gap in (3.33) changes sign. This is because the twist field $V^R_\sigma(x_0)$ introduces a flip in boundary condition $\psi_R(x_0+) = -\psi_R(x_0-)$ and corresponds to a change of sign in front of the fermion backscattering $i\psi_R\psi_L$. Alternatively, this can also be understood by identifying V_σ as a Jackiw-Rebbi soliton[98] or a zero energy Majorana bound state between a trivial and topological superconductor[5] in 1D.

Next a $\uparrow - \downarrow$ domain wall of opposite signs of the GEV (3.34) in the order phase traps an excitation in the fermion sector ψ. This can be seen by equating the order Ising phase to a 1D topological superconductor[5], where the two Ising ground states corresponds to the even and odd fermion parity states among the pair of boundary Majorana zero modes. Adding (or subtracting) a fermion therefore flips the parity as well as the GEV in (3.34). We notice this domain wall interpretation of excitations is consistent with the non-Abelian fusion rule

$$\sigma \times \sigma = 1 + \psi. \tag{3.35}$$

The trivial fusion channel corresponds to the annihilation of a domain wall pair such as

$$|\underbrace{\ldots\uparrow\uparrow}_{\text{order}}\underbrace{\leftarrow\leftarrow}_{\text{disorder}}\underbrace{\uparrow\uparrow\ldots}_{\text{order}}\rangle \xrightarrow{\text{fusion}} |\ldots\uparrow\uparrow\ldots\rangle \tag{3.36}$$

while the fermion fusion channel corresponds to joining the pair of "order - disorder" domain walls into a kink

$$|\underbrace{\ldots\uparrow\uparrow}_{\text{order}}\underbrace{\leftarrow\leftarrow}_{\text{disorder}}\underbrace{\downarrow\downarrow\ldots}_{\text{order}}\rangle \xrightarrow{\text{fusion}} |\ldots\uparrow\uparrow\downarrow\downarrow\ldots\rangle. \tag{3.37}$$

3.1.1.2 The special case: $so(4)_1 = su(2)_1 \times su(2)_1$

The case when $r = 2$ requires special attention. The $O(2)$ GN model (3.17) is a gapless Luttinger liquid because its bosonized form (3.19) contains no sine-Gordon terms and the rest only renormalizes velocities and the Luttinger parameter. As a result the fractionalization (or conformal embedding) $so(4)_1 \supseteq so(2)_1 \times so(2)_1$ of wires with $N = 4$ Majorana channels does not lead to a gapped theory. Instead we turn to an alternative fractionalization $so(4)_1 = su(2)_1^+ \times su(2)_1^-$ that only applies for $N = 4$.

The four Majorana ψ_y^a along each wire can be paired into Dirac channels $c_y^1 = (\psi_y^1 + i\psi_y^2)/\sqrt{2} = e^{i\widetilde{\phi}_y^1}$ and $c_y^2 = (\psi_y^3 + i\psi_y^4)/\sqrt{2} = e^{i\widetilde{\phi}_y^2}$. It would be more convenient if we express the bosons in the new basis using the simple roots of $so(4)$: $\widetilde{\phi}^1 = \phi^1 - \phi^2$ and $\widetilde{\phi}^2 = \phi^1 + \phi^2$. Unlike when $r > 2$, these bosons decouple in the Lagrangian density (2.22)

$$\mathcal{L}_0 = \frac{1}{2\pi}\sum_{y=-\infty}^{\infty}(-1)^y\sum_{J=1}^{2} 2\partial_x\phi_y^J\partial_t\phi_y^J. \tag{3.38}$$

This is equivalent to the fact that the Cartan matrix $K_{so(4)} = \mathrm{diag}(2,2)$ is diagonal so that the Lie algebra splits into the product $su(2)^+ \times su(2)^-$ of isoclinic rotations, each with Cartan matrix $K_{su(2)} = 2$.

The $su(2)_1$ current generators are given by $S_{\mathsf{z}}^I(z) = i\sqrt{2}\partial\phi^I(z)$ and $S_\pm^I(z) = (S_{\mathsf{x}}^I \pm iS_{\mathsf{y}}^I)/\sqrt{2} = e^{i2\phi^I(z)}$, and they satisfy the OPE

$$S_{\mathsf{i}}^I(z)S_{\mathsf{j}}^I(w) = \frac{\delta_{\mathsf{ij}}}{(z-w)^2} + \frac{i\sqrt{2}\varepsilon_{\mathsf{ijk}}}{z-w}S_{\mathsf{k}}^I(w) + \ldots \tag{3.39}$$

for $I = 1, 2 = +, -$. The $su(2)_1^+$ sector is completely decoupled from the $su(2)_1^-$ one as the OPE $S^1_{\mathsf{i}}(z)S^2_{\mathsf{j}}(w)$ is non-singular. They completely decomposes all low energy degrees of freedom as the energy momentum tensor splits into

$$\begin{aligned} T_{so(4)_1} &= -\frac{1}{2}\sum_{j=1}^{2}\partial\widetilde{\phi}^j(z)\partial\widetilde{\phi}^j(z) \\ &= -\sum_{J=1}^{2}\partial\phi^J(z)\partial\phi^J(z) = T_{su(2)_1^+} + T_{su(2)_1^-}. \end{aligned} \tag{3.40}$$

The gapping Hamiltonian is

$$\begin{aligned} \mathcal{H}_{\text{int}} &= u\sum_{y=-\infty}^{\infty}\mathbf{S}^2_y\cdot\mathbf{S}^1_{y+1} \\ &= 2u\sum_{y=-\infty}^{\infty}\partial_x\phi^2_y\partial_x\phi^1_{y+1} - 2\cos\left(4\Theta_{y+1/2}\right), \end{aligned} \tag{3.41}$$

$$\begin{aligned} 4\Theta_{y+1/2} &= 2\phi^1_{y+1} - 2\phi^2_y \\ &= \widetilde{\phi}^1_{y+1} + \widetilde{\phi}^2_{y+1} + \widetilde{\phi}^1_y - \widetilde{\phi}^2_y. \end{aligned} \tag{3.42}$$

The first kinetic term of the interacting Hamiltonian only renormalizes velocities and the Luttinger parameter. The second sine-Gordon term involves four-fermion interactions and is responsible for the energy gap as it back-scatters the $su(2)_1^-$ sector on the y^{th} wire to the $su(2)_1^+$ sector on the $(y+1)^{\text{th}}$ one. It pins the ground state expectation value (GEV)

$$\left\langle e^{i2\Theta_{y+1/2}(x)}\right\rangle = (-1)^{m_s} \tag{3.43}$$

which characterizes the two distinct ground states. Like the previous cases, quasiparticle excitations are kinks in the GEV. The fundamental excitation can be created by the vertex operator $V_s = e^{i\phi^1_{y+1}}$, which is the semionic primary field in the $su(2)_1^+$ sector along the $(y+1)^{\text{th}}$ wire.

3.1.2 Gapping odd Majorana cones

We now move on to the case when there are $N = 2r + 1 \geq 3$ chiral Majorana channels on each wire in the coupled Majorana wire model (2.4) (of figure 2.2). It corresponds to an odd number of Majorana cones on the surface of a 3D topological superconductor. The chiral degrees of freedom along each wire are described by a $so(N)_1$ WZW theory, which is going to be fractionalized into the pair $\mathcal{G}_N^+ \times \mathcal{G}_N^-$ according to (3.5). The $\mathcal{G}_N^-$ sector along the y^{th} wire will then be back-scattered onto the $\mathcal{G}_N^+$ sector along the $(y+1)^{\text{th}}$ one by the current-current interaction (3.8), which will introduce an energy gap.

Unlike the even N case where $so(N)_1$ can simply be split into a pair of $so(N/2)_1$'s, here the decomposition is less trivial but leads to more exotic surface topological order. We begin with the particular case where 9 Majorana channels can be bipartite into

$$so(9)_1 \supseteq so(3)_3 \times so(3)_3 \tag{3.44}$$

essentially by noticing that the tensor product $SO(3) \otimes SO(3)$ sits inside $SO(9)$. The two $so(3)_3$ WZW sectors carry decoupled current generators. They can then be back-scattered using the current-current interaction (3.8) onto adjacent wires in opposite directions (also see figure 2.2 and 3.2).

For a general odd $N \geq 9$, one can decompose the Majorana channels into $N = 9 + (N-9)$. The first 9 channels can be fractionalized by (3.44), which we will discuss in detail below, and the remaining even number of channels can be split using the previous method, namely $so(N-9)_1 = so\left(\frac{N-9}{2}\right)_1 \times so\left(\frac{N-9}{2}\right)_1$. In the case when N is smaller than 9, one can add $9 - N$ number of *non-chiral* Majorana channels to each wire. These additional degrees of freedom can be interpreted as surface reconstruction as they do not violate fermion doubling[70] and are not required to live on the boundary of a topological bulk. Now each wire consists of 9 right (or left) propagating Majorana channels and $9-N$ left (resp. right) propagating ones. We still refer the remaining even channels by $so(N-9)_1$ except now the negative $N-9$ signals the reverse propagating direction of these Majorana's.

The $so(9)_1$ and $so(N-9)_1$ sectors can then be bipartitioned independently. The fractionalization of a general odd number of Majorana channels is summarized by the sequence

$$so(N)_1 \supseteq so(9)_1 \times so(N-9)_1 \supseteq \mathcal{G}_N^+ \times \mathcal{G}_N^- \tag{3.45}$$

for $\mathcal{G}_N^\pm = so(3)_3 \times so\left(\frac{N-9}{2}\right)_1$. The "+" and "−" sectors can now be back-scattered independently using (3.8) onto adjacent wires in opposite directions. This removes all low energy degrees of freedom and opens up an energy gap.

3.1.2.1 The conformal embedding $so(9)_1 \supseteq so(3)_3^+ \times so(3)_3^-$

As a matrix Lie algebra, $so(3)$ is generated by the three anti-symmetric matrices $\mathbf{\Sigma} = (\Sigma_\mathsf{x}, \Sigma_\mathsf{y}, \Sigma_\mathsf{z})$

$$\Sigma_\mathsf{x} = \begin{pmatrix} 0 & 0 & 0 \\ 0 & 0 & 1 \\ 0 & -1 & 0 \end{pmatrix}, \quad \Sigma_\mathsf{y} = \begin{pmatrix} 0 & 0 & 1 \\ 0 & 0 & 0 \\ -1 & 0 & 0 \end{pmatrix}, \quad \Sigma_\mathsf{z} = \begin{pmatrix} 0 & 1 & 0 \\ -1 & 0 & 0 \\ 0 & 0 & 0 \end{pmatrix}.$$

They can be embedded into $so(9)$ by tensoring with $\mathbb{1}_3$, the 3×3 identity matrix, on the left or right

$$\mathbf{\Sigma}^+ = \mathbf{\Sigma} \otimes \mathbb{1}_3, \quad \mathbf{\Sigma}^- = \mathbb{1}_3 \otimes \mathbf{\Sigma}. \tag{3.46}$$

We denote $so(3)^\pm = \mathrm{span}\{\Sigma_\mathsf{x}^\pm, \Sigma_\mathsf{y}^\pm, \Sigma_\mathsf{z}^\pm\}$ to be the two mutually commuting subalgebras in $so(9)$.

Recall the free field representation (2.9) of the $so(9)_1$ WZW current generators $J^\beta = i\psi^a t^\beta_{ab}\psi^b/2$ for t^β an antisymmetric 9×9 matrix, the $so(3)_3^\pm$ current generators are given by the substitution of t^β:

$$\mathbf{J}_{so(3)_3^\pm}(z) = \frac{i}{2}\psi^a(z)\mathbf{\Sigma}^\pm_{ab}\psi^b(z) \tag{3.47}$$

for $z = e^{\tau+ix}$ and $\mathbf{J} = (J_\mathsf{x}, J_\mathsf{y}, J_\mathsf{z})$. Written explicitly,

$$\begin{aligned}
J^+_\mathsf{x} &= i(\psi^{23}+\psi^{56}+\psi^{89}), \quad & J^-_\mathsf{x} &= i(\psi^{47}+\psi^{58}+\psi^{69}) \\
J^+_\mathsf{y} &= i(\psi^{13}+\psi^{46}+\psi^{79}), \quad & J^-_\mathsf{y} &= i(\psi^{17}+\psi^{28}+\psi^{39}) \\
J^+_\mathsf{z} &= i(\psi^{12}+\psi^{45}+\psi^{78}), \quad & J^-_\mathsf{z} &= i(\psi^{14}+\psi^{25}+\psi^{36})
\end{aligned}$$

for $\psi^{ab} = \psi^a\psi^b$. Using Wick's theorem and the OPE $\psi^a(z)\psi^b(w) = \delta^{ab}/(z-w)+\ldots$, it is straightforward to deduce the $so(3)_3$ WZW current relations

$$J^\pm_\mathsf{i}(z)J^\pm_\mathsf{j}(w) = \frac{3\delta_\mathsf{ij}}{(z-w)^2} + \frac{i\varepsilon_\mathsf{ijk}}{z-w}J^\pm_\mathsf{k}(w)+\ldots \tag{3.48}$$

and $J^\pm_\mathsf{i}(z)J^\mp_\mathsf{j}(w)$ is non-singular, for $\mathsf{i},\mathsf{j} = \mathsf{x},\mathsf{y},\mathsf{z}$ and ε_ijk the antisymmetric tensor.

The $so(3)_3$ current relations (3.48) differs from the $so(3)_1$ ones (2.11) by the coefficient 3 of the most singular term. This sets the level of the affine Lie algebra. The $so(3)_3$ WZW theory is identical to $su(2)_6$ by noticing that the structure factor of $su(2)$ is $f_\mathsf{ijk} = \sqrt{2}\varepsilon_\mathsf{ijk}$ (see (3.39) and Ref.[26]). The $su(2)$ current generators thus need to be normalized by $\mathbf{S}_{su(2)_6^\pm} = \sqrt{2}\mathbf{J}_{so(3)_3^\pm}$ so that

$$S^\pm_\mathsf{i}(z)S^\pm_\mathsf{j}(w) = \frac{6\delta_\mathsf{ij}}{(z-w)^2} + \frac{i\sqrt{2}\varepsilon_\mathsf{ijk}}{z-w}S^\pm_\mathsf{k}(w)+\ldots \tag{3.49}$$

where the coefficient 6 of the most singular term sets the level of the $su(2)_6$ affine Lie algebra.

The Sugawara energy momentum tensors are the normal ordered product

$$T_{so(3)_3^\pm}(z) = \frac{1}{8}\mathbf{J}_{so(3)_3^\pm}(z) \cdot \mathbf{J}_{so(3)_3^\pm}(z). \tag{3.50}$$

Written explicitly in the fermion representation (3.47) and using the normal ordered product

$$\psi^a(z)\psi^b(z)\psi^a(z)\psi^b(z) = \psi^a(z)\partial\psi^a(z) + \psi^b(z)\partial\psi^b(z) \tag{3.51}$$

the energy momentum tensor takes the form

$$T_{so(3)_3^\pm}(z) = -\frac{1}{4}\sum_{a=1}^{9}\psi^a(z)\partial\psi^a(z) \mp \frac{1}{4}\mathcal{O}_\psi(z) \tag{3.52}$$

$$\begin{aligned}\mathcal{O}_\psi(z) &= \psi^{1245} + \psi^{1278} + \psi^{4578} + \psi^{1346} + \psi^{1379} \\ &\quad + \psi^{4679} + \psi^{2356} + \psi^{2389} + \psi^{5689}\end{aligned} \tag{3.53}$$

for $\psi^{abcd} = \psi^a(z)\psi^b(z)\psi^c(z)\psi^d(z)$. The four-fermion terms in $\mathcal{O}_\psi$ cancel when combining the "$\pm$" sectors, and therefore the energy momentum tensor (2.12) completely decomposes

$$T_{so(9)_1} = -\frac{1}{2}\sum_{a=1}^{9}\psi^a\partial\psi^a = T_{so(3)_3^+} + T_{so(3)_3^-}. \tag{3.54}$$

Moreover, as the OPE between $\mathbf{J}_{so(3)_3^+}$ and $\mathbf{J}_{so(3)_3^-}$ is non-singular, so is the OPE between $T_{so(3)_3^+}$ and $T_{so(3)_3^-}$. Each sector carries half the total central charge of 9 Majorana channels

$$c_{so(3)_3^\pm} = 9/4. \tag{3.55}$$

The primary fields of $so(3)_3 = su(2)_6$ are characterized by half-integral "angular momenta" $s = 0, 1/2, \ldots, 3$.[26] Each primary field $\mathbf{V}_s = (V_s^{-s}, V_s^{-s+1}, \ldots, V_s^s)$ irreducibly represents the WZW algebra

$$S_{\mathsf{i}}(z)V_s^m(w) = \frac{1}{z-w}\sum_{m'=-s}^{s} (S_{\mathsf{i}}^s)^m_{m'}\, V_s^{m'}(w) + \ldots \tag{3.56}$$

for $\mathsf{i} = \mathsf{x}, \mathsf{y}, \mathsf{z}$ and S_{i}^s the $su(2)$ generators in the spin-s matrix representation. We label the seven primary fields by greek letters $\mathbf{V}_s = 1, \alpha_\pm, \gamma_\pm, \beta, f$, each has conformal dimension $h_s = s(s+1)/8$ (see table 3.1). In particular $1 = \mathbf{V}_0$ is the vacuum and $f = \mathbf{V}_3$ is Abelian and fermionic with spin 3/2.

$\mathbf{V}_s$	1	α_+	γ_+	β	γ_-	α_-	f
s	0	1/2	1	3/2	2	5/2	3
h_s	0	3/32	1/4	15/32	3/4	35/32	3/2
d_s	1	$\sqrt{2+\sqrt{2}}$	$1+\sqrt{2}$	$\sqrt{4+2\sqrt{2}}$	$1+\sqrt{2}$	$\sqrt{2+\sqrt{2}}$	1

Table 3.1: The "angular momenta" s, conformal dimensions h_s and quantum dimensions d_s of primary fields $\mathbf{V}_s$ of $so(3)_3 = su(2)_6$.

The rest of the primary fields are non-Abelian. They obey multi-channel fusion rules

$$\mathbf{V}_{s_1} \times \mathbf{V}_{s_2} = \sum_s N^s_{s_1 s_2}\mathbf{V}_s \tag{3.57}$$

where the fusion matrix element $N^s_{s_1 s_2} = 0, 1$ is determined by the Verlinde formula[99]

$$N^s_{s_1 s_2} = \sum_{s'} \frac{\mathcal{S}_{s_1 s'}\mathcal{S}_{s_2 s'}\mathcal{S}_{s s'}}{\mathcal{S}_{0 s'}} \tag{3.58}$$

and the modular S-matrix[26]

$$\mathcal{S}_{s_1 s_2} = \frac{1}{2}\sin\left[\frac{\pi(2s_1+1)(2s_2+1)}{8}\right] \tag{3.59}$$

which is symmetric and orthogonal. Explicitly, the fusion rules are given by

$$\begin{gathered} f\times f=1,\quad f\times\gamma_\pm=\gamma_\mp,\quad f\times\alpha_\pm=\alpha_\mp,\quad f\times\beta=\beta \\ \gamma_\pm\times\gamma_\pm=1+\gamma_++\gamma_-,\quad \alpha_\pm\times\alpha_\pm=1+\gamma_+ \\ \beta\times\beta=1+\gamma_++\gamma_-+f \\ \alpha_\pm\times\gamma_\pm=\alpha_++\beta,\quad \beta\times\gamma_\pm=\alpha_++\alpha_-+\beta \\ \alpha_\pm\times\beta=\gamma_++\gamma_- \end{gathered} \tag{3.60}$$

The quantum dimension d_s of the primary field $\mathbf{V}_s$ is defined to be the largest eigenvalue of the fusion matrix $N_s = \left(N_{ss_1}^{s_2}\right)$. It coincides with the modular S matrix element $\mathcal{S}_{0s}/\mathcal{S}_{00}$ and respects fusion rules so that

$$d_{s_1}d_{s_2}=\sum_s N_{s_1s_2}^s d_s. \tag{3.61}$$

They are listed in table 3.1.

3.1.2.2 $\mathbb{Z}_6$ parafermions

We first study the simplest odd case when there are 9 Majorana cones mimicked by the coupled Majorana wire model (2.4) with 9 chiral Majorana channels per wire. Now that we have bipartite the degrees of freedom according to the two $so(3)_3^\pm$ WZW current algebras in (3.47), they can be backscattered independently to adjacent wires in opposite directions (see eq.(3.8) and figure 2.2). As the $so(3)_3^+$ sector completely decomposes from the $so(3)_3^-$ one, the current backscattering $\mathbf{J}^{y-1}_{so(3)_3^-}\cdot\mathbf{J}^y_{so(3)_3^+}$ between the $(y-1)^{\mathrm{th}}$ and y^{th} wire does not compete with the next pair $\mathbf{J}^y_{so(3)_3^-}\cdot\mathbf{J}^{y+1}_{so(3)_3^+}$.

The current-current interaction consists of four-fermion terms and is marginally relevant. This can be seen from the RG equation (3.16) using the operator product expansion $(\mathbf{J}^y\cdot\mathbf{J}^{y+1})^2\sim+\mathbf{J}^y\cdot\mathbf{J}^{y+1}$. (Recall the time reversal symmetric convention

(3.11) and that $\mathbf{J}^y\mathbf{J}^y \sim i(-1)^y\mathbf{J}^y$.) To see that the interaction indeed opens up an excitation energy gap, it suffices to focus on a single pair of wires with the Hamiltonian

$$\mathcal{H}_{\text{int}} = u\mathbf{J}^R_{so(3)^-_3} \cdot \mathbf{J}^L_{so(3)^+_3} \tag{3.62}$$

where R/L labels the counter-propagating directions along wire y and $y+1$.

First we further decompose the $so(3)_3$ WZW theory by the coset construction[26]

$$so(3)_3 = u(1)_6 \times \text{“}\mathbb{Z}_6\text{”}, \quad \text{“}\mathbb{Z}_6\text{”} = \frac{so(3)_3}{so(2)_3} = \frac{su(2)_6}{u(1)_6} \tag{3.63}$$

where “$\mathbb{Z}_6$” refers to the $\mathbb{Z}_6$ parafermion CFT model by Zamolodchikov and Fateev[44, 45]. This is done by noticing that $SO(3)$ (or equivalently $SU(2)$) contains the Abelian subgroup $SO(2)$ (resp. $U(1)$) of rotations about the z-axis, and on the CFT level, the $so(2)_3$ WZW sub-theory of $so(3)_3$ (resp. $u(1)_6 \subseteq su(2)_6$) can be bosonized and single-out. To do this we first group three pairs of Majorana fermions into three Dirac fermions on each chiral sector

$$\begin{aligned}
c^1_R &= \frac{\psi^1_R + i\psi^4_R}{\sqrt{2}}, & c^2_R &= \frac{\psi^2_R + i\psi^5_R}{\sqrt{2}}, & c^3_R &= \frac{\psi^3_R + i\psi^6_R}{\sqrt{2}} \\
c^1_L &= \frac{\psi^1_L + i\psi^2_L}{\sqrt{2}}, & c^2_L &= \frac{\psi^4_R + i\psi^5_L}{\sqrt{2}}, & c^3_L &= \frac{\psi^7_L + i\psi^8_L}{\sqrt{2}}
\end{aligned}$$

and bosonize

$$c^j_{R/L} \sim \frac{1}{\sqrt{l_0}} \exp\left(i\widetilde{\phi}^j_{R/L}\right) \tag{3.64}$$

for $j = 1, 2, 3$. The $so(2)_3$ subalgebra in the R and L sectors are generated by the J^-_{z} and J^+_{z} currents operators in (3.47)

$$J^R_{\mathsf{z}} = -3i\partial\phi^\rho_R, \quad J^L_{\mathsf{z}} = 3i\partial\phi^\rho_L \tag{3.65}$$

where the boson field of the "charge" sector is the average

$$\phi^{\rho}_{R/L} = \frac{\widetilde{\phi}^1_{R/L} + \widetilde{\phi}^2_{R/L} + \widetilde{\phi}^3_{R/L}}{3}. \tag{3.66}$$

The "neutral" sector is carried by the three boson fields

$$\phi^{\sigma,j}_{R/L} = \widetilde{\phi}^j_{R/L} - \phi^{\rho}_{R/L} \tag{3.67}$$

which are not independent as $\phi^{\sigma,1} + \phi^{\sigma,2} + \phi^{\sigma,3} = 0$.

It is straightforward to check that the "charge" and the "neutral" sectors completely decouple from each other. For instance, the Lagrangian density decomposes

$$\begin{aligned}\mathcal{L}_{R/L} &= \frac{(-1)^{R/L}}{2\pi}\sum_{j=1}^{3}\partial_x\widetilde{\phi}^j_{R/L}\partial_t\widetilde{\phi}^j_{R/L} \\ &= \frac{(-1)^{R/L}}{2\pi}\left[3\partial_x\phi^{\rho}_{R/L}\partial_t\phi^{\rho}_{R/L} + \sum_{j=1}^{3}\partial_x\phi^{\sigma,j}_{R/L}\partial_t\phi^{\sigma,j}_{R/L}\right]\end{aligned} \tag{3.68}$$

where the remaining fermions $\psi^{7,8,9}_R, \psi^{3,6,9}_L$ are suppressed, and $(-1)^R = 1$, $(-1)^L = -1$.

The Lagrangian density (3.68) involves more degrees of freedom in $so(9)^{R/L}_1$ than just $so(3)^{R,-}_3$ or $so(3)^{L,+}_3$. Therefore, a priori, it is not obvious that this $\rho - \sigma$ decomposition is a splitting of $so(3)_3$, and in fact it is not. Only the charge sector $\phi^{\rho}_{R/L}$ is entirely belonging to $so(3)^{R,-}_3$ or $so(3)^{L,+}_3$. To show this, we go back to the energy-momentum tensor $T_{so(3)^{\pm}_3}$ in (3.52), say for R movers.

$$T_{so(3)^{R,\pm}_3}(z) = \frac{1}{2}T_{so(9)^R_1}(z) \mp \frac{1}{4}\mathcal{O}_{\psi}(z) \tag{3.69}$$

where the total energy-momentum tensor in partially bosonized basis is

$$T_{so(9)^R_1} = -\frac{1}{2}\Bigg[3\partial\phi^\rho_R\partial\phi^\rho_R + \sum_{j=1}^{3}\partial\phi^{\sigma,j}_R\partial\phi^{\sigma,j}_R \\ + \psi^7_R\partial\psi^7_R + \psi^8_R\partial\psi^8_R + \psi^9_R\partial\psi^9_R\Bigg] \quad (3.70)$$

and the operator $\mathcal{O}_\psi$ defined in (3.53) is now

$$\mathcal{O}_\psi = -3\partial\phi^\rho_R\partial\phi^\rho_R + \frac{1}{2}\sum_{j=1}^{3}\partial\phi^{\sigma,j}_R\partial\phi^{\sigma,j}_R \quad (3.71) \\ - 2i\left[\cos\left(\phi^{\sigma,1}_R - \phi^{\sigma,2}_R\right)\psi^{78}_R + \cos\left(\phi^{\sigma,1}_R - \phi^{\sigma,3}_R\right)\psi^{97}_R \\ + \cos\left(\phi^{\sigma,2}_R - \phi^{\sigma,3}_R\right)\psi^{89}_R\right].$$

Eq.(3.71) is deduced by substituting the fermions by the boson fields (3.64), whose OPE can be found in (D.1,D.2,D.3) in appendix D. For instance, the factor of i in (3.71) is a result of mutually non-commuting $\phi^{\sigma,j}$. More importantly, ϕ^ρ, ϕ^σ and $\psi^{7,8,9}$ are completely decoupled. As the "charge" sector ϕ^ρ_R only appears in $T_{so(3)^{R,-}_3}$, it belongs entirely in $so(3)^{R,-}_3$. Similarly ϕ^ρ_L belongs entirely in $so(3)^{L,+}_3$. The "$\mathbb{Z}_6$" energy-momentum is defined by subtracting the decoupled "charge" sector from $so(3)_3$.

$$T_{so(2)^R_3} = \frac{1}{6}J_z J_z = -\frac{1}{2}3\partial\phi_\rho\partial\phi_\rho \quad (3.72)$$

$$T^R_{\mathbb{Z}_6} = T_{so(3)^{R,-}_3} - T_{so(2)^R_3} \quad (3.73) \\ = -\frac{1}{4}\sum_{a=7}^{9}\psi^a_R\partial\psi^a_R - \frac{1}{8}\sum_{j=1}^{3}\partial\phi^{\sigma,j}_R\partial\phi^{\sigma,j}_R \\ - \frac{i}{2}\left[\cos\left(\phi^{\sigma,1}_R - \phi^{\sigma,2}_R\right)\psi^{78}_R + \cos\left(\phi^{\sigma,1}_R - \phi^{\sigma,3}_R\right)\psi^{97}_R \\ + \cos\left(\phi^{\sigma,2}_R - \phi^{\sigma,3}_R\right)\psi^{89}_R\right]$$

and similarly for the L movers.

The remaining current operators $J_\pm = (J_\mathsf{x} \pm iJ_\mathsf{y})/\sqrt{2}$ of $so(3)_3^-$ in the R sector and $so(3)_3^+$ in the L sector (see eq.(3.47)) now split into "charge" and "netrual" parafermion components

$$J_\pm^{R/L} = \mp\sqrt{3}e^{\mp i\phi^\rho_{R/L}}\Psi^\mp_{R/L} \tag{3.74}$$

where the $\mathbb{Z}_6$ parafermions are given by the combinations

$$\begin{aligned}\Psi_R &= \frac{1}{\sqrt{3}}\left(e^{i\phi_R^{\sigma,1}}\psi_R^7 + e^{i\phi_R^{\sigma,2}}\psi_R^8 + e^{i\phi_R^{\sigma,3}}\psi_R^9\right)\\ \Psi_L &= \frac{1}{\sqrt{3}}\left(e^{i\phi_L^{\sigma,1}}\psi_L^3 + e^{i\phi_L^{\sigma,2}}\psi_L^6 + e^{i\phi_L^{\sigma,3}}\psi_L^9\right)\end{aligned} \tag{3.75}$$

for $\Psi^+_{R/L} = \Psi_{R/L}$ and $\Psi^-_{R/L} = \Psi^\dagger_{R/L}$. Unlike the ϕ^σ's, here the "neutral" $\mathbb{Z}_6$ parafermions $\Psi_{R/L}$ belongs entirely in $so(3)_3^{R,-}$ or $so(3)_3^{L,+}$. This is because $\mathbf{J}^{R/L}$ and $\phi^\rho_{R/L}$ both completely sit inside the $so(3)_3$'s as seen above. Otherwise one can verified this by computing the OPE with the energy-momentum tensor (3.70) explicitly

$$\begin{aligned}T_{so(3)_3^{R,-}}(z)\Psi_R(w) &= \frac{5/6}{(z-w)^2}\Psi_R(w) + \frac{\partial\Psi_R(w)}{z-w} + \ldots\\ T_{so(3)_3^{R,-}}(z)e^{\pm i\phi_R^\rho(w)} &= \frac{1/6}{(z-w)^2}e^{\pm i\phi_R^\rho(w)} + \frac{\partial e^{\pm i\phi_R^\rho(w)}}{z-w} + \ldots\end{aligned} \tag{3.76}$$

and $T_{so(3)_3^{R,+}}(z)\Psi_R(w)$ and $T_{so(3)_3^{R,+}}(z)e^{\pm i\phi_R^\rho(w)}$ are both non-singular. Similar OPE hold for the L sector. The primary fields (3.75) generate the rest of the $\mathbb{Z}_6$ parafermions (see (D.5) in appendix D) and they obey the known $\mathbb{Z}_6$ structure by Zamolodchikov and Fateev[45].

3.1.2.3 Gapping potential

Now that we have further decomposed the $so(3)_3^\pm$ currents in each wire into $so(2)_3 = U(1)_6$ and $\mathbb{Z}_6$ parafermion components (see eq.(3.74)), the current-current backscattering interaction (3.62) between a pair of wires takes the form of

$$\mathcal{H}_{\text{int}} = 9u\partial_x\phi_R^\rho\partial_x\phi_L^\rho + 3u\left[e^{i(\phi_L^\rho-\phi_R^\rho)}\Psi_R^\dagger\Psi_L + h.c.\right]. \tag{3.77}$$

The first term only renormalizes the velocity of the boson in the $so(2)_3$ sector. The second term is responsible for openning an excitation energy gap. It extracts a $\mathbb{Z}_6$ parafermion Ψ and a quasiparticle $e^{i\phi^\rho}$ from the $so(3)_3^+$ sector on the y^{th} wire and backscatter them onto the $so(3)_3^-$ sector along the $(y+1)^{th}$ wire. This freezes all low energy degrees of freedom and the ground state is characterized by the $\mathbb{Z}_6$ expectation value (GEV)

$$\left\langle\Psi_R^\dagger(x)\Psi_L(x)\right\rangle \sim -e^{i\left\langle\phi_R^\rho(x)-\phi_L^\rho(x)\right\rangle} = e^{2\pi im/6} \tag{3.78}$$

for m an integer.

Like the $O(N)$ Gross-Neveu model we discussed in section 3.1.1.1, quasiparticle excitations here also manifest as kinks or domain walls between segments with different GEV's. The primary fields $\alpha_\pm, \gamma_\pm, \beta$ of the chiral $so(3)_3$ WZW theory in table 3.1 decompose into components in the "$\mathbb{Z}_6$" and $so(2)_3$ sectors.

$$\begin{aligned}\alpha_+ = [\sigma_1]\times[e^{i\phi^\rho/2}], \quad \alpha_- = [\sigma_5]\times[e^{-i\phi^\rho/2}]\\ \gamma_+ = [\sigma_2]\times[e^{i\phi^\rho}], \quad \gamma_- = [\sigma_4]\times[e^{-i\phi^\rho}]\\ \beta = [\sigma_3]\times[e^{i3\phi^\rho/2}]\end{aligned} \tag{3.79}$$

where σ_l are primary fields in the chiral $\mathbb{Z}_6$ parafermion theory so that $\sigma_l^R\sigma_l^L$ take the roles of the order parameters of the $\mathbb{Z}_6$ model[44, 45]. They satisfy the exchange relations

$$\Psi(x)\sigma_l(x') = \sigma_l(x')\Psi(x)e^{-2\pi i\frac{l}{6}\theta(x-x')} \tag{3.80}$$

for R sector, and similar relations hold for the L sector with the $\mathbb{Z}_6$ phases conjugated. Therefore adding the operators $\alpha_\pm(x), \gamma_\pm(x), \beta(x)$ to the ground state create kinks of different hights in the GEV (3.78)

$$\begin{aligned}
\left\langle \alpha_\pm^\dagger(x_0)\Psi_R^\dagger(x)\Psi_L(x)\alpha_\pm(x_0)\right\rangle &\sim e^{\frac{\pi i}{3}(m\pm\theta(x-x_0))} \\
\left\langle \gamma_\pm^\dagger(x_0)\Psi_R^\dagger(x)\Psi_L(x)\gamma_\pm(x_0)\right\rangle &\sim e^{\frac{\pi i}{3}(m\pm 2\theta(x-x_0))} \\
\left\langle \beta^\dagger(x_0)\Psi_R^\dagger(x)\Psi_L(x)\beta(x_0)\right\rangle &\sim e^{\frac{\pi i}{3}(m+3\theta(x-x_0))}
\end{aligned} \tag{3.81}$$

where $\theta(s) = (s/|s|+1)/2$ is the unit step function.

The fermionic supersector f in $so(3)_3$ (see table 3.1) consists of operators that admit free field representations. Again we focus on the the $so(3)_3^{R,-}$ sector. The operators

$$\begin{aligned}
V_f^0 = \Psi^3, \quad V_f^{\pm 1} = e^{\mp i\phi^\rho}\Psi^{\mp 2} \\
V_f^{\pm 2} = e^{\mp 2i\phi^\rho}\Psi^{\mp}, \quad V_f^{\pm 3} = e^{\mp 3i\phi^\rho}
\end{aligned}$$

span a $s=3$ representation of the affine $so(3)_3$ Lie algebra, where $\Psi^{-m} = \Psi^{6-m}$ are the $\mathbb{Z}_6$ parafermions satisfying the OPE $\Psi^m(z)\Psi^{m'}(w) \sim (z-w)^{-mm'/3}\Psi^{m+m'}$ (see appendix D for explicit definitions). From (3.80), they create a kink to the order parameter $\langle b\rangle = \langle \beta_R(x)\beta_L(x)\rangle$

$$\left\langle \mathbf{V}_f^R(x_0)^\dagger \beta_R(x)\beta_L(x)\mathbf{V}_f^R(x_0)\right\rangle = \langle b\rangle(-1)^{\theta(x-x_0)} \tag{3.82}$$

in the order phase.

The gapping potential can now be generalized to an arbitrary odd number of Majorana channels per wire. Using the decomposition (3.45), the N Majorana channels are first split into $9+(N-9)$. The first 9 channels are fractionalized into $so(3)_3^+ \times so(3)_3^-$ while the remaining $N-9$ can be split into $so(\frac{N-9}{2})_1^+ \times so(\frac{N-9}{2})_1^-$ because $N-9$ is even. The interwire current backscattering (3.8) takes the form

$$\mathcal{H}_{\text{int}} = u \sum_{y=-\infty}^{\infty} \mathbf{J}^{y}_{so(3)_3^-} \cdot \mathbf{J}^{y+1}_{so(3)_3^+} + \mathbf{J}^{y}_{so\left(\frac{N-9}{2}\right)_1^-} \cdot \mathbf{J}^{y+1}_{so\left(\frac{N-9}{2}\right)_1^+} \tag{3.83}$$

where different terms act on completely decoupled degrees of freedom. They also gap out *all* low energy degrees freedom as the energy-momentum tensor of the CFT along each wire decomposes

$$\begin{aligned} T_{so(N)_1} &= T_{so(9)_1} + T_{so(N-9)_1} \\ &= T_{so(3)_3^+} + T_{so(3)_3^-} + T_{so\left(\frac{N-9}{2}\right)_1^+} + T_{so\left(\frac{N-9}{2}\right)_1^-} \end{aligned} \tag{3.84}$$

using (3.54) and the fact that

$$T_{so(m+n)_1} = -\frac{1}{2}\sum_{a=1}^{m+n} \psi^a \partial \psi^a = T_{so(m)_1} + T_{so(n)_1}. \tag{3.85}$$

3.1.3 Gapping by fractional quantum Hall stripes

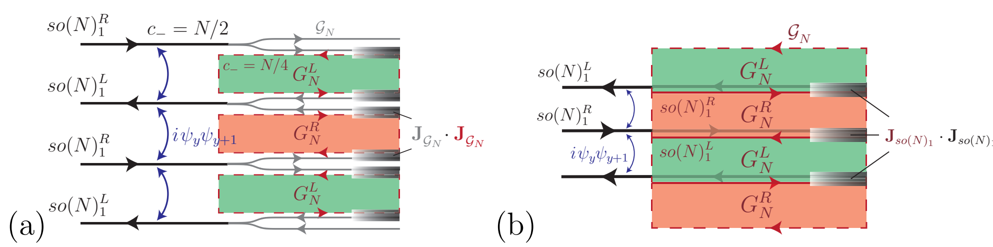

Figure 3.3: Gapping N surface Majorana cones by inserting $(2+1)$D G_N stripe state and removing edge modes by current-current backscattering interaction.

Previously, we designed interwire interactions that gap all Majorana modes without breaking time reversal symmetry. Here we provide an alternative where each chiral Majorana wire is gapped by backscattering onto the edges of two topological stripes sandwiching the wire (see figure 3.3). The topological stripes could be fractional quantum Hall states for instance. Similar construction has been proposed to describe surface states of topological insulators[69].

First we consider inserting between each pairs of Majorana wire a (2+1)D topological state. It supports chiral boundary modes which move in a reverse direction to its neighboring Majorana wire. As adjacent wires have opposite propagation directions, the chiralities of the topological states also alternates. This alternating topological stripe state can be regarded as a surface reconstruction of the 3D topological superconductor. It preserves the antiferrormagnetic time reversal symmetry (2.2), which relates adjacent topological stripes by reversing their chirality. Unlike the coupled Majorana wire mode, the topological stripe state itself is a pure $(2+1)$D time reversal symmetric system and is not supported by a $(3+1)$D bulk. It has a gapless energy spectrum that is identical to N surface Majorana cones and is carried by the interface modes between stripes (see figure 3.3(b)). However the topological stripe state also carry non-trivial anyonic excitations between wires. This distinguishes it from the coupled Majorana wire model and allows it to exist non-holographically in a pure $(2+1)$D setting.

The Majorana modes along the chiral wires then can be backscattered onto the boundaries or interfaces of the topological stripes by current-current couplings. In order for the boundary or interface modes to exactly cancel the Majorana modes along each wire, the topological stripes must carry specific topological orders. We take a G_N topological state (see eq.(3.91)) so that its boundary carries a $\mathcal{G}_N$ Kac-Moody current, for $\mathcal{G}_N$ the affine Lie algebra of G_N defined in (3.5). G_N^R and G_N^L denote stripes with opposite chiralities. The $(2+1)$D G_N topological state itself can be constructed using a coupled wire construction similar to that in Ref.[52, 100] and will not be discussed here.

There are two ways the Majorana modes can be backscattered onto the topological stripes. The first is shown in figure 3.3(a). The N Majorana modes along each chiral wire is bipartite into a pair of WZW theories $\mathcal{G}_N^+ \times \mathcal{G}_N^-$ according to (3.4). Each WZW theory is identical to the CFT along the boundary of an neighboring topological stripe but propagates in an opposite direction. It can be then be gapped out by the current-current backscattering

$$\mathcal{H}_{\rm int} = u\mathbf{J}^{\rm wire}_{\mathcal{G}_N} \cdot \mathbf{J}^{\rm stripe}_{\mathcal{G}_N}. \tag{3.86}$$

Alternatively, one could first glue the topological stripes together (see figure 3.3(b)) so that the line interface sandwiched between adjacent G_N^R and G_N^L states hosts a chiral $so(N)_1$ CFT. The stripes can then be put on top of the Majorana wire array so that each interface is sitting on top of a wire with opposite chirality. The current-current backscattering

$$\mathcal{H}_{\rm int} = u\mathbf{J}^{\rm wire}_{so(N)_1} \cdot \mathbf{J}^{\rm interface}_{so(N)_1} \tag{3.87}$$

between each Majorana wire and stripe interface gaps out all low energy degrees of freedom.

3.2 Surface topological order

In the previous section, we described how a coupled Majorana wire model, which mimics the surface Majorana modes of a 3D bulk topological superconductor (TSC), can be gapped by interwire current-current backscattering interaction without breaking time reversal (TR) symmetry. In this section, we pay more attention to the topological order and the anyon types[101, 23, 102] of gapped excitations. The ground states are time reversal symmetric and there are no non-vanishing order parameters that breaks time reversal spontaneously. There is a finite ground state degeneracy that does not depend on system size. This signifies a non-trivial topological order[103, 104, 105].

The surface topological order can be inferred from bulk-boundary correspondence[106,

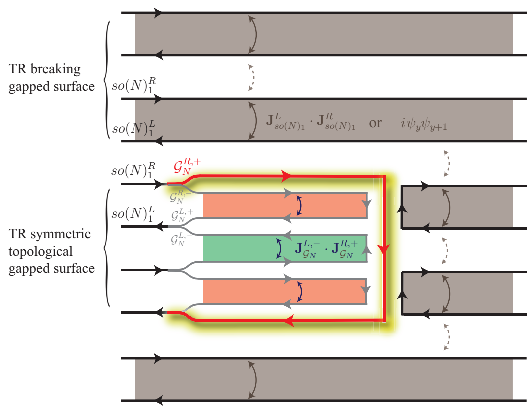

Figure 3.4: Chiral interface (highlighted line) between a time reversal breaking gapped region and a TR symmetric topologically ordered gapped region.

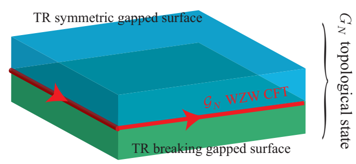

Figure 3.5: The G_N topological order of a quasi-2D slab with time reversal symmetric gapped top surface and time reversal breaking gapped bottom surface

107, 108, 73]. There is a one-to-one correspondence between the primary fields of the CFT along the (1+1)D gapless boundary and the anyon types in the (2+1)D gapped topological bulk. The conformal scaling dimension or spin $h = h_R - h_L$ of a primary field corresponds to the exchange statistical phase $\theta = e^{2\pi i h}$ of the corresponding anyon. The fusion rules of primary fields are identical to that of the anyons. And the modular S-matrix of the CFT at the boundary equals the braiding S-matrix[73]

$$\mathcal{S}_{\mathbf{ab}} = \frac{1}{\mathcal{D}} \sum_{\mathbf{c}} d_{\mathbf{c}} N_{\mathbf{ab}}^{\mathbf{c}} \frac{\theta_{\mathbf{c}}}{\theta_{\mathbf{a}}\theta_{\mathbf{b}}} \tag{3.88}$$

in the bulk, where the non-negative integers $N_{\mathbf{ab}}^{\mathbf{c}}$ are the degeneracies of the fusion rules

$$\mathbf{a} \times \mathbf{b} = \sum_{\mathbf{c}} N_{\mathbf{ab}}^{\mathbf{c}} \mathbf{c} \tag{3.89}$$

between anyons, and the total quantum dimension $\mathcal{D} = \sqrt{\sum_{\mathbf{a}} d_{\mathbf{a}}^2}$ quantifies topological entanglement[19] and can be evaluated by knowing the quantum dimensions $d_{\mathbf{a}} \geq 1$ of each anyon $\mathbf{a}$ by solving the fusion identities

$$d_{\mathbf{a}} d_{\mathbf{b}} = \sum_{\mathbf{c}} N_{\mathbf{ab}}^{\mathbf{c}} d_{\mathbf{c}}. \tag{3.90}$$

On the surface of a topological superconductor, where there are no boundaries, the $(2+1)$D topological order corresponds to a $(1+1)$D interface that separate the time reversal symmetric topologically ordered domain and a time reversal breaking domain. This interface hosts a chiral gapless modes (see figure 3.4). This geometry can be wrapped onto the surface of a slab where the TR symmetric and breaking domains occupy the top and bottom surface of a 3D bulk (see figure 3.5). The quasi-2D system has an energy gap except along its boundary which is previously the interface that carries the $\mathcal{G}_N$ WZW CFT. The bulk-boundary correspondence then determines a bulk G_N topological order on the quasi-2D slab.

$$G_N = \begin{cases} SO(r)_1, & \text{for } N = 2r \\ SO(3)_3 \boxtimes_b SO(r)_1, & \text{for } N = 9 + 2r \end{cases} \tag{3.91}$$

where both N and r can be extended to negative integers.

Wires in the trivial TR-breaking domain are gapped by non-uniform current backscattering

$$\begin{aligned} \mathcal{H}_{\mathrm{TR-breaking}} = & \sum_y \Delta \mathbf{J}^{2y-1}_{so(N)_1} \cdot \mathbf{J}^{2y}_{so(N)_1} \\ & + \delta \mathbf{J}^{2y}_{so(N)_1} \cdot \mathbf{J}^{2y+1}_{so(N)_1} \end{aligned} \tag{3.92}$$

or single-body fermion backscattering perturbation

$$\mathcal{H}_{\mathrm{TR-breaking}} = \sum_y i\Delta \boldsymbol{\psi}_{2y-1}^T \boldsymbol{\psi}_{2y} + i\delta \boldsymbol{\psi}_{2y}^T \boldsymbol{\psi}_{2y+1} \tag{3.93}$$

to the coupled Majorana wire model (2.4), for $\Delta > \delta$ and $\boldsymbol{\psi}_y = (\psi_y^1, \ldots, \psi_y^N)$. This violates the antiferrormagnetic time reversal symmetry (2.2) and leads to a gapped surface with trivial topological order. This TR breaking half-plane is put side by side against a TR symmetric gapped half-plane, where the N Majorana channels per wire is *fractionalized* into $so(N)_1 \supseteq \mathcal{G}_N^+ \times \mathcal{G}_N^-$, for $\mathcal{G}_N$ previously defined in (3.5). Each $\mathcal{G}_N$ sector is then paired with the adjacent one on the next wire and are gapped by current-current backscattering $\mathbf{J}_{\mathcal{G}_N^-} \cdot \mathbf{J}_{\mathcal{G}_N^+}$. The interface between the TR-symmetric and TR-breaking regions leaves behind one single unpaired fractional $\mathcal{G}_N$ channel. This can be regarded as a 2D analogue of the fractional boundary modes in the the Haldane integral spin chain[86, 87] and the AKLT spin chain[109].

As eluded in the introduction, when the coupled wire model involves only current-current backscattering interaction, it is a boson model where the bosonic current operators, rather than Majorana fermions, are treated as fundamental local objects. It is therefore more natural for us to use the current backscattering Hamiltonian (3.92) instead of the fermionic single-body one (3.93) to introduce a time reversal breaking gap. In this case, π-fluxes are deconfined anyonic excitations realized as π-kinks along a stripe where there is no energy cost in separating a flux-antiflux pair. If the fermionic TR-breaking Hamiltonian (3.93) were used instead, π-fluxes would be confined on the bottom layer and Majorana fermions would become local. We however will mostly be focusing on the former bosonic case, although the fermionic scenario may be more realistic in a superconducting medium.

The bulk-interface correspondence depends on the orientation of the time reversal breaking order. In eq.(3.92), if the backscattering tunneling strengths are reversed so that $\delta > \Delta$, figure 3.4 will need to be shifted by $y \to y+1$ and all propagating directions will need to be inverted. As a result, the interface CFT will also be reversed to its time reversal partner $\mathcal{G}_N \to \overline{\mathcal{G}_N}$. This will flip the spins of all primary fields $h_{\mathbf{a}} \to h_{\bar{\mathbf{a}}} = -h_{\mathbf{a}}$ and conjugates all exchange phases $\theta_{\mathbf{a}} \to \theta_{\bar{\mathbf{a}}} = \theta_{\mathbf{a}}^*$.

An interface with a particular orientation therefore corresponds to a time reversal breaking topological order. This is also apparent in the slab geometry in figure 3.5 where the TR breaking order on the bottom surface can have opposite orientations. Unlike the conventional case on the surface of a topological superconductor where time reversal is local, here time reversal involves a half translation $y \to y+1$ and relates a stripe gapped by $\mathbf{J}_y^- \cdot \mathbf{J}_{y+1}^+$ to its neighbor $\mathbf{J}_{y+1}^- \cdot \mathbf{J}_{y+2}^+$. As anyonic excitations are realized as kinks or domain walls that separate distinct ground states along a stripe, time reversal non-locally translates anyons on an even stripe (green) to an odd one (red) or vice versa (see figure 3.4). However an interface with a particular orientation can only correspond to anyons on stripes with a particular parity. For example the bulk-interface correspondence in figure 3.4 singles out anyons on even stripes gapped by $\mathbf{J}_{2y}^- \cdot \mathbf{J}_{2y+1}^+$. There is therefore no reason to expect the anyon theory would be closed under time reversal.

3.2.1 Summary of anyon contents

	r even				r odd		
$\mathbf{x}$	1	ψ	s_+	s_-	1	ψ	σ
$d_{\mathbf{x}}$	1	1	1	1	1	1	$\sqrt{2}$
$\theta_{\mathbf{x}}$	1	-1	$e^{\pi i r/8}$	$e^{\pi i r/8}$	1	-1	$e^{\pi i r/8}$

Table 3.2: The exchange phase $\theta_{\mathbf{x}} = e^{2\pi i h_{\mathbf{x}}}$ and quantum dimensions of anyons $\mathbf{x}$ in a $(2+1)$D $SO(r)_1$ topological phase.

The interface carries chiral gapless degrees of freedom, which are captured by the $\mathcal{G}_N$ WZW theory whose primary fields corresponds to the anyon content of the TR symmetry gapped surface. For even $N = 2r$, the surface carries a

$$G_N = SO(r)_1 \tag{3.94}$$

topological order summarized in table 3.2. Its anyonic excitations obey the abelian fusion rules

$$\begin{aligned} \psi \times \psi = 1, \quad s_\pm \times \psi = s_\mp \\ s_\pm \times s_\pm = \begin{cases} 1, & \text{for } r \equiv 0 \bmod 4 \\ \psi, & \text{for } r \equiv 2 \bmod 4 \end{cases} \end{aligned} \tag{3.95}$$

for r even, or the Ising fusion rules

$$\psi \times \psi = 1, \quad \psi \times \sigma = \sigma, \quad \sigma \times \sigma = 1 + \psi \tag{3.96}$$

for r odd. Eq.(3.95) and (3.96) follows directly from the fusion properties of the primary fields in the $so(r)_1$ Kac-Moody algebra (see section 2.1.1 and appendix B and C). The exchange phase (also known as topological spin) $\theta_{\mathbf{x}} = e^{2\pi i h_{\mathbf{x}}}$ can be read off from the conformal dimension $h_{\mathbf{x}}$ of the primary field $V_{\mathbf{x}}$ in $so(r)_1$ that corresponds to the anyon type $\mathbf{x}$. Again we extend r to negative integers by defining $SO(-r)_1 = \overline{SO(r)_1}$ to be the time reversal conjugate of the $SO(r)_1$ topological state.

$\mathbf{x}$	1	α_+	γ_+	β	γ_-	α_-	f
$d_{\mathbf{x}}$	1	$\sqrt{2+\sqrt{2}}$	$1+\sqrt{2}$	$\sqrt{4+2\sqrt{2}}$	$1+\sqrt{2}$	$\sqrt{2+\sqrt{2}}$	1
$\theta_{\mathbf{x}}$	1	$e^{\pi i \frac{3+2r}{16}}$	$e^{i\pi/2}$	$e^{\pi i \frac{15+2r}{16}}$	$e^{-i\pi/2}$	$e^{\pi i \frac{3+2r}{16}}$	-1

r even

$\mathbf{x}$	1	α_+	γ_+	β	γ_-	α_-	f
$d_{\mathbf{x}}$	1	$\sqrt{2+\sqrt{2}}$	$1+\sqrt{2}$	$\sqrt{4+2\sqrt{2}}$	$1+\sqrt{2}$	$\sqrt{2+\sqrt{2}}$	1
$\theta_{\mathbf{x}}$	1	$e^{\pi i \frac{15+2r}{16}}$	$e^{i\pi/2}$	$e^{\pi i \frac{3+2r}{16}}$	$e^{-i\pi/2}$	$e^{\pi i \frac{15+2r}{16}}$	-1

r odd

Table 3.3: The exchange phase $\theta_{\mathbf{x}} = e^{2\pi i h_{\mathbf{x}}}$ and quantum dimensions of anyons $\mathbf{x}$ in a (2 + 1)D $SO(3)_3 \boxtimes_b SO(r)_1$ topological phase.

For odd $N = 9 + 2r$, the $\mathcal{G}_N$ WZW CFT at the interface corresponds the TR symmetric gapped surface that carries a topological order given by the *relative* tensor product

$$G_N = SO(3)_3 \boxtimes_b SO(r)_1 \tag{3.97}$$

where the fermion pair $b = \psi_{SO(3)_3} \times \psi_{SO(r)_1}$ is condensed. The concept of anyon condensation[110] will be demonstrated more explicitly later in section 3.2.2. The topological state carries seven anyon types and are summarized in table 3.3. For instance, the anyon structure matches the primary field content of the $so(3)_3$ WZW theory (see table 3.1) when $r = 0$. The quasiparticle fusion rules of G_N are similar to the $so(3)_3$ ones in (3.60)

$$\begin{gathered} f \times f = 1, \quad f \times \gamma_\pm = \gamma_\mp, \quad f \times \alpha_\pm = \alpha_\mp, \quad f \times \beta = \beta \\ \gamma_\pm \times \gamma_\pm = 1 + \gamma_+ + \gamma_-, \quad \alpha_\pm \times \beta = \gamma_+ + \gamma_- \\ \beta \times \beta = 1 + \gamma_+ + \gamma_- + f, \quad \beta \times \gamma_\pm = \alpha_+ + \alpha_- + \beta \end{gathered} \tag{3.98}$$

except the following modifications that dependent on $r = (N - 9)/2$.

$$\begin{gathered} \alpha_\pm \times \alpha_\pm = \begin{cases} 1 + \gamma_+, & \text{for } r \equiv 0 \bmod 4 \\ f + \gamma_+, & \text{for } r \equiv 1 \bmod 4 \\ f + \gamma_-, & \text{for } r \equiv 2 \bmod 4 \\ 1 + \gamma_-, & \text{for } r \equiv 3 \bmod 4 \end{cases} \\ \alpha_\pm \times \gamma_\pm = \begin{cases} \alpha_+ + \beta, & \text{for } r \text{ even} \\ \alpha_- + \beta, & \text{for } r \text{ odd} \end{cases} \end{gathered} \tag{3.99}$$

This quasiparticle spin and fusion structure will be shown later in section 3.2.2. The braiding S-matrices of the G_N states are summarized in appendix E.

The G_N sequence extends the sixteenfold periodic anyon structure[73, 111, 112] $SO(r+16)_1 \cong SO(r)_1$ to a periodic class of thirty two topological states

$$G_{N+32} \cong G_N. \tag{3.100}$$

This seemingly contradicts the sixteenfold prediction of topologically ordered surface states from Ref.[29, 30, 31, 32, 33, 34, 35]. This is due to the non-local nature of the "antiferromagnetic" time reversal symmetry in the coupled Majorana wire model. On the other hand, in general there are multiple possible gapping potentials that leads to distinct topological order. For instance, we will show in a subsequent section that for $N = 16$, there is an extended E_8 symmetry or an alternative conformal embedding that would allow a different set of gapping terms but would forbid all electronic quasiparticle excitations.

The thirty two topological states here follow a $\mathbb{Z}_{32}$ tensor product algebraic structure

$$G_{N_1} \boxtimes_b G_{N_2} \cong G_{N_1+N_2} \tag{3.101}$$

where certain maximal set of mutually local bosons from G_{N_1} and G_{N_2} are pair condensed in the relative tensor product. We will discuss this in more detail below.

3.2.2 The 32-fold tensor product structure

We first explain the relative tensor product that defines the G_N topological state in eq.(3.97). We begin with the tensor product state $SO(3)_3 \otimes SO(r)_1$ which consists of decoupled $SO(3)_3 = SU(2)_6$ and $SO(r)_1$ topological states. The primary fields of the $su(2)_6$ WZW CFT are labeled by seven half-integral "spins" $s = \mathbf{0}, \mathbf{1/2}, \mathbf{1}, \mathbf{3/2}, \mathbf{2}, \mathbf{5/2}, \mathbf{3}$ and are summarized in table 3.1 and eq.(3.60). These correspond to the anyon structure of the $(2+1)$D $SO(3)_3$ topological state. The topological order of $SO(r)_1$ is well-known[73] and was summarized earlier in this section. For instance, "spin" $\mathbf{3}$ corresponds to the BdG fermion quasiparticle f, and the half-integral "spins" $\mathbf{1/2}$, $\mathbf{3/2}$ and $\mathbf{5/2}$ are π-fluxes that give a -1 monodromy phase of an orbiting fermion.

In the coupled Majorana wire model where there are $N = 9{+}2r$ Majorana channels per wire, the gapping term explicitly seperates the first 9 and final $2r$ channels and the current backscattering potential does not mix these two sectors. This model would therefore give a decouple $SO(3)_3 \otimes SO(r)_1$ topological state. However, there could be additional local time reversal symmetric terms, such as intrawire forward scattering $i\psi_a^R\psi_b^R$ and $i\psi_a^L\psi_b^L$, that mixes the two sectors and condenses the fermion pair $b = f_{SO(3)_3} \otimes \psi_{SO(r)_1}$. In fact, fermion pair condensation is natural in a superconducting medium where the ground state consists of Cooper pairs. The condensation of the bosonic anyon b results in the confinement of certain quasiparticles that have non-trivially monodromy around it.[110] These includes all the π fluxes $\mathbf{1/2}$, $\mathbf{3/2}$ and $\mathbf{5/2}$ in the $SO(3)_3$ sector, $s_\pm$ (or σ) in $SO(r)_1$ for r even (resp. odd), as well as the tensor product $\mathbf{1/2} \otimes \psi$, $\mathbf{3/2} \otimes \psi$, $\mathbf{5/2} \otimes \psi$, $\mathbf{1} \otimes s_\pm$, $\mathbf{2} \otimes s_\pm$ and $\mathbf{3} \otimes s_\pm$ (or $\mathbf{1} \otimes \sigma$, $\mathbf{2} \otimes \sigma$ and $\mathbf{3} \otimes \sigma$). The remaining anyons are local with respect to the boson b and survive the condensation, but certain pairs are identified if they differ only by the boson condensate, $\mathbf{a} \times b \equiv \mathbf{a}$. This includes $\mathbf{3} \equiv \psi$, $\mathbf{1} \otimes \psi \equiv \mathbf{2}$, $\mathbf{2} \otimes \psi \equiv \mathbf{1}$, $\mathbf{1/2} \otimes s_\pm \equiv \mathbf{5/2} \otimes s_\mp$ and $\mathbf{3/2} \otimes s_+ \equiv \mathbf{3/2} \otimes s_-$ for even r, or $\mathbf{1/2} \otimes \sigma \equiv \mathbf{5/2} \otimes \sigma$ for r odd. Special care has to be taken for the tensor product $\mathbf{3/2} \otimes \sigma$ when r is odd. After condensation, the fusion rule of a pair of $\mathbf{3/2} \otimes \sigma$ becomes

$$\begin{aligned}(\mathbf{3/2} \otimes \sigma) \times (\mathbf{3/2} \otimes \sigma) &= (\mathbf{0} + \mathbf{1} + \mathbf{2} + \mathbf{3}) \otimes (1 + \psi) \\ &\equiv \mathbf{0} + \mathbf{0} + \mathbf{1} + \mathbf{1} + \mathbf{2} + \mathbf{2} + \mathbf{3} + \mathbf{3} \end{aligned} \tag{3.102}$$

which has two vacuum fusion channels and indicates that $\mathbf{3/2} \otimes \sigma$ cannot be a simple object. This leads to the decomposition

$$\mathbf{3/2} \otimes \sigma \equiv \alpha_+ + \alpha_- \tag{3.103}$$

where $\alpha_\pm$ are simple anyons with identical exchange statistics but opposite fermion parity $\alpha_\pm \times f = \alpha_\mp$ and obey the fusion rules (3.99).

	1	α_+	γ_+	β	γ_-	α_-	f
r even	$\mathbf{0}$	$\mathbf{1/2} \otimes s_+$	$\mathbf{1}$	$\mathbf{3/2} \otimes s_\pm$	$\mathbf{2}$	$\mathbf{5/2} \otimes s_+$	$\mathbf{3}$
r odd	$\mathbf{0}$	$(\mathbf{3/2} \otimes \sigma)_+$	$\mathbf{1}$	$\mathbf{1/2} \otimes \sigma$	$\mathbf{2}$	$(\mathbf{3/2} \otimes \sigma)_-$	$\mathbf{3}$

Table 3.4: Identification of the seven anyon types in table 3.3 as tensor products.

We summarize the identification of the seven anyon types in $G_N = SO(3)_3 \boxtimes_b SO(r)_1$ as tensor products in table 3.4. This explains the exchange statistics and quantum dimensions of the quasiparticles in table 3.3

$$\theta_{\mathbf{a}\otimes\mathbf{b}} = \theta_{\mathbf{a}}\theta_{\mathbf{b}}, \quad d_{\mathbf{a}\otimes\mathbf{b}} = d_{\mathbf{a}}d_{\mathbf{b}} \tag{3.104}$$

with the exception of the non-simple object $\mathbf{3/2} \otimes \sigma$ in (3.103) where each component $\alpha_\pm$ carries half of its dimension. The fusion rules in (3.98) and (3.99) are explained by the tensor product

$$(\mathbf{a}_1 \otimes \mathbf{b}_1) \times (\mathbf{a}_2 \otimes \mathbf{b}_2) = (\mathbf{a}_1 \times \mathbf{a}_2) \otimes (\mathbf{b}_1 \times \mathbf{b}_2) \tag{3.105}$$

except in the odd r cases where again the non-simple object $\mathbf{3/2} \otimes \sigma = \alpha_+ + \alpha_-$ requires special attention.

The fusion rules (3.99) of $\alpha_\pm$ in the odd r cases are fixed by modular invariance. The braiding S-matrix (3.88) is determined by fusion rules and quasiparticle exchange statistics. On the other hand fusion rules can also be determined by the S-matrix using the Verlinde formula (3.58).[99] Moreover one can define the T-matrix according to the quasiparticle exchange statistics

$$T_{\mathbf{ab}} = \delta_{\mathbf{ab}}\theta_{\mathbf{a}} \tag{3.106}$$

which corresponds to the modular T-transformation in the CFT along the boundary. As a consequence they satisfies the $SL(2;\mathbb{Z})$ algebraic relation[73]

$$\left(\mathcal{S}T^{\dagger}\right)^3 = e^{-2\pi i c_-/8}\mathcal{S}^2 \tag{3.107}$$

where $c_- = c_R - c_L$ is the chiral central charge of the corresponding CFT along the boundary

$$c_-(G_N) = c_-(so(3)_3) + c_-(so(r)_1) = \frac{9}{4} + \frac{r}{2} = \frac{N}{4}. \tag{3.108}$$

These put a very restrictive constraint on the allowed topological field theory and fix the fusion rules (3.99) for $\alpha_\pm$ when r is odd. The braiding S matrices can be found in appendix E.

The relative tensor product structure of the sixteenfold $SO(r)_1$ sequence itself can also be understood using anyon condensation

$$SO(r_1)_1 \boxtimes_b SO(r_2)_1 \cong SO(r_1+r_2)_1 \tag{3.109}$$

where the fermion pair $\psi_1 \otimes \psi_2$ is condensed. This can be verified by a similar condensation procedure as the one presented above. For instance, if r_1 and r_2 are both odd, the tensor product $\sigma_1 \otimes \sigma_2$ will become non-simple after condensation and decompose into a pair of abelian π-fluxes, $s_+ + s_-$, with identical exchange statistics but opposite fermion parities $s_\pm \times \psi = s_\mp$ and are related by an anyonic symmetry[111, 112].

Next we move on to explaining the general relative tensor product structure (3.101) of the 32-fold G_N states. Eq.(3.109) describes the cases when both N_1 and N_2 are even, i.e. $G_{2r_1} \boxtimes_b G_{2r_2} \cong G_{2r_1+2r_2}$. A similar anyon condensation procedure that defined the relative tensor product $SO(3)_3 \boxtimes_b SO(r)_1$ above would prove that

$$G_N \boxtimes_b SO(r)_1 \cong G_{N+2r} \tag{3.110}$$

for N odd, where the fermion pair $b = f_{G_N} \otimes \psi_{SO(r)_1}$ is condensed.

When both $N_1 = 9 + 2r_1$ and $N_2 = 9 + 2r_2$ are odd, each of the two $G_{N_i} = SO(3)_3 \boxtimes_b SO(r_i)_1$ theories contains seven anyon types $1, \alpha^i_\pm, \gamma^i_\pm, \beta^i, f^i$. The tensor product state $G_{N_1} \otimes G_{N_2}$ contains three non-trivial bosons

$$b = \{b_0, b_+, b_-\} = \left\{f^1 \otimes f^2, \gamma^1_+ \otimes \gamma^2_-, \gamma^1_- \otimes \gamma^2_+\right\} \tag{3.111}$$

as $\gamma_\pm$ have conjugate exchange phases $\theta_{\gamma_\pm} = \pm i$. Moreover, these bosons are mutually local. Firstly, b_0 have trivial monodromy around $b_\pm$ as $\gamma_\pm$ are local with respect to the fermion f. Secondly, as there are bosonic fusion channels $b_\pm \times b_\pm = 1 + b_+ + b_- + \ldots$ and $b_\pm \times b_\mp = b_0 + b_+ + b_- + \ldots$, $b_\pm$ are local among themselves because their mutual monodromy phases are trivial. We first condensed the Abelian fermion pair $b_0 = f^1 \otimes f^2$. The resulting theory contains the following set of (non-confined) anyon types

$$G_{N_1} \boxtimes_{b_0} G_{N_2} = \left\langle \begin{array}{c} 1, f, \gamma^1_\pm, \gamma^2_\pm, \gamma^1_+\gamma^2_+, \gamma^1_+\gamma^2_-, \\ \alpha^1_+\alpha^2_+, \alpha^1_+\alpha^2_-, \alpha^1_+\beta^2, \beta^1\alpha^2_+, \beta^1\beta^2 \end{array} \right\rangle \tag{3.112}$$

where some anyon types are identified by the b_0 condensate, such as $f \equiv f^1 \equiv f^2$ and $\gamma^1_-\gamma^2_- = \gamma^1_+\gamma^2_+ \times b_0$, and are therefore not listed. Next we condense the non-Abelian boson $b_+ = \gamma^1_+\gamma^2_-$, which is already equated with $b_- = b_+ \times b_0$. The general condensation procedure of a non-Abelian boson was proposed by Bais and Slingerland in Ref.[110]. In the present case, it begins with the fusion theory $\mathcal{F}$ of $G_{N_1} \boxtimes_{b_0} G_{N_2}$ that only encodes the associative fusion content but neglects the braiding structure of the anyons. As the boson b_+ is condensed, it decomposes as $b_+ = \gamma_+^1 \gamma_-^2 = 1 + \ldots$, which now contains the vacuum channel 1. This reduces the fusion theory $\mathcal{F}$ into a new fusion theory $\mathcal{F}'$, where the certain anyons in (3.112) become non-simple objects and decompose into simpler components while others are identified by the boson condensate. This new fusion category $\mathcal{F}'$ contains the non-confined anyons in the resulting state as well as confined non-point-like objects.

We start with the first line of anyons in (3.112), which are all local with respect to the fermion f. The semion γ_+^1 is self-conjugate as $\gamma_+^1 \times \gamma_+^1 = 1 + \gamma_+^1 + \gamma_-^1$. However γ_-^2 is now also an antiparticle of γ_+^1 since $\gamma_+^1 \times \gamma_-^2 = b_+ = 1 + \ldots$ also contains the vacuum channel. The uniqueness of antipartner guarantees the identifications

$$\gamma_+ \equiv \gamma_+^1 \equiv \gamma_-^2, \quad \gamma_- \equiv \gamma_-^1 \equiv \gamma_+^2 \tag{3.113}$$

which obey the usual fusion rules $\gamma_\pm \times \gamma_\pm = 1 + \gamma_+ + \gamma_-$ and $f \times \gamma_\pm = \gamma_\mp$. This in turn determines the decomposition of the non-Abelian boson

$$b_+ = \gamma_+^1 \gamma_-^2 \equiv \gamma_+ \times \gamma_+ = 1 + \gamma_+ + \gamma_- \tag{3.114}$$

which is consistent with the boson quantum dimension $d_{b_+} = d_\gamma^2 = 1 + 2d_\gamma$. Moreover the non-Abelian fermion also decomposes

$$\gamma_+^1 \gamma_+^2 \equiv \gamma_+ \times \gamma_- = f + \gamma_+ + \gamma_-. \tag{3.115}$$

Next we move on to the second line of anyons in (3.112), which are π fluxes with respect to the fermion f. From the original fusion rules (3.98), (3.99) and the identification (3.113), (3.114) and (3.115), the π fluxes satisfy the fusion rules

$$(\alpha^1_+\alpha^2_+) \times (\alpha^1_+\alpha^2_+) = \begin{cases} 1 + f + 2\gamma_+ + 2\gamma_-, & \text{for } r_1 + r_2 \text{ even} \\ 1 + 1 + \gamma_+ + \gamma_- + 2\gamma_\pm, & \text{for } r_1 + r_2 \equiv 3 \bmod 4 \\ f + f + \gamma_+ + 3\gamma_-, & \text{for } r_1 + r_2 \equiv 1 \bmod 4 \end{cases} \tag{3.116}$$

$$(\alpha^1\beta^2) \times (\alpha^1\beta^2) = 1 + 1 + f + f + 4\gamma_+ + 4\gamma_- \tag{3.117}$$

$$(\beta^1\beta^2) \times (\beta^1\beta^2) = 4(1 + f + 2\gamma_+ + 2\gamma_-) \tag{3.118}$$

$$(\alpha^1_+\alpha^2_+) \times (\alpha^1_+\beta^2) = 1 + f + 3\gamma_+ + 3\gamma_- \tag{3.119}$$

$$(\alpha^1_+\alpha^2_+) \times (\beta^1\beta^2) = 1 + 1 + f + f + 4\gamma_+ + 4\gamma_- \tag{3.120}$$

for $N_1 = 9 + 2r_1$ and $N_2 = 9 + 2r_2$.

These show $\alpha^1\beta^2$ and $\beta^1\beta^2$ must be non-simple because their corresponding fusion rules contain multiple vacuum channels. The decomposition of $\beta^1\beta^2$ is simplest and applies to all r_1, r_2

$$\beta^1\beta^2 = \alpha^1_+\alpha^2_+ + \alpha^1_+\alpha^2_- \tag{3.121}$$

where $\alpha^1_+\alpha^2_- = \alpha^1_+\alpha^2_+ \times f$. For instance, it is straightforward to check that this decomposition is consistent with the fusion rules. $\alpha^1_+\beta^2$ and $\alpha^1_-\beta^2$ are clearly identified as they differ only by the Abelian boson $b_0 = f^1f^2$. We therefore will simply denote them as $\alpha^1\beta^2$. Moreover, one can show that $\alpha^1\beta^2$ and $\beta^1\alpha^2$ are also identified after the condensation of the non-Abelian boson $\gamma^1_+\gamma^2_- = 1 + \gamma_+ + \gamma_-$ in (3.114). This can be verify by equating the fusion equations $(\alpha^1\beta^2) \times (\gamma^1_+\gamma^2_-) = (\alpha^1\beta^2) \times (1 + \gamma_+ + \gamma_-)$. The decomposition of $\alpha^1\beta^2 \equiv \beta^1\alpha^2$ depends on the parity of $r_1 + r_2$.

When $r_1 + r_2$ is even, the pair fusion rule for $\alpha^1_+\alpha^2_+$ allows it to be simple since there is a unique vacuum channel. Moreover as the pair fusion rule is unaltered by the addition of a fermion f, it is identical to $(\alpha^1_+\alpha^2_+) \times (\alpha^1_+\alpha^2_-)$. This shows $\alpha^1_\pm\alpha^2_-$ conjugates and therefore identifies with $\alpha^1_\pm\alpha^2_+$, which is self-conjugate.

$$\alpha^1\alpha^2 \equiv \alpha^1_\pm\alpha^2_\pm \equiv \alpha^1_\pm\alpha^2_\mp. \tag{3.122}$$

In this case, $\alpha^1\beta^2$ is decomposed into

$$\alpha^1\beta^2 = \sigma + \alpha^1\alpha^2 \tag{3.123}$$

where we introduce the Ising anyon σ that obey

$$\begin{gathered} \sigma \times \sigma = 1 + f, \quad \sigma \times f = \sigma \\ \sigma \times \alpha^1\alpha^2 = \gamma_+ + \gamma_-, \quad \sigma \times \gamma_\pm = \alpha^1\alpha^2. \end{gathered} \tag{3.124}$$

The decomposition (3.123) is consistent with the fusion rules (3.119) and (3.117). The reduced fusion category after condensing the boson (3.114) is therefore generated by the following simple objects

$$\mathcal{F}'_{\text{even}} = \left\langle 1, f, \sigma, \gamma_\pm, \alpha^1\alpha^2 \right\rangle \tag{3.125}$$

when $r_1 + r_2$ is even. It has the fusion rules (3.124) together with $\gamma_\pm \times \alpha^1\alpha^2 = \sigma + 2\alpha^1\alpha^2$.

When $r_1 + r_2$ is odd, we need to further separate into two cases. When $r_1 + r_2 \equiv 3 \mod 4$, the fusion rule of a pair of $\alpha^1_+\alpha^2_+$ in (3.116) forbids it to be simple. It decomposes into

$$\alpha^1_+\alpha^2_+ = s_+ + \gamma_+ \quad \text{or} \quad s_+ + \gamma_- \tag{3.126}$$

where $s_\pm$ are Abelian anyons that satisfy the fusion rules

$$s_\pm \times s_\pm = 1, \quad s_\pm \times f = s_\mp, \quad s_+ \times \gamma_\pm = \gamma_\pm \tag{3.127}$$

and the fermion parity $\gamma_\pm$ in (3.126) depends on $(r_1, r_2) \equiv (0,3)$ or $(1,2)$ mod 4 but is unimportant for the current discussion. The decomposition (3.126) is consistent with the fusion rule (3.116). In this case, the fusion rules $(\alpha_+^1\alpha_+^2) \times (\alpha^1\beta^2)$ in (3.119) requires a different decomposition of $\alpha^1\beta^2$ than (3.123).

$$\alpha^1\beta^2 = \gamma_+ + \gamma_-. \tag{3.128}$$

The reduced fusion category after condensing the boson (3.114) is therefore generated by the following simple objects

$$\mathcal{F}_3' = \langle 1, f, s_\pm, \gamma_\pm \rangle \tag{3.129}$$

when $r_1 + r_2 \equiv 3$ mod 4.

When $r_1 + r_2 \equiv 1$ mod 4, the fusion rule (3.116) again forbids $\alpha_+^1\alpha_+^2$ to be simple. Moreover as the vacuum channel is absent, it is no longer self-conjugate but instead is conjugate with $\alpha_+^1\alpha_-^2$ since it has opposite fermion parity and $(\alpha_+^1\alpha_+^2) \times (\alpha_+^1\alpha_-^2) = 1 + 1 + 3\gamma_+ + \gamma_-$. We decompose

$$\alpha_+^1\alpha_+^2 = s_+ + g_+ \tag{3.130}$$

where $s_\pm$ are Abelian anyons and $g_\pm$ are non-Abelian objects that satisfy

$$s_\pm \times s_\pm = f, \quad s_\pm \times f = s_\mp, \quad g_\pm = \gamma_+ \times s_\pm. \tag{3.131}$$

The decomposition of $\alpha^1\beta^2$ also needs to be modified

$$\alpha^1\beta^2 = g_+ + g_-. \tag{3.132}$$

One can check that these decompositions are consistent with the original fusion rules. The reduced fusion category after condensing the boson (3.114) is therefore generated by the following simple objects

$$\mathcal{F}_1' = \langle 1, f, s_\pm, \gamma_\pm, g_\pm \rangle \tag{3.133}$$

when $r_1 + r_2 \equiv 1 \bmod 4$.

Not all objects in the reduced fusion theories $\mathcal{F}_{\text{even}}'$, $\mathcal{F}_1'$ and $\mathcal{F}_3'$ in (3.125), (3.133) and (3.129) are non-confined anyons in the new topological states. Some may be non-local with respect to the boson b_+ (3.114) and are therefore not point-like objects when b_+ is condensed. They are equipped with a physical string or branch cut that extends. The anyon theory, which encodes both fusion and braiding information, after condensation excludes these confined extended objects. To determine which objects in the reduced fusion categories $\mathcal{F}'$ are non-confined anyons, we look at the possible monodromy around the condensed boson b_+. Suppose $\mathbf{a}_1 \otimes \mathbf{a}_2$ and $\mathbf{b}_1 \otimes \mathbf{b}_2$ are anyons in the tensor product state $G_{N_1} \boxtimes_{b_0} G_{N_2}$ (3.112) that are related by the fusion rule $b_+ \times (\mathbf{a}_1 \otimes \mathbf{a}_2) = \mathbf{b}_1 \otimes \mathbf{b}_2 + \ldots$, the monodromy under this fixed fusion channel is[110]

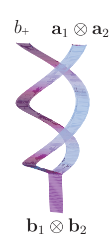

$=$

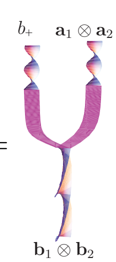

$$= \frac{\theta_{\mathbf{b}_1\otimes\mathbf{b}_2}}{\theta_{b_+}\theta_{\mathbf{a}_1\otimes\mathbf{a}_2}} = \frac{\theta_{\mathbf{b}_1\otimes\mathbf{b}_2}}{\theta_{\mathbf{a}_1\otimes\mathbf{a}_2}} \tag{3.134}$$

as b_+ is a boson with $\theta_{b_+} = 1$. In other words trivial monodromy simply reqires the invariance of exchange statistics upon an addition of the boson.

Given any simple object $\mathbf{x}$ in the reduced fusion category $\mathcal{F}'$ in (3.125), (3.133) or (3.129), it may be *lifted* to multiple anyons in the tensor product state $G_{N_1} \boxtimes_{b_0} G_{N_2}$ in (3.112) in the sense that it belongs in distinct decompositions $\mathbf{a}_1 \otimes \mathbf{a}_2 = \mathbf{x} + \ldots$ and $\mathbf{b}_1 \otimes \mathbf{b}_2 = \mathbf{x} + \ldots$. For instance, $\gamma_\pm$ are components of the boson $\gamma_+^1 \gamma_-^2 = 1 + \gamma_+ + \gamma_-$ as well as the fermion $\gamma_+^1 \gamma_+^2 = f + \gamma_+ + \gamma_-$ (see (3.114) and (3.115)). If $\mathbf{x}$ is an object not confined by the boson condensation, then its exchange statistics should be independent from the choices of lift

$$\theta_{\mathbf{x}} = \theta_{\mathbf{a}_1 \otimes \mathbf{a}_2} = \theta_{\mathbf{b}_1 \otimes \mathbf{b}_2} \tag{3.135}$$

since the monodromy (3.134) should be trivial. Otherwise, the object $\mathbf{x}$ has to be non-point-like and extended as it does not have well defined statistics. For example since $\gamma_\pm$ belongs to the decomposition of a non-Abelian boson and fermion, they have to be confined objects after condensation.

The relative tensor product $G_{N_1} \boxtimes_b G_{N_2}$ with the condensation of the set of bosons b (3.111) contains non-confined anyons in the reduced fusion categories $\mathcal{F}'_{\text{even}}$, $\mathcal{F}'_1$ and $\mathcal{F}'_3$ in (3.125), (3.133) and (3.129). For example when $r_1 + r_2$ is even, the simple object $\alpha^1 \alpha^2$ in (3.125) is confined and is not an anyon because it can be lifted into $\alpha^1 \beta^2$ and $\beta^1 \beta^2$, which have distinct statistics, in (3.123) and (3.121). When $r_1 + r_2 \equiv 1 \bmod 4$, the simple objects $g_\pm$ are also confined because they belong in $\alpha^1 \beta^2$ and $\alpha_+^1 \alpha_\pm^2$, which have different spins, in (3.132) and (3.130). This shows $G_{N_1} \boxtimes_b G_{N_2}$ is generated by the non-confined anyons

$$G_{N_1} \boxtimes_b G_{N_2} = \begin{cases} \langle 1, f, \sigma \rangle, & \text{for } r_1 + r_2 \text{ even} \\ \langle 1, f, s_\pm \rangle, & \text{for } r_1 + r_2 \text{ odd} \end{cases} \tag{3.136}$$

The exchange statistics of σ and $s_\pm$ are determined by that of their lifts. For instance,

$$\theta_\sigma = \theta_{\alpha^1\beta^2} = \theta_\alpha\theta_\beta = e^{\pi i \frac{9+r_1+r_2}{8}} = e^{\pi i(N_1+N_2)/16} \tag{3.137}$$

using table 3.3 when $r_1 + r_2$ is even. This shows

$$G_{N_1} \boxtimes_b G_{N_2} = SO\left(\frac{N_1+N_2}{2}\right)_1 \tag{3.138}$$

when both N_1 and N_2 are odd and concludes the 32-fold tensor product algebraic structure of the G_N-series.

3.3 Other possibilities

In the previous sections, we proposed time reversal symmetric interactions that gap the coupled Majorana wire model and lead to a G_N topological order (see eq.(3.94) and (3.97)). The interwire current-current backscattering interactions depend on a particular fractionalization, $so(N)_1 \supseteq \mathcal{G}_N \times \mathcal{G}_N$, of the N Majorana channels per wire. However, in special cases, we have already seen that alternative decompositions exist and correspond to different gapping interactions and topological orders. For example, at the beginning of section 3.1, we showed when there are even Majorana channels per wire, the model could simply be gapped by a single-body backscattering potential (see (3.1)) and have trivial topological order. This is consistent with the $\mathbb{Z}_2$ classification of gapless Majorana modes protected by the "antiferromagnetic" time reversal symmetry (2.2). Another example was given in section 3.1.1.2 for the special case when there are $N = 4$ Majorana channels per wire where the decomposition needs to be changed into $so(4)_1 \supseteq su(2)_1 \times su(2)_1$. The resulting gapped state carries the $SU(2)_1$ semion topological order instead of $G_4 = SO(2)_1$.

Moreover the sixteenfold classification of topological superconductors (TSC) with the presence of interaction[29, 30, 31, 32, 33, 34, 35] suggests the 32-fold G_N-series could have redundancies. On the other hand, the $\mathbb{Z}_{16}$ classification of TSC is based on the canonical local time reversal symmetry, which is fundamentally different from the non-local "antiferrormagnetic" time reversal considered in this manuscript. The $\mathbb{Z}_{32}$ structure of surface topological order could be an artifact of such unconventional time reversal symmetry. Nonetheless, here in section 3.3.1 and 3.3.2, we discuss altenative gapping interactions when $N = 16$ that removes all electronic quasiparticles.

3.3.1 Consequence of the emergent E_8 when $N = 16$

We design alternative interwire backscattering terms in the coupled wire model (2.4) with $N = 16$ Majorana channels per wire. They open a time reversal symmetric energy gap among 16 surface Majorana cones with the same chirality. In general, these terms can also apply when the number of chiral Majorana channel per wire is larger than 16 by acting on a subset of channels. We begin with the bosonized description presented previously in section 2.1.2, where each wire consists of an 8-component chiral $U(1)$ boson $\widetilde{\boldsymbol{\phi}} = (\tilde{\phi}^1, \ldots, \tilde{\phi}^8)$ that bosonizes the complex fermions $c_j = (\psi_{2j-1} + i\psi_{2j})/\sqrt{2} = \exp(i\tilde{\phi}^j)$. This theory is special because it carries non-trivial bosonic primary fields, which can condense. For example the two spinor representations $s_\pm$ correspond to *bosonic* primary fields of $so(16)_1$ with conformal dimension $h_{s_\pm} = 1$ (see eq.(2.18)). In particular we will focus on the even sector s_+. It consists of vertex operators

$$V_{s_+}^{\boldsymbol{\varepsilon}} = e^{i\boldsymbol{\varepsilon}\cdot\widetilde{\boldsymbol{\phi}}/2}, \quad \boldsymbol{\varepsilon} = (\varepsilon_1, \ldots, \varepsilon_8) \tag{3.139}$$

(see eq.(B.24)) for $\varepsilon_j = \pm 1$ with $\varepsilon_1 \ldots \varepsilon_8 = +1$. The $128 = 2^7$ number of combinations naturally matches with the dimension of the even spinor representation of $so(16)$ (see appendix A). These $V_{s_+}^{\boldsymbol{\varepsilon}}$ are related to each other through the OPE with the raising and lowering operators $E^{\boldsymbol{\alpha}} = e^{i\boldsymbol{\alpha}\cdot\widetilde{\boldsymbol{\phi}}} = e^{i(\pm\tilde{\phi}^i \pm\tilde{\phi}^j)}$ of $so(16)_1$ (see (B.8) in appendix B). The 128 lattice vectors $\boldsymbol{\varepsilon}/2$ extend the 112 roots $\boldsymbol{\alpha}$ of $so(16)$ to the root lattice of the exceptional simple Lie algebra E_8 with size 240.[26] The unit dimensional vertex operators $V_{s_+}^{\boldsymbol{\varepsilon}}$ themselves can be regarded as raising and lowering operators that enlarge the $so(16)_1$ current algebra to E_8 at level 1. This extends the current algebra of each wire

$$so(16)_1 \subseteq (E_8)_1 \tag{3.140}$$

and is intimately related to the fact that the surface state can be gapped out without leaving electronic quasiparticles which are non-local with respect to the boson s_+.

The gapping strategy is to condense primary fields in the bosonic sector s_+ between adjacent wires. This is facilitated by interwire backscattering interactions that bipartite the emergent E_8 symmetry.

$$E_8 \supseteq \widetilde{so(8)}_1^+ \times \widetilde{so(8)}_1^- \tag{3.141}$$

However, these $\widetilde{so(8)}_1$ subalgebras are distinct from the ones in the decomposition $so(16)_1 \supseteq so(8)_1 \times so(8)_1$. In particular, we will see that they do not support electronic primary fields $c_j = e^{i\tilde{\phi}^j}$. Out of 128 $\boldsymbol{\varepsilon}$ lattice vectors in (3.139), there is a (non-unique) maximal set of 8 orthonormal vectors $\boldsymbol{\varepsilon}_{(1)}, \ldots, \boldsymbol{\varepsilon}_{(8)}$

$$\frac{1}{2}\boldsymbol{\varepsilon}_{(m)} \cdot \frac{1}{2}\boldsymbol{\varepsilon}_{(n)} = 2\delta_{mn}. \tag{3.142}$$

We choose the set containing the highest weight vector $\boldsymbol{\varepsilon}_{(1)} = (1,1,1,1,1,1,1,1)$:

$$\begin{pmatrix} | & & | \\ \boldsymbol{\varepsilon}_{(1)} & \dots & \boldsymbol{\varepsilon}_{(8)} \\ | & & | \end{pmatrix} = \begin{pmatrix} 1 & 1 & 1 & 1 & 1 & 1 & 1 & 1 \\ 1 & 1 & 1 & 1 & -1 & -1 & -1 & -1 \\ 1 & 1 & -1 & -1 & 1 & 1 & -1 & -1 \\ 1 & 1 & -1 & -1 & -1 & -1 & 1 & 1 \\ 1 & -1 & 1 & -1 & 1 & -1 & 1 & -1 \\ 1 & -1 & 1 & -1 & -1 & 1 & -1 & 1 \\ 1 & -1 & -1 & 1 & 1 & -1 & -1 & 1 \\ 1 & -1 & -1 & 1 & -1 & 1 & 1 & -1 \end{pmatrix}. \tag{3.143}$$

From (2.20), they give 8 mutually commuting bosons $\boldsymbol{\varepsilon}_{(n)} \cdot \boldsymbol{\phi}_y/2$ per wire

$$\begin{aligned} &\left[\frac{1}{2}\boldsymbol{\varepsilon}_{(m)} \cdot \boldsymbol{\phi}_y(x,t), \frac{1}{2}\boldsymbol{\varepsilon}_{(n)} \cdot \boldsymbol{\phi}_{y'}(x',t)\right] \\ &= 2\pi i \delta_{mn}(-1)^y \delta_{yy'} \mathrm{sgn}(x'-x) \end{aligned} \tag{3.144}$$

up to a constant integral multiple of $2\pi i$.

We separate the 8 vectors into two groups $\mathcal{S}^+ = \{\boldsymbol{\varepsilon}_{(1)}, \boldsymbol{\varepsilon}_{(2)}, \boldsymbol{\varepsilon}_{(3)}, \boldsymbol{\varepsilon}_{(4)}\}$ and $\mathcal{S}^- = \{\boldsymbol{\varepsilon}_{(5)}, \boldsymbol{\varepsilon}_{(6)}, \boldsymbol{\varepsilon}_{(7)}, \boldsymbol{\varepsilon}_{(8)}\}$. They defines the two $\widetilde{so(8)}_1^\pm$ subalgebras in E_8, whose roots lie in the root lattice of E_8 orthogonal to $\mathcal{S}^\mp$ respectively. One could pick the simple roots

$$\begin{aligned} &\widetilde{\boldsymbol{\alpha}}_1^+ = \boldsymbol{\varepsilon}_{(1)}/2,\ \widetilde{\boldsymbol{\alpha}}_2^+ = \mathbf{e}_1 + \mathbf{e}_2,\ \widetilde{\boldsymbol{\alpha}}_2^+ = \mathbf{e}_3 + \mathbf{e}_4,\ \widetilde{\boldsymbol{\alpha}}_4^+ = \mathbf{e}_5 + \mathbf{e}_6 \\ &\widetilde{\boldsymbol{\alpha}}_1^- = \boldsymbol{\varepsilon}_{(5)}/2,\ \widetilde{\boldsymbol{\alpha}}_2^- = \mathbf{e}_2 - \mathbf{e}_1,\ \widetilde{\boldsymbol{\alpha}}_2^- = \mathbf{e}_4 - \mathbf{e}_3,\ \widetilde{\boldsymbol{\alpha}}_4^- = \mathbf{e}_6 - \mathbf{e}_5 \end{aligned}$$

so that their inner product recover the Cartan matrix of $so(8)$

$$\widetilde{\boldsymbol{\alpha}}_I^\pm \cdot \widetilde{\boldsymbol{\alpha}}_J^\pm = K_{IJ}, \quad K = \begin{pmatrix} 2 & -1 & -1 & -1 \\ -1 & 2 & 0 & 0 \\ -1 & 0 & 2 & 0 \\ -1 & 0 & 0 & 2 \end{pmatrix} \tag{3.145}$$

while opposite sectors decouple $\widetilde{\boldsymbol{\alpha}}_I^\pm \cdot \widetilde{\boldsymbol{\alpha}}_J^\mp = 0$.

The new gapping potential is constructed by backscattering the two decoupled

$\widetilde{so(8)}^{\pm}_1$ currents to adjacent wires in opposite directions.

$$\mathcal{H}_{\text{int}} = u \sum_{y=-\infty}^{\infty} \mathbf{J}^y_{\widetilde{so(8)}^-_1} \cdot \mathbf{J}^{y+1}_{\widetilde{so(8)}^+_1} \tag{3.146}$$

However not every terms can be written down as 4-fermion interactions. In particular $\mathcal{H}_{\text{int}}$ contains interwire s_+ quasiparticle backscattering

$$V^{\varepsilon}_y V^{-\varepsilon'}_{y+1} + h.c. \sim \cos\left(\sum_{j=1}^{8} \frac{\varepsilon_j}{2}\tilde{\phi}^j_y - \frac{\varepsilon'_j}{2}\tilde{\phi}^j_{y+1}\right) \tag{3.147}$$

for $\varepsilon_j, \varepsilon'_j = \pm 1$, that condenses pairs of s_+'s along adjacent wires and confines all electronic excitations. The $\widetilde{so(8)}^{\pm}_1$ WZW CFT carries three emergent fermionic primary fields

$$\widetilde{c}^{\pm}_p = \exp\left[\frac{i}{2}\left(\tilde{\phi}^{2p-1} \pm \tilde{\phi}^{2p} - \tilde{\phi}^7 \mp \tilde{\phi}^8\right)\right] \tag{3.148}$$

for $p = 1, 2, 3$. All of which have neutral electric charge and even fermion parity with respect to the original electronic operators $c_j = e^{i\tilde{\phi}^j}$. This is because the $\widetilde{c}^{\pm}_p$'s are invariant under the $U(1)$ gauge transformation $\tilde{\phi}^j \to \tilde{\phi}^j + \varphi$. As a result, the interaction (3.146) corresponds to a gapped $\widetilde{SO(8)}_1$ topological order but contains no electron-like anyon excitations. Lastly we notice that this matches with the surface topological order of a type-II topological paramagnet.[113, 32]

3.3.2 Alternative conformal embeddings

The fractionalization $so(9)_1 \supseteq so(3)_3 \otimes so(3)_3$ in 3.1.2.1 is the corner stone for the construction of symmetric gapping interactions when there is an odd number of Majorana species. However, this is not the unique decomposition. In general when the number of Majorana channels is a whole square, the wire can be bipartitioned into $so(n^2)_1 \supseteq so(n)_n \otimes so(n)_n$.[26, 83, 84, 85]

For instance, this provides yet another alternative when $N = 16$ where each wire is fractionalized into a pair of $so(4)_4 = su(2)_4 \times su(2)_4$. The $so(4)_4^\pm$ current operators can be constructed in a similar fashion as those in the $so(3)_3^\pm$ case, $\mathbf{J} = \frac{i}{2}\mathbf{\Sigma}_{ab}^\pm \psi^a \psi^b$ for $\mathbf{\Sigma}^+ = \mathbf{\Sigma} \otimes \mathbb{1}_4$ and $\mathbf{\Sigma}^- = \mathbb{1}_4 \otimes \mathbf{\Sigma}$ where $\mathbf{\Sigma}$ are antisymmetric 4×4 matrices generating $so(4)$. After introducing the current-current backscattering interactions $\mathbf{J}^y_{so(4)_4^-} \cdot \mathbf{J}^{y+1}_{so(4)_4^+}$, the surface would carry a $SO(4)_4 = SU(2)_4 \times SU(2)_4$ topological order. Each $SU(2)_4$ theory contains five anyon types $j = \mathbf{0}, \mathbf{1/2}, \mathbf{1}, \mathbf{3/2}, \mathbf{2}$ with spins $h_j = j(j+1)/6$. The $SO(4)_4$ topological state does not carry fermionic excitations, and therefore, like the previous example in 3.3.1, this gapping potential also removes all electronic quasiparticle excitations.

The gapped symmetric states for N odd are not unique either. For example, the decomposition $so(25)_1 \supseteq so(5)_5 \otimes so(5)_5$ leads to a surface $SO(5)_5$ topological order which is inequivalent to $G_{25} = SO(3)_3 \boxtimes_b SO(8)_1$.

Chapter 4

3D fractional topological insulators (FTI)

Topological insulators (TI) [13, 14, 15, 16] are time-reversal (TR) and charge ($U(1)$) symmetric electronic band insulators. In (3+1)D, they host massless Dirac fermions on the surface that is protected by these symmetries. On the other hand Fractional topological insulators (FTI) [17, 114, 115, 116, 117, 118, 119] in (3+1)D are long range entangled topologically ordered electronic phases. One can not describe FTI using a single-body Hamiltonian. They also exhibit TR and $U(1)$ symmetries, which enriches it's topological order in the sense that a symmetric surface must be anomalous and cannot be realized non-holographically by a true $(2+1)$D system. For this thesis, I considered a series of fermionic FTI, labeled by integers n, whose magneto-electric response is characterized by the θ-angle $\theta = \pi/(2n+1)$ (modulo $2\pi/(2n+1)$) that associates an electric charge of $e^*/2 = e/2(2n+1)$ to each magnetic monopole [120], for e the electric charge of the electron. It is shown before that such FTI support deconfined fermionic parton excitations ψ in the bulk, each carrying a fractional electric charge of $e^* = e/(2n+1)$. The electron decomposes as $\psi_{\mathrm{el}} \sim \psi_1 \ldots \psi_{2n+1}$. There is an emergent gauge symmetry these partons exhibit, for example $\psi_i \to \psi e^{i2\pi g/2n+1}$ for an integer g makes electron a gauge invariant object. In [115] many consistent gauge theories are considered for the FTI with $\nu = 1/(2n+1)$, but here we will consider only the discrete $\mathbb{Z}_{2n+1}$ gauge theory. The $(3+1)$-D TO we discuss is based on this discrete $\mathbb{Z}_{2n+1}$ gauge theory [115]. This theory supports electrically neutral string-like gauge flux Φ, so that a monodromy phase $e^{2\pi i g/(2n+1)}$ is obtained each time ψ orbits around Φ. In other words, ψ carries g gauge charges. g and $2n+1$, both integers, should be relatively prime so that all local quasi-particle must be combinations of the electronic quasi-particles $\psi_{\rm el}$ and must carry integral electric charges and trivial gauge charges.

For TI, the Dirac fermions on the surface can acquire mass in a Ferromagnetic heterostructure where TR symmetry is broken.They also acquire mass in a superconducting heterostructure that breaks the $U(1)$ symmetry. Within the mean-field description such mass terms in the Hamiltonian are of single-body type. It was also shown that in presence of many-body interaction term the surface of TI is gapped but symmetric and has topological order called the "$\mathcal{T}$-Pfaffian"($\mathcal{T}$-Pf) surface state. Such topological order Such Generalizing the surface state of a conventional TI , the surface of a FTI hosts massless Dirac partons coupling with a $\mathbb{Z}_{2n+1}$ gauge theory. Unlike its non-interacting counterpart whose gapless Dirac surface state is symmetry protected in the single-body picture, a FTI is strongly interacting to begin with and there is no topological reason for its surface state to remain gapless. Similar to the TI case, FTI can support different gapped surfaces that corresponds to different symmetries that are broken. Three types of gapped surface states in FTI will be discussed– ferromagnetic surfaces that break TR , superconducting surfaces that break charge $U(1)$, and symmetric gapped surfaces which we denote as generalized $\mathcal{T}$-Pf* surfaces that generalize the $\mathcal{T}$-Pf surface states of a conventional TI .

4.1 Ferromagetic heterostructure

Let's begin with a slab that has opposite TR breaking order which is possible with the opposite orientation of the magnetic field from the ferromagnet. In this slab, in addition to the single-body Dirac mass m for the surface parton, the $\mathbb{Z}_{2n+1}$ gauge sector also shows TR breaking signature. The $\mathbb{Z}_{2n+1}$ gauge theory is only present inside the FTI , and when a flux line Φ terminates at the surface, the TR breaking boundary condition confines an electrically neutral surface gauge quasi-particles, denoted by ζ^a, with gauge charge a at the flux-surface junction (see Fig. 4.1). This gauge flux-charge composite, referred to as a dyon $\delta = \Phi \times \zeta^a$, carries fractional spin $h_\delta = a/(2n+1)$ because a 2π-rotation about the normal axis braids a gauge charges around Φ and results in the monodromy quantum phase of $e^{2\pi i a/(2n+1)}$. TR conjugates all quantum phases so, $a \not\equiv 0$ modulo $2n+1$ breaks TR .

The one-dimensional interface between the two TR conjugate ferromagnetic surface domains hosts a fractional chiral channel. For example, the interface between two ferromagnetic surface domains with opposite ferromagnetic orientations on the surface of a conventional TI bounds a chiral Dirac channel [74, 121, 122], where electrons propagate only in the forward direction. Alternatively, a TI slab with opposite TR breaking ferromagnetic surfaces is topologically identical to a quasi-$(2+1)$-D Chern insulator [123, 124] and supports a chiral Dirac edge mode. Similarly, in the FTI case, the low-energy content of the fractional chiral channel between a pair of TR conjugate ferromagnetic surfaces domains can be inferred by the edge mode of a FTI slab with TR breaking ferromagnetic surfaces that is topologically identical to a quasi-$(2+1)$-D fractional Chern insulator [125, 126, 127, 128] or fractional quantum Hall (FQH) state [129]. The chiral $(1+1)$-D channel is characterized by two response quantities [130, 131, 132, 133, 71, 76, 77, 73, 78] – the differential electric conductance $\sigma = dI/dV = \nu e^2/h$ that relates the changes of electric current and potential, and the differential thermal conductance $\kappa = dI_T/dT = c(\pi^2 k_B^2/3h)T$ that relates the changes of energy current and temperature. In the slab geometry, they are equivalent to the Hall conductance $\sigma = \sigma_{xy}$, $\kappa = \kappa_{xy}$. $\nu = N_e/N_\phi$ is also referred to as the filling fraction of the FTI slab and associates the gain of electric charge (in units of e) to the addition of a magnetic flux quantum hc/e. $c = c_R - c_L$ is the chiral central charge of the CFT [26] that effectively describes the low-energy degrees of freedom of the fractional chiral channel.

Since the top and bottom surfaces of the FTI slab are TR conjugate, their parton Dirac masses m and gauge flux-charge ratio a have opposite signs. The anyon content is generated by the partons and gauge dyons. When a gauge flux passes through the entire slab geometry from the bottom to the top surface, it associates with total $2a$ gauge charges at the two surface junctions. We denote this dyon by $\gamma = \Phi \times \zeta^{2a}$, which corresponds to an electrically neutral anyon in the slab with spin $h_\gamma = 2a/(2n+1)$. If a is relatively prime with $2n+1$, the primitive dyon generates the chiral Abelian topological field theory $\mathbb{Z}^{(2a)}_{2n+1}$ [134, 135], which consists of the dyons γ^m, for $m = 0, \dots, 2n$, with spins $h_{\gamma^m} = 2am^2/(2n+1)$ modulo 1 and fusion rules $\gamma^m \times \gamma^{m'} = \gamma^{m+m'}$, $\gamma^{2n+1} = \gamma^0 = 1$. In particular, when $a = -1$, γ^n now has spin $-2n^2/(2n+1) \equiv n/(2n+1)$ modulo 1, which is identical to that of the fundamental quasi-particle of the $SU(2n+1)$ Chern-Simons theory at level 1 [134, 135]. This identifies the Abelian theories $\mathbb{Z}^{(-2)}_{2n+1} \cong \mathbb{Z}^{(n)}_{2n+1} = SU(2n+1)_1$, which has chiral central charge $c_{\text{neutral}} = 2n$. For details refer appendix D.

The FTI slab also supports fractionally charged partons ψ, each carrying a gauge charge g. The electrically charged sector can be decoupled from the neutral $\mathbb{Z}^{(2a)}_{2n+1}$ sector by combining each parton with a specific number of dyons $\lambda = \psi \times \gamma^{-n^2 ug}$, where $ua + v(2n+1) = 1$ for some integer u, v, so that the combination is local (i.e. braids trivially) with any dyons γ^m. λ has fractional electric charge $q_\lambda = e^*$ and spin $h_\lambda = 1/2 + n^3 ug^2/(2n+1)$ modulo 1. The $\langle$charge$\rangle$ sector consists of the fractional Abelian quasi-particles products λ^m, where $\lambda^{2n+1} \sim \psi^{2n+1} \sim \psi_{\text{el}}$ corresponds to the local electronic quasi-particles. In particular, when $a = -1$ and $g = -2$, $h_\lambda = 1/2(2n+1)$ and therefore λ behaves exactly like the Laughlin quasi-particle of the FQH state $U(1)_{(2n+1)/2}$ with filling fraction $\nu = 1/(2n+1)$ and chiral central charge $c_{\text{charge}} = 1$. Combining the neutral and charge sectors, the FTI slab with TR breaking ferro-magnetic surface has the decoupled tensor product TO

$$\mathcal{F} = \langle \text{charge} \rangle \otimes \mathbb{Z}_{2n+1}^{(2a)}, \tag{4.1}$$

and in the special case when $a = -1$ and $g = -2$, it is identical to the Abelian state $U(1)_{(2n+1)/2} \otimes SU(2n+1)_1$, which has a total central charge $c = 2n+1$. In general, the filling fraction and chiral central charge are not definite and are subject to surface reconstruction. For instance, the addition of $2N$ electronic Dirac fermions per surface modifies the two response quantities by an equal amount $\nu \to \nu + 2N$, $c \to c + 2N$.

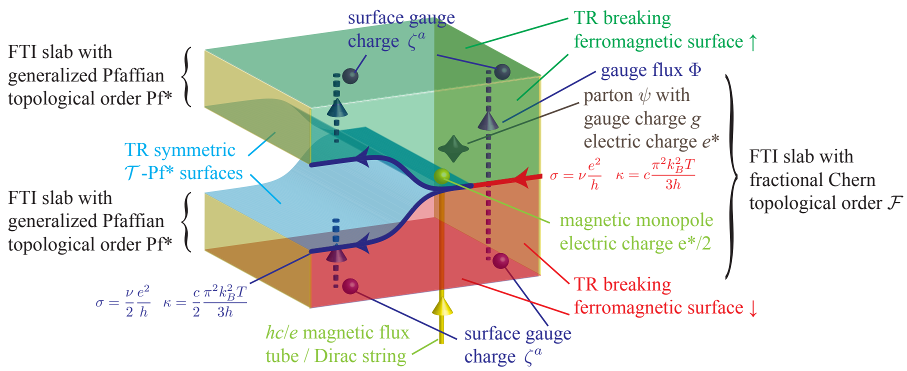

Figure 4.1: Summary of the quasi-particles and gauge flux content in FTI slabs. A pair of Pf* FTI slabs are merged into a fractional Chern FTI slab $\mathcal{F}$ by gluing the two TR symmetric $\mathcal{T}$-Pf* surfaces. Directed bold lines on the front surface are chiral edge modes of the Pf* and $\mathcal{F}$ FTI slabs.

4.2 Superconducting heterostructure

Next we move on to superconducting heterostructures. We begin with the fractional Chern FTI slab $\mathcal{F}$ in (4.1) and introduce weak superconducting pairing, perhaps induced by proximity with a bulk superconductor, without closing the bulk energy gap. In the simplest scenario, this condenses all parton pairs ψ^{2m}, which form a *Lagrangian subgroup* [136] – a maximal set of mutually local bosons – containing the Cooper pair $\psi_{\mathrm{el}}^2 = \psi^{2(2n+1)}$. Since the parton pair ψ^2 carries gauge charge $2g$, which is relatively prime with $2n+1$, the condensate confines all non-trivial dyons γ^m, which are non-local and have non-trivial monodromy with ψ^2. As the neutral sector $\mathbb{Z}_{2n+1}^{(2a)}$ is killed by pairing, the superconducting FTI slab with TR conjugate ferromagnetic surfaces has a trivial fermionic TO . It however still carries chiral fermionic edge modes with the same chiral central charge $c_{\mathcal{F}}$. On the other hand, these fermionic channels also live along the line interface between TR conjugate ferromagnetic domains on the surface of a weakly superconducting FTI . When the line interface hits a TR symmetric superconductor surface island (c.f. Fig. 4.1 by replacing the $\mathcal{T}$-Pf* surfaces by superconductor surface), these chiral channels split and divide along the pair of superconducting-ferromagnetic surface line interfaces. Both of these channels are electrically neutral as charge $U(1)$ symmetry is broken by the superconductor, and each of them carries half of the energy current of $\mathcal{F}$ and has chiral central charge $c_{\mathcal{F}}/2$. For example, the superconductor surface-ferromagnetic surface heterostructure on a conventional TI surface holds a chiral Majorana channel with $c = 1/2$ along the line tri-junction [121, 74]. In the specific fractional case when $a = -1$ and $g = -2$, each superconducting-ferromagnetic surface line interface holds $2n+1$ chiral Majorana fermions and is described by the Wess-Zumino-Witten $SO(2n+1)_1$ CFT with the central charge $c = (2n+1)/2$. Analogous to the conventional superconducting TI surface [137], the superconductor surfaces of the FTI supports a zero energy Majorana bound state (MBS) at a vortex core. Now that the condensate consists of parton pairs, vortices are quantized with the magnetic flux $hc/2e^* = (2n+1)hc/2e$. Each pair of MBS forms a two-level system distinguished by parton fermion parity.

4.3 Generalized $\mathcal{T}$-Pfaffian* surface

Here we describe the $\mathcal{T}$-Pf* surface state that preserves both TR and charge $U(1)$ symmetries of the FTI. Let's first discuss the $\mathcal{T}$-Pf surface state in TI . "Pfaffian" states generally describe non-abelian topological order in fractional quantum Hall states with even denominator filling fraction. The following many-electron wave-function was originally proposed by Moore and Read in [107] for $\nu = 1/q$ fractional quantum Hall state with q being an even integer.

$$\Psi_{Pf}(\{z_i\}) = \text{Pfaff}\left(\frac{1}{z_i - z_j}\right) \Pi_{i<j}\,(z_i - z_j)^q\, e^{-1/4\sum_i |z_i|^2} \tag{4.2}$$

Here z_j is the complex co-ordinate of electrons. The Pfaff() function gives an anti-symmetric matrix. The boundary of such 2+1 D topologically ordered state is characterized by fractional Hall conductance as well as thermal conductance. This boundary is described by a CFT as mentioned in chapter 1 and a particular CFT candidate is $U(1) \otimes Ising$ with central charge $c = 3/2$ describing $\nu = 1/2$ state. The non-trivial quasiparticles at this boundary consists of semions (quasi-particle with fractional charge and spin) co-propagating with neutral Majorana fermions. For the abelian $U(1)$ part of the CFT K-matrix is taken to be 8, hence the charge and spin (mod 1) of all the quasi-particles E_j are $(j/4, j^2/16)$. The Ising part of the CFT is charge neutral and only contributes to the spin of the quasi-particles as shown in table 4.1. The "Pfaffian" TO have quasi-particles $\mathbb{1}_j \equiv \mathbb{1}E_j$, $\Psi_j \equiv \Psi E_j$ and $\Sigma_j \equiv \Sigma E_j$ with spin $\frac{j^2}{16}$, $\frac{j^2}{16} + \frac{1}{2}$ and $\frac{j^2+1}{16}$ respectively. We can observe that this TO doesn't have TR and $U(1)$ symmetry as under these symmetries an anyon would transform to another anyon with opposite spin but same charge. From the table 4.1 we clearly see such partners don't exist within the same charge sectors i.e. for same j.

A related topologically ordered state was proposed in ([69, 36]) for the TR symmetric topologically ordered surface of TI, called the $\mathcal{T}$-Pf state. This TO is char-

Table 4.1: Charge and spin for 24 possible quasi-particles (anyons) in Moore-Read Pfaffian state.

Charge	E_0 0	E_1 e/4	E_2 e/2	E_3 e/4	E_4 e	E_5 5e/4	E_6 6e/4	E_7 7e/4
$\mathbb{1}$	0	1/16	1/4	9/16	1	9/16	1/4	1/16
Ψ	1/2	9/16	3/4	1/16	1/2	1/16	1/4	7/16
Σ	1/16	1/8	5/16	10/16	1/16	10/16	5/16	1/8

acterized by $U(1) \times \overline{Ising}$ CFT at the boundary. Here the charge neutral Majorana mode is counter-propagating with respect to the charged semion mode. The electrical conductance $\sigma = \frac{1}{2}\frac{e^2}{h}$ is same as in the boundary CFT of the Pfaffian state, but the thermal conductance κ alters as does the central charge, $c = \frac{1}{2}$ (see figure 4.2). Such topological ordered state can occur on the surface of TI in the presence of many-body interaction as shown in [69]. This CFT also gives 24 quasi-particles $\{\overline{\mathbb{1}}E_j \equiv \mathbb{1}_j, \overline{\Psi}E_j \equiv \Psi_j, \overline{\Sigma}E_j \equiv \Sigma_j\}$ like in 4.1 although with different spins. Only 12 quasi-particles among these, $\mathbb{1}_{j \text{ even}}$, $\Psi_{j \text{ even}}$ and $\Sigma_{j \text{ odd}}$, braid trivially with the electron quasi-particle Ψ_4 i.e they have trivial monodromy phase with electron (multiple of 2π). Assuming all the π-fluxes are confined then only these 12 quasi-particles are possible for this state.The fusion and braiding operations are product of the operations for $U(1)$ and Ising. This state has both TR as well as $U(1)$ symmetry. The symmetry transformation maps bosons and fermions to themselves and switches semions within the same charge sector.

$$\mathbb{1}_2 \leftrightarrow \Psi_2,\ \mathbb{1}_6 \leftrightarrow \Psi_6 \tag{4.3}$$

The square of TR is a local unitary symmetry which assigns phase to each anyon in the T-Pf state, $T^2|a\rangle \rightarrow e^{i\phi(x)}|a\rangle$[38, 39]. A *Kramers doublet* is assigned a phase $T^2 = -1$ and a *Kramers singlet* is assigned a phase $T^2 = -1$. According to Kramer's theorem, fermions form doublets and bosons form singlets. But for $\mathcal{T}$-Pf state $\mathbb{1}_4$ with integer topological spin turns out to be a *Kramers doublet*. Similarly, Ψ_0 with half-integer topological spin is a *Kramers singlet*. In addition to such anomaly in the time-reversal property[138, 139], the state also exhibits chiral anomaly. Hence, $\mathcal{T}$-Pf TO can not be realized in a pure 2D system and must be supported by a 3D bulk.

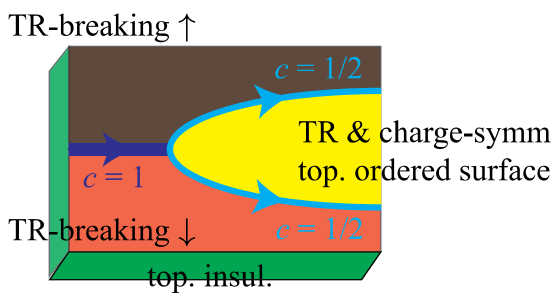

Figure 4.2: Gapped surfaces on TI. Splitting of central charge showing TO with $c = 1/2$ boundary CFT on the TR symmetric gapped surface.

Generalizing the $\mathcal{T}$-Pf surface state of a conventional TI , the FTI version – referred here as $\mathcal{T}$-Pf* – consists of the Abelian surface anyons $\mathbb{1}_j$ and Ψ_j, for j even, and the non-Abelian Ising-like anyons Σ_j, for j odd. The index j corresponds to the fractional electric charge $q_j = je/4(2n+1)$. $n = 1$ corresponds to $\mathcal{T}$-Pf state.The surface anyons satisfy the fusion rules

$$\begin{aligned} \mathbb{1}_j \times \mathbb{1}_{j'} = \Psi_j \times \Psi_{j'} = \mathbb{1}_{j+j'}, \quad \mathbb{1}_j \times \Psi_{j'} = \Psi_{j+j'}, \\ \Psi_j \times \Sigma_{j'} = \Sigma_{j+j'}, \quad \Sigma_j \times \Sigma_{j'} = \mathbb{1}_{j+j'} + \Psi_{j+j'}, \end{aligned} \tag{4.4}$$

and the spin statistics

$$h_{\mathbb{1}_j} = h_{\Psi_j} - \frac{1}{2} = \frac{j^2}{16}, \quad h_{\Sigma_j} = \frac{j^2-1}{16} \quad \text{modulo } 1 \tag{4.5}$$

so that $\mathbb{1}_j, \Psi_j$ are bosonic, fermionic or semionic, and Σ_j are bosonic or fermionic. The fermion Ψ_4 is identical to the super-selection sector of the bulk parton ψ, which is local with respect to all surface anyons and can escape from the surface and move into the bulk of FTI . TR symmetry acts on the surface anyons the same way it acts on those in the $\mathcal{T}$-Pf state for conventional TI [38, 140]. For example, the parton combinations

$\psi^{2j+1} = \Psi_{8j+4}$ (and $\psi^{2j} = \mathbb{1}_{8j}$) are Kramers doublet fermions (respectively Kramers singlet bosons), while Ψ_{8j} ($\mathbb{1}_{8j+4}$) are Kramers singlet fermions (respectively Kramers doublet bosons). Moreover, for identical reasons as in the conventional TI case, the $\mathcal{T}$-Pf* state is anomalous and can only be supported holographically on the surface of a topological bulk. For instance, the bosonic TO of the $\mathcal{T}$-Pf* state with all the quasi-particles including those with monodromy phase π w.r.t. electron (π-fluxes) i.e. after gauging fermion parity would necessarily violate TR symmetry. Please note that there are alternative surface TO that generalize those in Refs.[36, 37]. However I will only focus on the $\mathcal{T}$-Pf* state in this thesis.

The generalized Pfaffian state described by the following CFT contains the $\mathcal{T}$-Pf* state as a subset.

$$\text{Pf}^* = U(1) \otimes Ising \otimes \overline{Z_{2n+1}} \tag{4.6}$$

Here $\overline{Z_{2n+1}}$ is a chiral gauge theory that is charge neutral. The Ising part is also charge neutral and identical to either SO$(15-2n)$ or SO$(7-2n)$. The charge part, $U(1)$ can be described using an abelian Chern simons theory with k-matrix $8(2n+1)$ denoted by $U(1)_{4(2n+1)}$. One can check that this is a modular CFT and indeed contains $\mathcal{T}$-Pf* quasi-particles as a subset. In fact, note that for $n > 0$, the TO corresponding to $U(1) \otimes Ising$ CFT has no subset of anyons that can form a TR symmetric TO . The chiral $\overline{Z_{2n+1}}$ part adds quasi-particles such that a subset of the quasi-particles are closed under time-reversal transformation along with charge conservation. FTI bulk supports the emergent discrete Z_{2n+1} gauge theory which may give rise to the chiral $\overline{Z_{2n+1}}$ gauge theory on the surface. The $\mathcal{T}$-Pf* surface state and generalized Pfaffian state in a FTI slab geometry will be discussed next.

The FTI slab with a TR symmetric $\mathcal{T}$-Pf* top surface and a TR breaking bottom ferromagnet surface carries a novel quasi-(2+1)-D TO . Its topological content consists of the fractional partons coupled with the $\mathbb{Z}_{2n+1}$ gauge theory in the bulk and the $\mathcal{T}$-Pf* surface state (see Fig. 4.1). All surface anyons are confined to the TR symmetric surface except the parton combinations $\psi^{2j+1} = \Psi_{8j+4}$ and $\psi^{2j} = \mathbb{1}_{8j}$. Moreover, the TR breaking boundary condition confines a gauge quasi-particle ζ^a per gauge flux Φ ending on the ferromagnet surface. On the other hand, there is no gauge charge associated with a gauge flux ending on the $\mathcal{T}$-Pf* surface because of TR symmetry. Thus a gauge flux passing through the entire slab corresponds to the dyon $\delta = \Phi \times \zeta^a$ with spin $h_\delta = a/(2n+1)$ modulo 1. The $\mathcal{T}$-Pf* state couples non-trivially to the $\mathbb{Z}_{2n+1}$ gauge theory as the parton $\psi = \Psi_4$ carries a gauge charge g. The general surface anyons X_j, for $X = \mathbb{1}, \Psi, \Sigma$, must carry the gauge charge $z(j) \equiv n^2 gj$ modulo $2n+1$ and associate to the monodromy quantum phase $e^{2\pi i z(j)/(2n+1)}$ when orbiting around the dyon δ. For instance, as $2n \equiv -1$ modulo $2n+1$, $z(4j) \equiv gj$ counts the gauge charge of the parton combination ψ^j.

The TO of this FTI slab is therefore generated by combinations of the $\mathcal{T}$-Pf* anyons and the dyon δ. We denote the composite anyon by

$$\tilde{X}_{j,z} = X_j \otimes \delta^{z+n^3ugj}, \tag{4.7}$$

where $X = \mathbb{1}, \Psi$ for j even or Σ for j odd, $z = 0, \ldots, 2n$ modulo $2n+1$, and $ua + v(2n+1) = 1$. They satisfy the fusion rules

$$\begin{gathered}
\tilde{\mathbb{1}}_{j,z} \times \tilde{\mathbb{1}}_{j',z'} = \tilde{\Psi}_{j,z} \times \tilde{\Psi}_{j',z'} = \tilde{\mathbb{1}}_{j+j',z+z'}, \\
\tilde{\mathbb{1}}_{j,z} \times \tilde{\Psi}_{j',z'} = \tilde{\Psi}_{j+j',z+z'}, \quad \tilde{\Psi}_{j,z} \times \tilde{\Sigma}_{j',z'} = \tilde{\Sigma}_{j+j',z+z'}, \\
\tilde{\Sigma}_{j,z} \times \tilde{\Sigma}_{j',z'} = \tilde{\mathbb{1}}_{j+j',z+z'} + \tilde{\Psi}_{j+j',z+z'}.
\end{gathered} \tag{4.8}$$

They follow the spin statistics

$$\begin{aligned} h(\tilde{\mathbb{1}}_{j,z}) &= h(\tilde{\Psi}_{j,z}) - \frac{1}{2} = h(\tilde{\Sigma}_{j,z}) + \frac{1}{16} \\ &= \frac{j^2}{16} + \frac{az^2 - n^6 ug^2 j^2}{2n+1} \quad \text{modulo } 1. \end{aligned} \tag{4.9}$$

The j, z indices in (4.7) are defined in a way so that $\tilde{X}_{j,0}$ are local with respect to the dyons $\delta^z = \tilde{\mathbb{1}}_{0,z}$ and decoupled from the dyon sector $\mathbb{Z}^{(a)}_{2n+1}$. The $\mathcal{T}$-Pf* surface anyons belong to the subset $X_j = \tilde{X}_{j,-n^3ugj}$, which is a maximal sub-category that admits a TR symmetry. The electronic quasi-particle belongs to the super-selection sector $\psi_{\mathrm{el}} = \tilde{\Psi}_{4(2n+1),0}$, which is local with respect to all anyons. If one gauges fermion parity and includes anyons that associate -1 monodromy phase with ψ_{el}, i.e. if one includes $\tilde{\mathbb{1}}_{j,z}, \tilde{\Psi}_{j,z}$ for j odd and $\tilde{\Sigma}_{j,z}$ for j even, the $\langle\overline{\mathrm{Ising}}\rangle$ sector generated by $1 = \tilde{\mathbb{1}}_{0,0}$, $f = \tilde{\Psi}_{0,0}$, $\sigma = \tilde{\Sigma}_{0,0}$ is local with and decoupled from the $\langle\mathrm{charge}\rangle_{\mathrm{Pf}^*}$ sector generated by $\tilde{\mathbb{1}}_{j,0}$. The TO of the FTI slab thus takes the decoupled tensor product form after gauging fermion parity

$$\mathrm{Pf}^* = \langle\mathrm{charge}\rangle_{\mathrm{Pf}^*} \otimes \langle\overline{\mathrm{Ising}}\rangle \otimes \mathbb{Z}^{(a)}_{2n+1}. \tag{4.10}$$

Gauging fermion parity is not the focus of this thesis. Nevertheless, we notice in passing that there are inequivalent ways of fermion parity gauging, and in order for the Pf* theory to have the appropriate central charge, (4.10) needs to be modified by a neutral Abelian $SO(2n)_1$ sector [140]. However, the tensor product (4.10) is sufficient and correct to describe the fermionic TO of the FTI slab (with global ungauged fermion parity) by restricting to super-selection sectors $\tilde{X}_{j,z}$ that are local with respect to the electronic quasi-particle ψ_{el}. We refer to this fermionic TO as a generalized Pfaffian state. The next section discusses how this generalized Pfaffian state proposed is indeed consistent with our understanding of the ferromagnetic surfaces in FTI explained in sec (4.1).

4.4 Gluing $\mathcal{T}$-Pfaffian* surfaces

The chiral channel $\mathcal{F}$ in (4.1) between a pair of TR conjugate FS domains divides into a pair of fermionic Pf* in (4.10) at a junction where the two ferromagnetic surface domains sandwich a TR symmetric $\mathcal{T}$-Pf* surface domain (see Fig. 4.1). Conservation of charge and energy requires the filling fractions and chiral central charges to equally split, i.e. $2\nu_{\mathrm{Pf}^*} = \nu_{\mathcal{F}}$ and $2c_{\mathrm{Pf}^*} = c_{\mathcal{F}}$. For instance, in the prototype case when $a = -1$ and $g = -2$, $\nu_{\mathrm{Pf}^*} = 1/2(2n+1)$ and $c_{\mathrm{Pf}^*} = (2n+1)/2$. Similar to the aforementioned $\mathcal{F}$ case, these quantities are subjected to surface reconstruction $\nu \to \nu + N$, $c \to c + N$.

In addition to the response quantities, the TO of $\mathcal{F}$ for the FTI slab with TR conjugate ferromagnetic surface is related to that of the fermionic Pf* by a *relative tensor product*

$$\mathcal{F} = \mathrm{Pf}^* \boxtimes_b \mathrm{Pf}^*. \tag{4.11}$$

This can be understood by juxtaposing the TR symmetric surfaces of a pair of Pf* FTI slabs and condensing surface bosonic anyon pairs on the two $\mathcal{T}$-Pf* surfaces. This anyon condensation [110, 141, 142] procedure effectively glues the two FTI slabs together along the TR symmetric surfaces (see Fig. 4.1). The relative tensor product $\boxtimes_b$ involves first taking a decoupled tensor product $(\mathrm{Pf}^*)^A \otimes (\mathrm{Pf}^*)^B$ when the two Pf* FTI slabs denoted by A and B are put side by side. The quasi-particles in this decoupled tensor product are of the form $\tilde{X}^A_{j_a,z_a}\tilde{X}^B_{j_b,z_b}$ which consists of a pair of $\mathcal{T}$-Pf* anyons and a pair of dyons. Out of these we choose a set of Bosons that braid trivially with each other and condense them to the vaccum. All the quasi-particles identified as vaccum should be charge neutral and should braid trivially with all the other anyons in the condensed phase. A natural choice for vaccum is the parton pair $\Psi^A_4\Psi^B_{-4}$, which is combination of parton creation and anhilation operator. This is because partons are deconfined in FTI bulk. Anything that braids with it is confined.

We can derive braiding statistics with the ribbon formula, $\theta_{A,B} = h_{A\times B} - h_A - h_B$. The braiding phase from the anyon combination $\tilde{X}^A_{j_a,z_a}\tilde{X}^B_{j_b,z_b}$ around $\Psi^A_4\Psi^B_{-4}$ is the same as $(\delta^A)^{z_a+n^3ugj_a}(\delta^B)^{z_b+n^3ugj_b}$ around $\Psi^A_4\Psi^B_{-4}$. This is because the parton Ψ_4 braids trivially with anyons in the $\mathcal{T}$-Pf* surface state but non-trivially with partons because it carries "g" gauge charges, so this phase is $g(z_a + n^3ugj_a - z_b - n^3ugj_b)$. This is zero if the dyon number $z + n^3ugj$ is equal on the A and B particle. This ensures gauge fluxes must continue through both A and B slabs, i.e., gauge magnetic monopoles are confined. If we define the dyon pair which consist of continuos gauge flux , $\gamma^z \equiv \tilde{\mathbb{1}}^A_{0,z}\tilde{\mathbb{1}}^B_{0,z}$ then quasi-particles that are not confined are of the form $X^A_{j_a}X^B_{j_b}\gamma^z$.

Quasi-particles that differ by $\Psi^A_4\Psi^B_{-4}$ are now identified as follows

$$
\begin{aligned}
&\mathbb{1}^A_{j_a}\mathbb{1}^B_{j_b}\gamma^z \equiv \Psi^A_{j_a+4}\Psi^B_{j_b-4}\gamma^z \equiv \mathbb{1}^A_{j_a+8}\mathbb{1}^B_{j_b-8}\gamma^z,\\
&\mathbb{1}^A_{j_a}\Psi^B_{j_b}\gamma^z \equiv \Psi^A_{j_a+4}\mathbb{1}^B_{j_b-4}\gamma^z \equiv \mathbb{1}^A_{j_a+8}\Psi^B_{j_b-8}\gamma^z,\\
&\Sigma^A_{j_a}\Sigma^B_{j_b}\gamma^z \equiv \Sigma^A_{j_a+4}\Sigma^B_{j_b-4}\gamma^z,\\
&\mathbb{1}^A_{j_a}\Sigma^B_{j_b}\gamma^z \equiv \Psi^A_{j_a+4}\Sigma^B_{j_b-4}\gamma^z \equiv \mathbb{1}^A_{j_a+8}\Sigma^B_{j_b-8}\gamma^z \equiv \Psi^A_{j_a+12}\Sigma^B_{j_b-12}\gamma^z.
\end{aligned}
$$

Next we choose the fermion pair $\Psi^A_0\Psi^B_0$. Notice Σ braids with Ψ, so anything with just one Σ is confined. This brings the identification to

$$
\begin{aligned}
&\mathbb{1}^A_{j_a}\mathbb{1}^B_{j_b}\gamma^z \equiv \mathbb{1}^A_{j_a+4j}\mathbb{1}^B_{j_b-4j}\gamma^z \equiv \Psi^A_{j_a+4j}\Psi^B_{j_b-4j}\gamma^z,\\
&\mathbb{1}^A_{j_a}\Psi^B_{j_b}\gamma^z \equiv \mathbb{1}^A_{j_a+4j}\Psi^B_{j_b-4j}\gamma^z \equiv \Psi^A_{j_a+4j}\mathbb{1}^B_{j_b-4j}\gamma^z,\\
&\Sigma^A_{j_a}\Sigma^B_{j_b}\gamma^z \equiv \Sigma^A_{j_a+4j}\Sigma^B_{j_b-4j}\gamma^z.
\end{aligned}
$$

Next we can condense $\Psi^A_2\mathbb{1}^B_{-2}$, which when braided around $\mathbb{1}^A_{j_a}\mathbb{1}^B_{j_b}$ or $\Psi^A_{j_a}\mathbb{1}^B_{j_b}$ gives $4(j_a - j_b)/16$. So, they are not confined if $j_a - j_b = 0 \bmod 4$. When $\Psi^A_2\mathbb{1}^B_{-2}$ braids around $\Sigma^A_{j_a}\Sigma^B_{j_b}$ it gives $4(j_a - j_b)/16 + 1/2$ which is not confined if $j_a - j_b = 2 \bmod 4$.

The identification is now

$$
\begin{aligned}
\mathbb{1}^A_{j_a}\mathbb{1}^B_{j_b}\gamma^z &\equiv \mathbb{1}^A_{j_a+4j}\mathbb{1}^B_{j_b-4j}\gamma^z \equiv \Psi^A_{j_a+4j}\Psi^B_{j_b-4j}\gamma^z \\
&\equiv \mathbb{1}^A_{j_a+2}\Psi^B_{j_b-2}\gamma^z \equiv \mathbb{1}^A_{j_a+2+4j}\Psi^B_{j_b-2-4j}\gamma^z \\
&\equiv \Psi^A_{j_a+2+4j}\mathbb{1}^B_{j_b-2-4j}\gamma^z, \\
\Sigma^A_{j_a}\Sigma^B_{j_b}\gamma^z &\equiv \Sigma^A_{j_a+2j}\Sigma^B_{j_b-2j}\gamma^z.
\end{aligned}
$$

$\Sigma\Sigma$ pairs have quantum dimension 2 so they split into simpler Abelian components

$$
\Sigma^A_{j_a}\Sigma^B_{j_b} = S^+_{j_a,j_b} + S^-_{j_a,j_b}, \tag{4.12}
$$

where each $S^\pm$ carries the same spin as the original Ising pair but differs from each other by a unit fermion $S^\pm \times \Psi^{A/B} = S^\mp$. S^+ and S^- normally have non-trivial mutual monodromy. We choose to condense the electrically neutral $S^+_{1,-1}$ and its multiples, while confining $S^-_{1,-1}$. This means $\Sigma^A_1\Sigma^B_{-1}$ is condensed. The Σ pair around $\mathbb{1}^A_{j_a}\mathbb{1}^B_{j_b}$ gives a phase of $2(j_a-j_b)/16$ which is zero if $j_a - j_b = 0$ mod 8. The Σ pair around $\mathbb{1}^A_{j_a}\Psi^B_{j_b}$ gives a phase of $2(j_a-j_b)/16 + 1/2$ which is zero if $j_a - j_b = 4$ mod 8. The Σ pair around $\Sigma^A_{j_a}\Sigma^B_{j_b}$ gives a phase of $2(j_a-j_b)/16 \pm 1/4$ which is zero if $j_a - j_b = 2$ or 6 mod 8.

The condensate is now complete, and we have the identification

$$
\begin{aligned}
\mathbb{1}^A_{j_a}\mathbb{1}^B_{j_b}\gamma^z &\equiv \Psi^A_{j_a,z}\Psi^B_{j_b,z}\gamma^z \equiv \Psi^A_{j_a+2}\mathbb{1}^B_{j_b-2}\gamma^z \\
&\equiv \mathbb{1}^A_{j_a+2}\Psi^B_{j_b-2,z}\gamma^z \equiv S^\pm_{j_a\pm1,j_b\mp1}\gamma^z \\
&\equiv \mathbb{1}^A_{j_a+4}\mathbb{1}^B_{j_b-4}\gamma^z
\end{aligned} \tag{4.13}
$$

for $j_a \equiv j_b$ mod 8 and j_a, j_b both even. These residual quasi-particles are just the multiples of the parton $\mathbb{1}^A_0\Psi^B_4$ together with the dyons γ^z. They generate the FTI slab topological order, $\mathcal{F}$ when it has a pair of conjugate TR breaking surfaces.

Equation 4.13 are just parton combinations. For instance, $\psi^A = \Psi_4^A \mathbb{1}_0^B \equiv \mathbb{1}_4^A \Psi_4^B = \psi^B$ are now free to move inside both FTI slabs after gluing. The TO after the gluing is generated by the partons and dyons, which behave identically to those in $\mathcal{F}$ of (4.1). This proves (4.11). The anyon condensation or the gluing of a pair of $\mathcal{T}$-Pf* states preserves symmetries for the same reason it does for the conventional TI case [38, 140].

It is worth noting that a magnetic monopole can be mimicked by a magnetic flux tube / Dirac string (with flux quantum hc/e) that originates at the TR symmetric surface interface and passes through one of the two FTI slab, say the A slab. In the prototype $a = -2$ and $g = -1$, the filling fraction $\nu_{\mathrm{Pf}^*} = 1/2(2n+1)$ of the quasi-two-dimensional slab ensures, according to the Laughlin argument [130], that the monopole associates to the fractional charge $q = 1/2(2n+1)$, which is carried by the confined $\mathcal{T}$-Pf* surface anyons $\mathbb{1}_2^A$ or Ψ_2^A. This surface condensation picture therefore provides a simple verification of the Witten effect [120] for $\theta = \pi/(2n+1)$.

At last notice that in the band insulator case for $n = 0$, $\mathcal{F}$ in (4.1) reduces to the Chern insulator or the lowest Landau level (LLL), and Pf* in (4.10) is simply the particle-hole (PH) symmetric Pfaffian state [143, 144, 145]. The PH symmetry is captured by the relative tensor product (4.11), which can be formally rewritten into

$$\mathrm{Pf}^* = \mathcal{F} \boxtimes \overline{\mathrm{Pf}^*} \tag{4.14}$$

by putting Pf* on the other side of the equation. Here, the tensor product is relative with respect to some collection of condensed bosonic pairs, and $\overline{\mathrm{Pf}^*}$ is the TR conjugate of Pf*. Equation (4.14) thus equates Pf* with its PH conjugate, which is obtained by subtracting itself from the LLL . In the fractional case with $n > 0$, (4.14) suggests a generalized PH symmetry for Pf*, whose PH conjugate is the subtraction of itself from the FQH state $\mathcal{F}$.

Chapter 5

Conclusion

We constructed a coupled Majorana wire model in (2+1)D that imitates the massless Majorana modes on the surface of a topological superconductor. This model had a non-local "antiferromagnetic" time reversal symmetry and consequently was $\mathbb{Z}_2$ classified – rather than $\mathbb{Z}$ in the class DIII TSC case – under the single-body framework. Despite the difference, this model adequately described the surface behavior of a TSC when the number N of Majorana species was odd, and it was worth studying and interesting in and of itself.

We introduced the 4-fermion gapping potentials in section 3.1. They relied on the fractionalization or bipartition of the $so(N)_1$ current along each wire into a pair of $\mathcal{G}_N$ channels (see eq.(3.4) and (3.5)). The two fractional channels were then backscattered onto adjacent wires in opposite directions. This localized all the low energy degrees of freedom and opened an excitations energy gap without breaking the time reversal symmetry. When $N = 2r$ was even, each wire could simply be split into a pair of $\mathcal{G}_N = so(r)_1$ channels. The fractionalization was not as obvious when N was odd. We first made use of the conformal embedding that decomposed nine Majorana's into two subsectors, $so(9)_1 \supseteq so(3)_3 \otimes so(3)_3$ (see section 3.1.2.1). This division could be generalized by all odd cases by splitting a subset of 9 Majorana's into a pair of $so(3)_3$

and the remaining even number of Majorana's into a pair of $so(r)_1$. This could even be applied when N is less then 9 because each wire could be reconstructed by adding same number of right and left movers.

The surface G_N topological order was inferred from the bulk-boundary correspondence (see eq.(3.91)). These topological states followed a 32-fold periodicity $G_N \cong G_{N+32}$ and a relative tensor product structure $G_{N_1} \boxtimes_b G_{N_2} \cong G_{N_1+N_2}$. We presented the quasiparticle types as well as their fusion and braiding statistics properties. We explained the relative tensor product structure using the notion of anyon condenstion[110]. On a more fundamental level, one should be able to deduce the topological order without the knowledge of the boundary by studying the modular properties of the degenerate bulk ground states under a compact torus geometry[102], or by directly looking at the exchange and braiding behaviors of bulk excitations (i.e. on 2+1 D surface). In fact the coupled wire construction provided a fitting model for this purpose. Being an exactly solvable model, a ground state could be explicitly expressed as entangled superposition of tensor product ground states between each pair of wires. In the simplest case when the model is bosonizable i.e. for the even N, a ground state could be specified by the pinned angle variables of a collection of sine-Gordon potentials. The bulk excitations could be realized as kinks between a pair of wires and could be created by vertex operators. We couldn't find a straight-forward method to find the ground states for the odd N case. Finding the ground state for odd N case will also provide us the operators corresponding to the non-abelian anyons. The non-abelian anyons corresponding to $SO(3)_3$ TO has not appeared in any other system. Hence finding the ground state for this interacting Hamiltonian for $N = 9$ is an important problem and will be addressed in future.

We noticed that there were alternative ways of fractionalization that led to different gapping interactions and consequently different topological orders. We saw in section 3.1.1.2 that $N = 4$ was an exceptional case that requires the special bipartition

$so(4)_1 \supseteq su(2)_1 \times su(2)_1$ instead of two copies of $so(2)_1$. We also saw in section 3.3 that when $N = 16$, the surface could be gapped by alternative interactions that corresponded to a $\widetilde{SO(8)}_1$ or $SO(4)_4$ topological order, none of which contained electronic quasiparticle excitations. Other conformal embeddings $so(n^2)_1 \supseteq so(n)_n \otimes so(n)_n$ could give rise to multiple possibilities. Our 32-fold topological states, which only utilized $so(9)_1 \supseteq so(3)_3 \otimes so(3)_3$, therefore should belong into a wider universal framework. These is to be understood in future.

We also studied gapped FTI surface states with (i) TR breaking order, (ii) charge $U(1)$ breaking order, as well as (iii) symmetry preserving $\mathcal{T}$-pfaffian* topological order. The FTI was described using fractionally charged Dirac partons. We considered the simplest type of FTI where partons coupled with a discrete $\mathbb{Z}_{2n+1}$ gauge theory for integer n. We characterized the fractional interface channels sandwiched between different gapped surface domains by describing their charge and energy response, namely the differential electric and thermal conductance. The low-energy CFT for these fractional interface channels corresponded to the TO of quasi-(2+1) dimensional FTI slabs with the corresponding gapped top and bottom surfaces. In particular, a FTI slab with TR conjugate ferromagnetic surfaces behaved like a fractional Chern insulator with TO (4.1). For the specific values of the parameters in our model, $a = -1$ and $g = -2$, its charge sector was identical to that of the Laughlin $\nu = 1/(2n+1)$ fractional quantum Hall state. When $n = 3$, CFT at the interface is given by $U(1)_{3/2} \times SU(3)_1$ where the charged part $U(1)_{3/2}$ correspond to the CFT for the Laughlin state with filling fraction $\nu = \frac{1}{3}$. The neutral part $SU(3)_1$ corresponds to gauge degrees of freedom. In future we will explore how to write a coupled elecron wire model with inter-wire interaction, such that $U(1)_{3/2} \times SU(3)_1$ CFT will be left behind at the edge after all the electrons in the bulk are localized. Such model will give us the explicit electron interaction that results in $2+1$ D topologically ordered state with $SU(3)$ gauge theory.

We proposed a generalized $\mathcal{T}$-Pf* TR symmetric surface state for the surface of FTI slab. Combining the top TR symmetric $\mathcal{T}$-Pf* surface with the FTI bulk as well as the bottom TR breaking surface, this FTI slab exhibited a generalized Pfaffian TO ,Pf* (4.10). Here we have $2n+1$ times more anyons compared to the $\mathcal{T}$-Pf surface state. The anyons in this generalized state have additional gauge charges. The electromagnetic charge for these anyons were quantized in multiples of $\frac{j}{4(2n+1)}$ instead of $\frac{j}{4}$, which is charge quantum in $\mathcal{T}$-Pf state. In fact $n=0$ $\mathcal{T}$-Pf* state is the $\mathcal{T}$-Pf state. The CFT corresponding to the generalized Pfaffian TO at the interface between TR breaking gapped surface and TR symmetric gapped $\mathcal{T}$-Pf* surface were shown to have differential electrical conductance, $\sigma = \frac{dI}{dv} = \frac{1}{2n+1}\frac{e^2}{h}$ and thermal conductance, $\frac{1}{2}\frac{\pi^2 k_B^2 T}{3h}$(see figure 4.1). For general n, the CFT was shown to be $U(1) \times Ising \times \overline{Z_{2n+1}}$ where only $U(1)$ is a charged theory. $\overline{Z_{2n+1}}$ is the chiral part of Z_{2n+1} gauge theory. Such CFT may also appear at the edge of a fractional quantum Hall state and should be explored in future. Furthermore, we demonstrated the gluing of a pair of parallel $\mathcal{T}$-pfaffian* surfaces, which are supported by two FTI bulk on both sides. It was captured by an anyon condensation picture that killed the $\mathcal{T}$-pfaffian* TO and left behind deconfined partons and confined gauge and magnetic monopoles in the bulk. This condensation of a pair of generalized pfaffian TO to Laughlin-like $\mathcal{F}$ TO using the corresponding Chern-Simon's K- matrices will be explored in future.

A related work Ref. [140] also constructs the $\mathcal{T}$-pfaffian* state of the FTI from the field theoretic duality approach and is complementary to this work.

Appendix A

The $so(N)$ Lie algebra and its representations

The $so(N)$ Lie algebra are generated by real antisymmetric matrices $t^{(rs)} = \left(t_{ab}^{(rs)}\right)_{N\times N}$ with entries

$$t_{ab}^{(rs)} = \delta_a^r \delta_b^s - \delta_b^r \delta_a^s \tag{A.1}$$

for $r, s = 1, \ldots, N$. There are $N(N-1)/2$ linearly independent generators since $t^{(rs)} = -t^{(sr)}$ and $t^{(rr)} = 0$. In the main text, we write the basis labels as $\beta = (rs)$, for $r < s$, for conciseness. The generators obey the commutator relation

$$\left[t^{(rs)}, t^{(pq)}\right] = \sum_{m<n} f_{(rs)(pq)(mn)} t^{(mn)} \tag{A.2}$$

where the structure constant is

$$\begin{aligned} f_{(rs)(pq)(mn)} =& \delta_{mr}\delta_{nq}\delta_{sp} - \delta_{mr}\delta_{np}\delta_{sq} \\ &+ \delta_{ms}\delta_{rq}\delta_{np} - \delta_{ms}\delta_{nq}\delta_{rp}. \end{aligned} \tag{A.3}$$

The matrix representation (A.1) is referred as the fundamental representation of $so(N)$ and is labeled by ψ. In general the generators of $so(N)$ can have different irreducible matrix representations $t_\lambda^{(rs)} = t_\lambda^\beta$ labeled by λ. Since the quadratic Casimir operator

$$\hat{\mathcal{Q}}_\lambda = -\sum_\beta t_\lambda^\beta t_\lambda^\beta \tag{A.4}$$

commutes with all the generators, it must have a fixed eigenvalue $\mathcal{Q}_\lambda$ that (incompletely) characterizes the irreducible representation λ. For instance, the fundamental representation in (A.1), denoted by ψ, has quadratic Casimir value $\mathcal{Q}_\psi = N - 1$.

The spinor representation σ of $so(N)$ makes use of the Clifford algebra[146] $\{\gamma_a, \gamma_b\} = \gamma_a\gamma_b + \gamma_b\gamma_a = 2\delta_{ab}$ where $\gamma_1, \ldots, \gamma_N$ are hermitian matrices of dimension $d = 2^{N/2}$ for N even or $d = 2^{(N-1)/2}$ for N odd. The $so(N)$ generators are represented as the quadratic combination

$$t_\sigma^{(rs)} = \frac{1}{4}\sum_{ab} \gamma_a t_{ab}^{(rs)} \gamma_b = \frac{1}{2}\gamma_r\gamma_s \tag{A.5}$$

and satisfy (A.2). When N is even, the parity operator $(-1)^F = i^{N/2}\gamma_1 \ldots \gamma_N$ commutes with all $t_\sigma^{(rs)}$ and the representation is decomposable into $\sigma = s_+ \oplus s_-$, where $s_\pm$ are $2^{N/2-1}$-dimensional sectors with $(-1)^F = \pm 1$. The $so(N)$ generators are then irreducibly represented by

$$t_{s_\pm}^{(rs)} = P_\pm t_\sigma^{(rs)} P_\pm^\dagger \tag{A.6}$$

where $P_\pm$ are the projection operators onto the fixed parity subspaces. As $t_\sigma^{(rs)} t_\sigma^{(rs)} = -(1/4)\mathbb{1}$, the quadratic Casimir values (A.4) of spinor representations are

$$\mathcal{Q}_\sigma = \frac{N(N-1)}{8}, \quad \mathcal{Q}_{s_\pm} = \frac{N(N-1)}{8}. \tag{A.7}$$

The complexified $so(N)$ Lie algebra has an alternative set of *Cartan-Weyl* generators. It consists of a maximal set of commuting hermitian generators $H^1, \ldots, H^r$, and a finite set of raising of lowering operators $E^{\boldsymbol{\alpha}} = (E^{-\boldsymbol{\alpha}})^\dagger$, labeled by integral vectors $\boldsymbol{\alpha} = (\alpha^1, \ldots, \alpha^r) \in \Delta$ called roots. The root lattice is given by the set

$$\begin{aligned} \Delta_{so(2r)} &= \{\pm\mathbf{e}_I \pm \mathbf{e}_J : 1 \leq I < J \leq r\} \\ \Delta_{so(2r+1)} &= \Delta_{so(2r)} \cup \{\pm\mathbf{e}_I : 1 \leq I \leq r\} \end{aligned} \tag{A.8}$$

where $\mathbf{e}_I$ are unit basis vectors of $\mathbb{R}^r$. In particular, there are r simple roots $\boldsymbol{\alpha}_1, \ldots, \boldsymbol{\alpha}_r$ that forms a basis for the root lattice. For $so(N)$ they can be chosen to be

$$\boldsymbol{\alpha}_I = \begin{cases} \mathbf{e}_I - \mathbf{e}_{I+1}, & \text{for } I = 1, \ldots, r-1 \\ \mathbf{e}_r, & \text{for } I = r \text{ and } N \text{ odd} \\ \mathbf{e}_{r-1} + \mathbf{e}_r, & \text{for } I = r \text{ and } N \text{ even} \end{cases} . \tag{A.9}$$

The set of roots Δ consists of integral combinations of the simple roots $\boldsymbol{\alpha} = \sum_{J=1}^{r} b^J \boldsymbol{\alpha}_J$ so that its length is $|\boldsymbol{\alpha}| = \sqrt{2}$, for even N, or $|\boldsymbol{\alpha}| = 1$ or $\sqrt{2}$, for odd N.

The integer r is the rank of the $so(N)$ Lie algebra and is determined by $N = 2r$ for N even or $N = 2r+1$ for N odd. These generators satisfy

$$\left[H^i, E^{\boldsymbol{\alpha}}\right] = \alpha^i E^{\boldsymbol{\alpha}}, \quad \left[E^{\boldsymbol{\alpha}}, E^{-\boldsymbol{\alpha}}\right] = \frac{2}{|\boldsymbol{\alpha}|^2} \sum_{i=1}^{r} \alpha^i H^i \tag{A.10}$$

$$\left[E^{\boldsymbol{\alpha}}, E^{\boldsymbol{\beta}}\right] \propto \begin{cases} E^{\boldsymbol{\alpha}+\boldsymbol{\beta}}, & \text{if } \boldsymbol{\alpha}+\boldsymbol{\beta} \in \Delta \\ 0, & \text{if otherwise} \end{cases} , \quad \text{for } \boldsymbol{\alpha} \neq \boldsymbol{\beta}.$$

The Cartan matrix $K = (K_{IJ})_{r\times r}$ of the algebra is defined by the scalar product

$$K_{IJ} = \frac{2\boldsymbol{\alpha}_I^T \boldsymbol{\alpha}_J}{|\boldsymbol{\alpha}_J|^2} = \sum_{i=1}^{r} \frac{2\alpha_I^i \alpha_J^i}{|\boldsymbol{\alpha}_J|^2}. \tag{A.11}$$

$so(2r)$ is *simply-laced* in the sense that all roots have identical length and the Cartan matrix is therefore symmetric

$$K_{so(2r)} = \begin{pmatrix} 2 & -1 & 0 & \dots & 0 \\ -1 & 2 & \ddots & & \vdots \\ 0 & \ddots & 2 & -1 & -1 \\ \vdots & & -1 & 2 & 0 \\ 0 & \dots & -1 & 0 & 2 \end{pmatrix}. \tag{A.12}$$

Sometimes it would be convenient to use the *Chevalley* basis so that the commuting generators are redefined

$$h^I = \frac{2}{|\boldsymbol{\alpha}_I|^2} \sum_{i=1}^{r} \alpha_I^i H^i \tag{A.13}$$

so that the commutator relations (A.10) becomes

$$\left[h^I, E^{\pm\boldsymbol{\alpha}_J}\right] = \pm K_{IJ} E^{\pm\boldsymbol{\alpha}_J}, \quad \left[E^{\boldsymbol{\alpha}_J}, E^{-\boldsymbol{\alpha}_J}\right] = \delta^{IJ} h^J. \tag{A.14}$$

Appendix B

Bosonizing the $so(2r)_1$ current algebra

Here we review the bosonization[26, 27, 23] of a chiral wire with $N = 2r$ Majorana fermions, and express the $so(2r)_1$ current operators in bosonized form. The $2r$ Majorana (real) fermions can be paired into r Dirac (complex) fermions and bosonized into the normal ordered vertex operators

$$c^j(z) = \frac{\psi^{2j-1}(z) + i\psi^{2j}(z)}{\sqrt{2}} \sim \exp\left(i\widetilde{\phi}^j(z)\right). \tag{B.1}$$

Here we focus on a single wire, say at an even y, so that all fields depend on the holomorphic parameter $z = e^{\tau+ix}$. The r-component boson $\widetilde{\boldsymbol{\phi}} = (\widetilde{\phi}^1, \ldots, \widetilde{\phi}^r)$ is governed by the Lagrangian density

$$\mathcal{L}_0 = \frac{1}{2\pi}\sum_{j=1}^{r} \partial_x\widetilde{\phi}^j\partial_t\widetilde{\phi}^j = \frac{1}{2\pi}\partial_x\widetilde{\boldsymbol{\phi}}\partial_t\widetilde{\boldsymbol{\phi}} \tag{B.2}$$

and follows the algebraic relations

$$\left[\widetilde{\phi}^j(x,t), \widetilde{\phi}^{j'}(x',t)\right] = i\pi\left[\delta^{jj'}\mathrm{sgn}(x'-x) + \mathrm{sgn}(j-j')\right] \tag{B.3}$$

or equivalently the time-ordered correlation function

$$\langle\widetilde{\phi}^j(z)\widetilde{\phi}^{j'}(w)\rangle = -\delta^{jj'}\log(z-w) + \frac{i\pi}{2}\mathrm{sgn}(j-j') \tag{B.4}$$

for $\mathrm{sgn}(s) = s/|s|$ when $s \neq 0$ and $\mathrm{sgn}(0) = 0$. Operator product expansions between unordered vertex operators can be evaluated by $e^{A(z)}e^{B(w)} = e^{A(z)+B(w)+\langle A(z)B(w)\rangle}$, for A, B linear combination of the bosons $\widetilde{\phi}^j$. For instance, the vertex operators in (B.1) reproduce the product expansion of a pair of identical Dirac fermions

$$c^j(z)\left(c^j(w)\right)^\dagger = \frac{1}{z-w} + i\partial\widetilde{\phi}^j(w) + \dots \tag{B.5}$$

and the singular piece is dropped when the product is normal ordered in the limit $z \to w$. The non-singular sign factor $i\pi\mathrm{sgn}(j-j')$ ensures fermions with distinct flavors anticommutes

$$c^j(z)c^{j'}(w) = -c^{j'}(w)c^j(z). \tag{B.6}$$

The $so(2r)_1$ currents in the Cartan-Weyl basis can now be bosonized

$$\begin{aligned} H^j(z) &= c^j(z)c^j(z)^\dagger = i\partial_z\widetilde{\phi}^j(z) \\ E^{\boldsymbol{\alpha}}(z) &= \prod_{j=1}^{r} c^j(z)^{\alpha^j} = \exp\left(i\boldsymbol{\alpha}\cdot\widetilde{\boldsymbol{\phi}}(z)\right) \end{aligned} \tag{B.7}$$

where $\boldsymbol{\alpha} = (\alpha^1, \dots, \alpha^r) \in \Delta$ are roots of $so(2r)$ (see (A.8)) and the fermion products are normal ordered. For instance, $\boldsymbol{\alpha}$ has two and only two non-zero entries and $E^{\boldsymbol{\alpha}}$ must be of the form

$$E^{\boldsymbol{\alpha}}(z) = c^i(z)^{\pm}c^j(z)^{\pm} = e^{i(\pm\widetilde{\phi}^i(z)\pm\widetilde{\phi}^j(z))}. \tag{B.8}$$

Combining raising or lowering operators give

$$E^{\boldsymbol{\alpha}}(z)E^{\boldsymbol{\beta}}(w) = i^{-\boldsymbol{\alpha}\cdot\boldsymbol{\beta}}\epsilon(\boldsymbol{\alpha},\boldsymbol{\beta})\frac{e^{i(\boldsymbol{\alpha}\cdot\widetilde{\boldsymbol{\phi}}(z)+\boldsymbol{\beta}\cdot\widetilde{\boldsymbol{\phi}}(w))}}{(z-w)^{-\boldsymbol{\alpha}\cdot\boldsymbol{\beta}}} \tag{B.9}$$

where the vertex operator here is again normal ordered and the 2-cocyle is given by the star product

$$\epsilon(\boldsymbol{\alpha},\boldsymbol{\beta}) = (-1)^{\boldsymbol{\alpha}*\boldsymbol{\beta}} = (-1)^{\sum_{i>j}\alpha^i\beta^j}. \tag{B.10}$$

As $\sum_{i=1}^{r}\alpha^i$ is even for all roots, we have the following simplification when interchanging $\boldsymbol{\alpha}\leftrightarrow\boldsymbol{\beta}$

$$\epsilon(\boldsymbol{\alpha},\boldsymbol{\beta})\epsilon(\boldsymbol{\beta},\boldsymbol{\alpha}) = (-1)^{\boldsymbol{\alpha}\cdot\boldsymbol{\beta}}. \tag{B.11}$$

Using the boson OPE (B.4), the product of the two vertex operators above is singular only when (i) $\boldsymbol{\alpha} = -\boldsymbol{\beta}$, or (ii) $\boldsymbol{\alpha}\cdot\boldsymbol{\beta} = -1$ in other words $\boldsymbol{\alpha}+\boldsymbol{\beta}\in\Delta$. To summarize, the Cartan-Weyl generators satisfy the product expansion

$$\begin{aligned}
H^i(z)H^j(w) &= \frac{\delta^{ij}}{(z-w)^2} - \partial\widetilde{\phi}^i(w)\partial\widetilde{\phi}^j(w) + \dots\\
H^i(z)E^{\boldsymbol{\alpha}}(w) &= \frac{\alpha^i}{z-w}E^{\boldsymbol{\alpha}}(w) + \dots\\
E^{\boldsymbol{\alpha}}(z)E^{-\boldsymbol{\alpha}}(w) &= \frac{1}{(z-w)^2} + \sum_{i=1}^{r}\frac{\alpha^i}{z-w}H^i(w)\\
&\quad -\frac{1}{2}\left(\boldsymbol{\alpha}\cdot\partial\widetilde{\boldsymbol{\phi}}(w)\right)^2 + \dots\\
E^{\boldsymbol{\alpha}}(z)E^{\boldsymbol{\beta}}(w) &= \frac{i\epsilon(\boldsymbol{\alpha},\boldsymbol{\beta})}{z-w}E^{\boldsymbol{\alpha}+\boldsymbol{\beta}}(w) + \dots, \quad \text{if } \boldsymbol{\alpha}\cdot\boldsymbol{\beta} = -1.
\end{aligned} \tag{B.12}$$

For instance, the 2-cocyle coefficient $\epsilon(\boldsymbol{\alpha},\boldsymbol{\beta})$ ensures the OPE between $E^{\boldsymbol{\alpha}}(z)$ and $E^{\boldsymbol{\beta}}(w)$ commute as the sign in (B.11) when exchanging $\boldsymbol{\alpha}\leftrightarrow\boldsymbol{\beta}$ cancels that in $1/(z-w)$ when switching $z\leftrightarrow w$.

In certain derivations, especially when involving quasiparticle excitations, it may be more convenient to use the Chevalley basis. Here fields are expressed in terms of non-local bosons $\boldsymbol{\phi} = (\phi^1, \ldots, \phi^r)$, which are related to the original ones by the (non-unimodular) basis transformation

$$\widetilde{\phi}^i = \sum_{I=1}^{r} \alpha_I^i \phi^I \tag{B.13}$$

using the simple roots $\boldsymbol{\alpha}_I = (\alpha_I^1, \ldots, \alpha_I^r) \in \mathbb{Z}^r$ (see (A.9) in appendix A). The Lagrangian density (B.2) now becomes

$$\mathcal{L}_0 = \frac{1}{2\pi} \sum_{I,J=1}^{r} K_{IJ} \partial_x \phi^I \partial_t \phi^J \tag{B.14}$$

where $K = (K_{IJ})_{r\times r} = \boldsymbol{\alpha}_I \cdot \boldsymbol{\alpha}_J$ is the Cartan matrix of $so(2r)_1$ (see eq.(A.12)).

The current generators are rewritten in the Chevalley basis by

$$\begin{aligned} h_I(z) &= \sum_{i=1}^{r} \alpha_I^i H^i(z) = i \sum_{J=1}^{r} K_{IJ} \partial_z \phi^J(z) \\ E^{\mathbf{b}}(z) &= E^{\boldsymbol{\beta}}(z) = \exp\left(i \mathbf{b}^T K \boldsymbol{\phi}^J(z)\right) \end{aligned} \tag{B.15}$$

where $\boldsymbol{\beta} = \sum_J b^J \boldsymbol{\alpha}_J$ are roots expressed in integral combinations of the simple ones, for $\mathbf{b} = (b^1, \ldots, b^r) \in \mathbb{Z}^r$. The Chevalley generators satisfy the modified current relations from (B.12)

$$\begin{aligned} h_I(z) h_J(w) &= \frac{K_{IJ}}{(z-w)^2} + \ldots \\ h_I(z) E^{\mathbf{b}}(w) &= \frac{K_{IJ} b^J}{z-w} E^{\mathbf{b}}(w) + \ldots \\ E^{\mathbf{b}}(z) E^{-\mathbf{b}}(w) &= \frac{1}{(z-w)^2} + \sum_{I=1}^{r} \frac{b^I}{z-w} h_I(w) + \ldots \\ E^{\mathbf{b}_1}(z) E^{\mathbf{b}_2}(w) &= \frac{i\epsilon(\boldsymbol{\beta}_1, \boldsymbol{\beta}_2)}{z-w} E^{\mathbf{b}_1+\mathbf{b}_2}(w) + \ldots \end{aligned} \tag{B.16}$$

if $\mathbf{b}_1^T K \mathbf{b}_2 = -1$.

The (normal ordered) energy-momentum tensor can be turned from the Sugawara form (2.12) to the usual bosonic one

$$\begin{aligned} T(z) &= \frac{1}{2(N-1)} \left[\sum_{i=1}^{r} H^i(z) H^i(z) + \sum_{\boldsymbol{\alpha}\in\Delta} E^{\boldsymbol{\alpha}}(z) E^{-\boldsymbol{\alpha}}(z) \right] \\ &= -\frac{1}{2} \partial \widetilde{\boldsymbol{\phi}}(z) \cdot \partial \widetilde{\boldsymbol{\phi}}(z) = -\frac{1}{2} \partial \boldsymbol{\phi}(z) \cdot K \partial \boldsymbol{\phi}(z). \end{aligned} \tag{B.17}$$

Excitations in the CFT can be easily represented by vertex operators

$$V^{\mathbf{a}}(z) = \exp\left(i\mathbf{a} \cdot \boldsymbol{\phi}(z)\right) = \exp\left(i\mathbf{a}_\vee \cdot \widetilde{\boldsymbol{\phi}}(z)\right) \tag{B.18}$$

labeled by integral lattice vectors $\mathbf{a} = (a_1, \ldots, a_r)$, or equivalently dual root lattice vectors $\mathbf{a}_\vee = (a_\vee^1, \ldots, a_\vee^r)$ with rational entries

$$a_\vee^j = \sum_{IJ} a_I (K^{-1})^{IJ} \alpha_J^j. \tag{B.19}$$

The conformal dimension of $V^{\mathbf{a}}$ can be read off by the inner product

$$\begin{aligned} h_{\mathbf{a}} &= \frac{1}{2} \mathbf{a}^T K^{-1} \mathbf{a} = \frac{1}{2} (K^{-1})^{IJ} a_I a_J \\ &= \frac{1}{2} \mathbf{a}_\vee^T \mathbf{a}_\vee = \frac{1}{2} \delta_{ij} a_\vee^i a_\vee^j. \end{aligned} \tag{B.20}$$

This can be evaluated from definition (2.16) using the energy-momentum tensor (B.17) and the OPE

$$\partial_z \phi_I(z) \phi_J(w) = -(K^{-1})^{IJ} \log(z-w) + \ldots \tag{B.21}$$

which is equivalent to (B.4).

Most vertex operators (B.18) however are not WZW primary and do not represent the $so(2r)_1$ Kac-Moody algebra. The OPE with the current generators

$$\begin{aligned} h_I(z)V^{\mathbf{a}}(w) &= \frac{a_I}{z-w}V^{\mathbf{a}}(w) + \ldots \\ E^{\mathbf{b}}(z)V^{\mathbf{a}}(w) &= c^{\mathbf{b}}_{\mathbf{a}}(z-w)^{\mathbf{a}\cdot\mathbf{b}}V^{\mathbf{a}+K\mathbf{b}}(w) + \ldots \end{aligned} \tag{B.22}$$

would match the requirement (2.14) for a primary field only when the exponent of the singular term is bounded below, i.e. $\mathbf{a}\cdot\mathbf{b} \geq -1$ for all roots $\boldsymbol{\beta} = \sum_I b^I \boldsymbol{\alpha}_I$. Such lattice vectors $\mathbf{a}$ are called weights or *Dynkin labels* of $so(2r)$ at level 1. When the exponenet $\mathbf{a}\cdot\mathbf{b}$ in (B.22) is -1, the vertex operators $V^{\mathbf{a}}$ and $V^{\mathbf{a}+K\mathbf{b}}$ are related by the $SO(2r)_1$ symmetry and belong to the same primary field sector. For example the unit vector $\mathbf{a} = \mathbf{e}_1$ is the highest weight that generates the fermion sector ψ. Applying lowering operators $E^{-\mathbf{b}}$ to $V^{\mathbf{e}_1} = c^1$ gives all $2r$ Dirac fermions

$$\mathbf{V}_\psi = \mathrm{span}\left\{(c^j)^\pm = e^{\pm i\widetilde{\phi}^j} : j = 1, \ldots, r\right\} \tag{B.23}$$

which in turn irreducibly represent the $so(2r)_1$ algebra (see (2.14)) according to the fundamental vector representation.

The unit vectors $\mathbf{a} = \mathbf{e}_{r-1}$ and $\mathbf{e}_r$ generate the two spinor sectors s_- and s_+ respectively. Each of them consists of 2^{r-1} twist fields

$$\begin{aligned} \mathbf{V}_{s_\pm} &= \sigma^1 \ldots \sigma^{2r} \\ &= \mathrm{span}\left\{\exp\left(i\sum_{j=1}^{r}\frac{(-1)^{s_j}}{2}\widetilde{\phi}^j\right) : \prod_{j=1}^{r}(-1)^{s_j} = \pm 1\right\}. \end{aligned} \tag{B.24}$$

They irreducibly represent the $so(2r)_1$ algebra according to the even and odd spinor representations. These are the only primary fields of $so(2r)_1$ and their conformal dimensions are given by $h_\psi = 1/2$ and $h_{s_\pm} = r/8$.

The four primary fields $1, \psi, s_\pm$ obey a set of fusion rules, which are OPE keeping only primary fields.

$$s_\pm \times \psi = s_\mp \tag{B.25}$$

$$s_\pm \times s_\pm \begin{cases} 1, & \text{for } r \text{ even} \\ \psi, & \text{for } r \text{ odd} \end{cases}, \quad s_\pm \times s_\mp \begin{cases} \psi, & \text{for } r \text{ even} \\ 1, & \text{for } r \text{ odd} \end{cases}. \tag{B.26}$$

For instance, the OPE

$$\begin{aligned} V_{s_+}(z)c^r(w)^\dagger &= e^{i\frac{\widetilde{\phi}^1(z)+\ldots+\widetilde{\phi}^r(z)}{2}} e^{-i\widetilde{\phi}^r(w)} \\ &\propto (z-w)^{-\frac{1}{2}} e^{i\frac{\widetilde{\phi}^1(w)+\ldots+\widetilde{\phi}^r(w)-\widetilde{\phi}^r(w)}{2}} + \ldots \\ &= (z-w)^{-\frac{1}{2}} V_{s_-}(w) + \ldots \end{aligned} \tag{B.27}$$

shows $s_+ \times \psi = s_-$, and

$$e^{i\sum_j \widetilde{\phi}^j(z)/2} e^{-i\sum_j \widetilde{\phi}^j(w)/2} \propto (z-w)^{-\frac{r}{4}} + \ldots \tag{B.28}$$

shows $s_+ \times s_+ = 1$ for r even, or $s_+ \times s_- = 1$ for r odd.

Appendix C

Bosonizing the $so(2r+1)_1$ current algebra

A chiral wire with $N = 2r + 1$ Majorana fermions can be partially bosonized by grouping $\psi^1, \ldots, \psi^{2r}$ in pairs to form r Dirac fermions (see (B.1)). This leaves a single Majorana ψ^{2r+1} behind. In order for the fermions to obey the correct anticommutation relations, the bosonized complex fermions (B.1) have to be modified by a Klein factor

$$c^j(z) = (-1)^{\Pi} e^{i\widetilde{\phi}^j(z)} = e^{i\widetilde{\phi}^j(z)+i\pi\Pi} \tag{C.1}$$

where $(-1)^{\Pi}$ is the fermion parity operator that anticommutes with ψ^{2r+1}, and both Π and ψ_{2r+1} commute with the rest of the bosons $\widetilde{\phi}^j$. In a non-chiral system, $(-1)^{\Pi}$ can be chosen to be the combination $i\gamma_L\gamma_R$, for $\gamma_{L/R}$ the zero mode of $\psi^{2r+1}_{L/R}$. In the chiral case, it can be defined by $i\gamma\gamma_\infty$ using an additional Majorana zero mode γ_∞ that completes the Cliffort algebra $\{\gamma, \gamma_\infty\} = 0$.

The $so(2r+1)_1$ current algebra extends the $so(2r)_1$ algebra by the short roots with length 1 (see (A.8)). It contains the $so(2r)_1$ generators $H^j = i\partial\widetilde{\phi}^j$ and $E^{\boldsymbol{\alpha}} = e^{i\boldsymbol{\alpha}\cdot\widetilde{\boldsymbol{\phi}}}$ (see (B.7) in apendix B), for $\boldsymbol{\alpha} \in \Delta_{so(2r)}$ the long roots with length $|\boldsymbol{\alpha}| = \sqrt{2}$. The remaining raising and lowering operators with the short roots are represented by the normal ordered products

$$E^{\pm \mathbf{e}_j}(z) = e^{\pm i\widetilde{\phi}^j(z)}\psi^{2r+1}(z). \tag{C.2}$$

In addition to (B.12), the Cartan-Weyl generators satisfy the current relations

$$\begin{aligned}
H^i(z)E^{\pm\mathbf{e}_j}(w) &= \frac{\pm\delta^{ij}}{z-w}E^{\pm\mathbf{e}_j}(w) + \dots \\
E^{\mathbf{e}_j}(z)E^{-\mathbf{e}_j}(w) &= \frac{1}{(z-w)^2} + \frac{1}{z-w}H^j(w) \\
&\quad - \frac{1}{2}\partial\widetilde{\phi}^j(w)\partial\widetilde{\phi}^j(w) \\
&\quad - \psi^{2r+1}(w)\partial\psi^{2r+1}(w) + \dots \\
E^{s_1\mathbf{e}_{j_1}}(z)E^{s_2\mathbf{e}_{j_2}}(w) &= \frac{i^{-s_1 s_2}\epsilon(\mathbf{e}_{j_1},\mathbf{e}_{j_2})}{z-w}E^{s_1\mathbf{e}_{j_1}+s_2\mathbf{e}_{j_2}}(w) \\
&\quad + \dots
\end{aligned} \tag{C.3}$$

for $j_1 \neq j_2$ and $s_1, s_2 = \pm 1$. Moreover, when $\boldsymbol{\alpha}\cdot(\pm\mathbf{e}_j) = -1$, i.e. $\boldsymbol{\alpha}\pm\mathbf{e}_j \in \Delta_{so(2r+1)}$,

$$E^{\boldsymbol{\alpha}}(z)E^{\pm\mathbf{e}_j}(w) = \frac{i\epsilon(\boldsymbol{\alpha},\mathbf{e}_j)(-1)^{\sum_j \alpha^j/2}}{z-w}E^{\boldsymbol{\alpha}\pm\mathbf{e}_j}(w) + \dots$$

where $\epsilon(\mathbf{m},\mathbf{n}) = (-1)^{\mathbf{m}*\mathbf{n}}$ is defined in (B.10).

The (normal ordered) energy-momentum tensor can be turned from the Sugawara form (2.12) to the usual bosonic and fermionic one

$$\begin{aligned}
T(z) &= \frac{1}{2(N-1)}\left[\sum_{i=1}^{r} H^i(z)H^i(z) + \sum_{\boldsymbol{\alpha}\in\Delta} E^{\boldsymbol{\alpha}}(z)E^{-\boldsymbol{\alpha}}(z)\right. \\
&\qquad \left. + \sum_{j=1}^{r} E^{\mathbf{e}_j}(z)E^{-\mathbf{e}_j}(z) + E^{-\mathbf{e}_j}(z)E^{\mathbf{e}_j}(z)\right] \\
&= -\frac{1}{2}\partial\widetilde{\boldsymbol{\phi}}(z)\cdot\partial\widetilde{\boldsymbol{\phi}}(z) - \frac{1}{2}\psi^{2r+1}(z)\partial\psi^{2r+1}(z).
\end{aligned} \tag{C.4}$$

There are only two non-trivial primary fields ψ and σ. The fermion sector ψ consists of the $2r$ Dirac fermions $c^j, (c^j)^\dagger$ in (B.23) as well as the remaining Majorana fermion ψ^{2r+1}. The σ sector consists of 2^r twist fields

$$\begin{aligned}\mathbf{V}_\sigma &= \sigma^1 \ldots \sigma^{2r+1} \\ &= \mathrm{span}\left\{ \exp\left(i \sum_{j=1}^{r} \frac{(-1)^{s_j}}{2} \widetilde{\phi}^j \right) \sigma^{2r+1} : s_j = 0, 1 \right\}\end{aligned} \tag{C.5}$$

which represents $so(2r+1)_1$ according to the spinor representation. Their conformal dimensions are given by $h_\psi = 1/2$ and $h_\sigma = (2r+1)/16$.

Appendix D

$\mathbb{Z}_6$ parafermion model

Here we represent the $\mathbb{Z}_6$ parafermions using bosonized fields and Majorana fermions in the $so(9)_1$ CFT. We focus on a single Majorana wire containing 9 right moving real fermions. The CFT is fractionalized using the conformal embedding into $so(9)_1 \supseteq so(3)_3^+ \times so(3)_3^-$ (see section 3.1.2.1). Each $so(3)_3$ sector is then further decomposed into $so(2)_3 \times$ "$\mathbb{Z}_6$" using the coset construction "$\mathbb{Z}_6$" $= so(3)_3/so(2)_3$ (see section 3.1.2.2). We now provide a more detail description of the $\mathbb{Z}_6$ parafermion sector. We will focus on the one in $so(3)_3^-$.

First we pair six Majorana channels into three Dirac fermions and bosonize $c^1 = (\psi^1 + i\psi^4)/\sqrt{2} = e^{i\widetilde{\phi}^1}$, $c^2 = (\psi^2 + i\psi^5)/\sqrt{2} = e^{i\widetilde{\phi}^2}$ and $c^3 = (\psi^3 + i\psi^6)/\sqrt{2} = e^{i\widetilde{\phi}^3}$. The Lagrangian density of the boson fields are given in (3.68). Like the $so(N)_1$ case, extra care is required so that the Dirac fermions c^j satisfies the appropriate mutual anticommutation relations. Here we use a slightly different but more convenient convention

$$\left\langle \widetilde{\phi}^i(z)\widetilde{\phi}^j(w)\right\rangle = -\delta^{ij}\log(z-w) + \frac{i\pi}{2}S^{ij} \tag{D.1}$$

$$S^{ij} = \begin{cases} 0 & \text{if } i=j \\ 1 & \text{if } i-j\equiv 1 \bmod 3 \\ -1 & \text{if } i-j\equiv -1 \bmod 3 \end{cases}$$

so that the constant phases S^{ij} have a threefold cyclic symmetry. The $so(2)_3$ subtheory is generated by the "charged" boson $\phi_\rho = (\widetilde{\phi}^1+\widetilde{\phi}^2+\widetilde{\phi}^3)/3$. It satisfies

$$\langle \phi_\rho(z)\phi_\rho(w)\rangle = -\frac{1}{3}\log(z-w). \tag{D.2}$$

The remaining "neutral" bosons $\phi^j_\sigma = \widetilde{\phi}^j - \phi_\rho$ are linearly dependent $\phi^1_\sigma+\phi^2_\sigma+\phi^3_\sigma=0$ and obey the OPE

$$\left\langle \phi^i_\sigma(z)\phi^j_\sigma(w)\right\rangle = -\left(\delta^{ij}-\frac{1}{3}\right)\log(z-w) + \frac{i\pi}{2}S^{ij}. \tag{D.3}$$

The "charge" and "neutral" sector completely decoupled so that $\langle\phi_\rho(z)\phi^j_\sigma(w)\rangle = 0$. Lastly, there are three remaining Majoranan fermions $\psi^{7,8,9}$ in the $so(9)_1$ theory. They completely decouple with ϕ_σ and ϕ_ρ. Although the vertex $e^{i\phi_\rho}$ anticommutes with $\psi^{7,8,9}$, this has no effect on any of our derivations. More importantly the "neutral" vertices $e^{i\phi^j_\sigma}$ commute with the remaining fermions.

In section 3.1.2.2, we defined the $\mathbb{Z}_6$ parafermion (3.75)

$$\Psi = \frac{1}{\sqrt{3}}\left(e^{i\phi^1_\sigma}\psi^7 + e^{i\phi^2_\sigma}\psi^8 + e^{i\phi^3_\sigma}\psi^9\right) \tag{D.4}$$

which is part of the $so(3)^-_3$ current (see (3.74)). It generates the rest of the $\mathbb{Z}_6$

parafermions

$$\begin{aligned}
\Psi^2 &= \frac{1}{\sqrt{15}}\left[\sum_{j=1}^{3} e^{i2\phi_\sigma^j}\right.\\
&\qquad \left. + 2i\left(e^{-i\phi_\sigma^1}\psi^{89} + e^{-i\phi_\sigma^2}\psi^{97} + e^{-i\phi_\sigma^3}\psi^{78}\right)\right]\\
\Psi^3 &= \sqrt{\frac{2}{5}}\left[i\psi^{789} - \cos\left(\phi_\sigma^1 - \phi_\sigma^2\right)\psi^9\right.\\
&\qquad \left. - \cos\left(\phi_\sigma^2 - \phi_\sigma^3\right)\psi^7 - \cos\left(\phi_\sigma^3 - \phi_\sigma^1\right)\psi^8\right]\\
\Psi^4 &= \left(\Psi^2\right)^\dagger, \quad \Psi^5 = \left(\Psi_1\right)^\dagger, \quad \Psi^0 = \Psi^6 = 1
\end{aligned} \tag{D.5}$$

where $\psi^{ab} = \psi^a\psi^b$ and $\psi^{abc} = \psi^a\psi^b\psi^c$. Their conformal dimensions

$$h_{\Psi^m} = \frac{m(6-m)}{6} \tag{D.6}$$

as well as the fusion rules

$$\begin{aligned}
\Psi^m(z)\Psi^{m'}(w) &= \frac{c^{mm'}}{(z-w)^{mm'/3}}\Psi^{m+m'}(w) + \dots \\
\Psi^m(z)\Psi^{6-m}(w) &= \frac{1}{(z-w)^{2h_{\Psi^m}}}\\
&\quad \times\left[1 + \frac{2h_{\Psi^m}}{c_{\mathbb{Z}_6}}(z-w)^2 T_{\mathbb{Z}_6} + \dots\right]
\end{aligned} \tag{D.7}$$

match with the known result by Zamolodchikov and Fateev[45], for $T_{\mathbb{Z}_6}$ the energy-momentum tensor (3.73) with central charge $c_{\mathbb{Z}_6} = 5/4$ and

$$c^{mm'} = \sqrt{\frac{(m+m')!(6-m)!(6-m')!}{m!m'!(6-m-m')!6!}}. \tag{D.8}$$

Appendix E

The S-matrices of the G_N state

The surface topological orders of the time reversal symmetric gapped coupled wire model are described in section 3.2. There are thirty two distinct topological states defined in eq.(3.94) and (3.97), which we repeat here.

$$G_N = \begin{cases} SO(r)_1, & \text{for } N = 2r \\ SO(3)_3 \boxtimes_b SO(r)_1, & \text{for } N = 9 + 2r \end{cases} . \tag{E.1}$$

In this appendix we summarize the modular properties of these states. In particular we present there braiding S-matrices (3.88)

$$\mathcal{S}_{\mathbf{ab}} = \frac{1}{\mathcal{D}} \sum_{\mathbf{c}} d_{\mathbf{c}} N_{\mathbf{ab}}^{\mathbf{c}} \frac{\theta_{\mathbf{c}}}{\theta_{\mathbf{a}}\theta_{\mathbf{b}}} \tag{E.2}$$

which are identical to the modular S-matrix[26] of the $\mathcal{G}_N$ WZW CFT. The fusion matrices $N_{\mathbf{ab}}^{\mathbf{c}}$ that characterize fusion rules $\mathbf{a} \times \mathbf{b} = \sum_{\mathbf{c}} N_{\mathbf{ab}}^{\mathbf{c}} \mathbf{c}$ can in turned be determined by S-matrix throught the Verlinde formula[99] (3.58)

$$N_{s_1 s_2}^{s} = \sum_{s'} \frac{\mathcal{S}_{s_1 s'} \mathcal{S}_{s_2 s'} \mathcal{S}_{s s'}}{\mathcal{S}_{0 s'}}. \tag{E.3}$$

The G_N state is Abelian and carries four anyon types $1, \psi, s_+, s_-$ when N is a multiple of four. It is non-Abelian otherwise and carries three anyon types $1, \psi, \sigma$ when N is 2 mod 4, or seven anyon types $1, \alpha_+\gamma_+, \beta, \gamma_-, \alpha_-, f$ when N is odd. The quasiparticle exchange statistics $\theta_{\mathbf{x}}$ and quantum dimensions $d_{\mathbf{x}}$ are summarized in table 3.2 and 3.3. The total quantum dimensions $\mathcal{D} = \sqrt{\sum_{\mathbf{x}} d_{\mathbf{x}}^2}$ are given by

$$\mathcal{D}_{G_N} = \begin{cases} 2 & \text{for } N \text{ even} \\ 2\csc(\pi/8) & \text{for } N \text{ odd} \end{cases} \tag{E.4}$$

where $\csc(\pi/8) = \sqrt{4 + 2\sqrt{2}}$.

The S-matrices of G_N for $N = 2r$ even are well-known and are given by those of the $SO(r)_1$ states.[73, 111]

$$\mathcal{S}_{G_N} = \frac{1}{\mathcal{D}_{G_N}} \begin{pmatrix} 1 & 1 & 1 & 1 \\ 1 & 1 & -1 & -1 \\ 1 & -1 & i^n & -i^n \\ 1 & -1 & -i^n & i^n \end{pmatrix}, \quad \text{for } N = 4n, \tag{E.5}$$

$$\mathcal{S}_{G_N} = \frac{1}{\mathcal{D}_{G_N}} \begin{pmatrix} 1 & 1 & \sqrt{2} \\ 1 & 1 & -\sqrt{2} \\ \sqrt{2} & -\sqrt{2} & 0 \end{pmatrix}, \quad \text{for } N = 4n+2. \tag{E.6}$$

The S-matrices for the odd N cases are modification of the $G_9 = SO(3)_3$ prototype (3.59)

$$\mathcal{S}^{SO(3)_3}_{s_1 s_2} = \frac{1}{2} \sin\left[\frac{\pi(2s_1+1)(2s_2+1)}{8}\right] \tag{E.7}$$

where $s_j = 0, 1/2, 1, 3/2, 2, 5/2, 3$ label the seven anyon types $1, \alpha_+, \gamma_+, \beta, \gamma_-, \alpha_-, f$ (see table 3.1). For $N = 9 + 2r$ mod 32, the S-matrix of G_N is given by

$$\mathcal{S}_{G_N} = \mathcal{F}^r S^e(\lceil r/2 \rceil)\mathcal{F}^{-r} \tag{E.8}$$

where $\lceil r/2 \rceil \geq r/2$ is the smallest integral ceiling of $r/2$, $\mathcal{S}^e(n)$ is the S-matrix when

$r = 2n$ is even

$$\mathcal{S}^{e}(n)_{s_1 s_2} = i^{n(4 s_1 s_2)^2} \mathcal{S}^{SO(3)_3}_{s_1 s_2} \tag{E.9}$$

and $\mathcal{F}$ is the operator that flips the fermion parity of $\alpha_+ \leftrightarrow \alpha_-$ and $\gamma_+ \leftrightarrow \gamma_-$

$$\mathcal{F} = \begin{pmatrix} 1 & & & & & & \\ & & & & & 1 & \\ & & & & 1 & & \\ & & & 1 & & & \\ & & 1 & & & & \\ & 1 & & & & & \\ & & & & & & 1 \end{pmatrix}. \tag{E.10}$$

Appendix F

Abelian Chern-Simons theory of dyons

The fractional topological insulator slab with time-reversal conjugate surfaces has anyons which are dyons and partons. The neutral sector consists of only dyons. A dyon γ is composed of a number of $\mathbb{Z}_{2n+1}$ gauge charge on each surface associated with an unit gauge flux through the bulk. The dyons γ^m where $m = 0, 1, \ldots, 2n$, with $1 = \gamma^0$ being the vacuum, form the anyon content of an Abelian topological state denoted as $\mathbb{Z}^{(2a)}_{2n+1}$. They have spins $h_{\gamma^m} = \frac{2am^2}{2n+1}$ modulo 1 and satisfy the $\mathbb{Z}_{2n+1}$ fusion rule $\gamma^m \times \gamma^{m'} = \gamma^{[m+m']}$, where $[m + m']$ is the remainder between 0 and $2n$ when dividing $m + m'$ by $2n + 1$. For the case when $a = -1$, the Abelian topological theory becomes $\mathbb{Z}^{(-2)}_{2n+1}$, which is actually identical to $\mathbb{Z}^{(n)}_{2n+1}$. This is because the dyon $\mathbf{e} = \gamma^n$ has spin $\frac{-2n^2}{2n+1} \equiv \frac{n}{2n+1}$ modulo 1. The collection $\{\mathbf{e}^l : l = 0, 1, \ldots, 2n\}$ is of 1-1 correspondence with $\{\gamma^m : m = 0, 1, \ldots, 2n\}$. For instance $\gamma = \mathbf{e}^{-2} = \mathbf{e}^{2n-1}$. At the same time, $\mathbb{Z}^{(n)}_{2n+1} = \{\mathbf{e}^l : l = 0, 1, \ldots, 2n\}$ is the anyon content of the Abelian Chern-Simons $SU(2n + 1)_1$ theory with Lagrangian density $\mathcal{L}_{2+1} = \frac{1}{4\pi} \int_{2+1} K_{IJ}\alpha^I \wedge d\alpha^J$, where α^I for $I = 1, \ldots, 2n$ are $U(1)$ gauge fields, and

$$K_{SU(2n+1)} = \begin{pmatrix} 2 & -1 & & & & \\ -1 & 2 & -1 & & & \\ & -1 & 2 & & & \\ & & & \ddots & & \\ & & & & 2 & -1 \\ & & & & -1 & 2 \end{pmatrix} \tag{F.1}$$

is the Cartan matrix of $SU(2n+1)$.

Bibliography

[1] K. v. Klitzing, G. Dorda, and M. Pepper. New method for high-accuracy determination of the fine-structure constant based on quantized hall resistance. *Phys. Rev. Lett.*, 45:494–497, Aug 1980.

[2] D. Hsieh, D. Qian, L. Wray, Y. Xia, Y. S. Hor, R. J. Cava, and M. Z. Hasan. A topological dirac insulator in a quantum spin hall phase. *Nature*, 452:970 EP –, 04 2008.

[3] M. Z. Hasan and C. L. Kane. Colloquium: Topological insulators. *Rev. Mod. Phys.*, 82:3045–3067, Nov 2010.

[4] W. P. Su, J. R. Schrieffer, and A. J. Heeger. Solitons in polyacetylene. *Phys. Rev. Lett.*, 42:1698–1701, Jun 1979.

[5] A. Yu Kitaev. Unpaired majorana fermions in quantum wires. *Phys.-Usp.*, 44:131, 2001.

[6] Lukasz Fidkowski and Alexei Kitaev. Topological phases of fermions in one dimension. *Phys. Rev. B*, 83:075103, Feb 2011.

[7] Alexander Altland and Martin R. Zirnbauer. Nonstandard symmetry classes in mesoscopic normal-superconducting hybrid structures. *Phys. Rev. B*, 55:1142, 1997.

[8] M. Z. Hasan and C. L. Kane. Topological insulators. *Rev. Mod. Phys.*, 82:3045, 2010.

[9] Xiao-Liang Qi and Shou-Cheng Zhang. Topological insulators and superconductors. *Rev. Mod. Phys.*, 83:1057, 2011.

[10] Ching-Kai Chiu, Jeffrey C. Y. Teo, Andreas P. Schnyder, and Shinsei Ryu. Classification of topological quantum matter with symmetries. *Rev. Mod. Phys.*, 88:035005, Aug 2016.

[11] Andreas P. Schnyder, Shinsei Ryu, Akira Furusaki, and Andreas W. W. Ludwig. Classification of topological insulators and superconductors in three spatial dimensions. *Phys. Rev. B*, 78:195125, 2008.

[12] Alexei Kitaev. Periodic table for topological insulators and superconductors. *AIP Conf. Proc.*, 1134:22, 2008.

[13] Liang Fu, C. L. Kane, and E. J. Mele. Topological insulators in three dimensions. *Phys. Rev. Lett.*, 98:106803, 2007.

[14] Rahul Roy. Topological phases and the quantum spin hall effect in three dimensions. *Phys. Rev. B*, 79:195322, 2009.

[15] J. E. Moore and L. Balents. Topological invariants of time-reversal-invariant band structures. *Phys. Rev. B*, 75:121306(R), 2007.

[16] Xiao-Liang Qi, Taylor L. Hughes, and Shou-Cheng Zhang. Topological field theory of time-reversal invariant insulators. *Phys. Rev. B*, 78:195424, 2008.

[17] Joseph Maciejko, Xiao-Liang Qi, Andreas Karch, and Shou-Cheng Zhang. Fractional topological insulators in three dimensions. *Phys. Rev. Lett.*, 105:246809, 2010.

[18] Esko Keski-Vakkuri and Xiao-Gang Wen. The ground state structure and modular transformations of fractional quantum hall states on a torus. *Int. J. Mod. Phys. B*, 7:4227, 1993.

[19] Alexei Kitaev and John Preskill. Topological entanglement entropy. *Phys. Rev. Lett.*, 96:110404, 2006.

[20] Frank Wilczek. Magnetic flux, angular momentum, and statistics. *Phys. Rev. Lett.*, 48:1144, 1982.

[21] Frank Wilczek. Quantum mechanics of fractional-spin particles. *Phys. Rev. Lett.*, 49:957, 1982.

[22] F. J. Burnell. Anyon condensation and its applications. *ArXiv e-prints*, June 2017.

[23] Eduardo Fradkin. *Field Theories of Condensed Matter Physics*. Cambridge University Press, second edition, 2013.

[24] J. Wess and B. Zumino. Consequences of anomalous ward identities. *Physics Letters B*, 37(1):95 – 97, 1971.

[25] Edward Witten. Global aspects of current algebra. *Nuclear Physics B*, 223(2):422 – 432, 1983.

[26] P. Di Francesco, P. Mathieu, and D. Senechal. *Conformal Field Theory*. Springer, 1999.

[27] Edward Witten. Nonabelian bosonization in two dimensions. *Comm. Math. Phys.*, 92(4):455–472, 1984.

[28] Jan von Delft and H. Schoeller. Bosonization for beginners: Refermionization for experts. *Annalen Phys.*, 7:225–305, 1998.

[29] Lukasz Fidkowski, Xie Chen, and Ashvin Vishwanath. Non-abelian topological order on the surface of a 3d topological superconductor from an exactly solved model. *Phys. Rev. X*, 3:041016, Nov 2013.

[30] M. A. Metlitski, L. Fidkowski, X. Chen, and A. Vishwanath. Interaction effects on 3D topological superconductors: surface topological order from vortex condensation, the 16 fold way and fermionic Kramers doublets. *ArXiv e-prints*, June 2014.

[31] Chong Wang and T. Senthil. Interacting fermionic topological insulators/superconductors in three dimensions. *Phys. Rev. B*, 89:195124, May 2014.

[32] T. Senthil. Symmetry Protected Topological phases of Quantum Matter. *ArXiv e-prints*, May 2014.

[33] A. Kapustin, R. Thorngren, A. Turzillo, and Z. Wang. Fermionic Symmetry Protected Topological Phases and Cobordisms. *ArXiv e-prints*, June 2014.

[34] Xiao-Liang Qi, Edward Witten, and Shou-Cheng Zhang. Axion topological field theory of topological superconductors. *Phys. Rev. B*, 87:134519, Apr 2013.

[35] Edward Witten. Fermion path integrals and topological phases. *arXiv:1508.04715*, 2015.

[36] Chong Wang, Andrew C. Potter, and T. Senthil. Gapped symmetry preserving surface state for the electron topological insulator. *Phys. Rev. B*, 88:115137, Sep 2013.

[37] Max A. Metlitski, C. L. Kane, and Matthew P. A. Fisher. Symmetry-respecting topologically ordered surface phase of three-dimensional electron topological insulators. *Phys. Rev. B*, 92:125111, Sep 2015.

[38] X. Chen, L. Fidkowski, and A. Vishwanath. Symmetry enforced non-Abelian topological order at the surface of a topological insulator. *prb*, 89:165132, April 2014.

[39] P. Bonderson, C. Nayak, and X.-L. Qi. A time-reversal invariant topological phase at the surface of a 3D topological insulator. *J. Stat. Mech.*, 9:16, September 2013.

[40] David J. Gross and André Neveu. Dynamical symmetry breaking in asymptotically free field theories. *Phys. Rev. D*, 10:3235–3253, Nov 1974.

[41] Alexandre B. Zamolodchikov and Alexey B. Zamolodchikov. Exact s matrix of gross-neveu elementary fermions. *Physics Letters B*, 72(4):481 – 483, 1978.

[42] Edward Witten. Some properties of the $(\bar{\psi}\psi)^2$ model in two dimensions. *Nuclear Physics B*, 142(3):285 – 300, 1978.

[43] R. Shankar and E. Witten. The s-matrix of the kinks of the $(\bar{g}\bar{\gamma}\psi)^2$ model. *Nuclear Physics B*, 141(4):349 – 363, 1978.

[44] V.A. Fateev and A.B. Zamolodchikov. Self-dual solutions of the star-triangle relations in zn-models. *Physics Letters A*, 92(1):37 – 39, 1982.

[45] A. B. Zamolodchikov and V. A. Fateev. Nonlocal (parafermion) currents in two-dimensional conformal quantum field theory and self-dual critical points in zn-symmetric statistical systems. *Sov. Phys. JETP*, 62:215, 1985.

[46] C. S. O'Hern, T. C. Lubensky, and J. Toner. Sliding phases in XY models, crystals, and cationic lipid-dna complexes. *Phys. Rev. Lett.*, 83:2745–2748, Oct 1999.

[47] V. J. Emery, E. Fradkin, S. A. Kivelson, and T. C. Lubensky. Quantum theory of the smectic metal state in stripe phases. *Phys. Rev. Lett.*, 85:2160–2163, Sep 2000.

[48] Ashvin Vishwanath and David Carpentier. Two-dimensional anisotropic non-fermi-liquid phase of coupled luttinger liquids. *Phys. Rev. Lett.*, 86:676–679, Jan 2001.

[49] S. L. Sondhi and Kun Yang. Sliding phases via magnetic fields. *Phys. Rev. B*, 63:054430, Jan 2001.

[50] Ranjan Mukhopadhyay, C. L. Kane, and T. C. Lubensky. Crossed sliding luttinger liquid phase. *Phys. Rev. B*, 63:081103, Feb 2001.

[51] C. L. Kane, Ranjan Mukhopadhyay, and T. C. Lubensky. Fractional quantum hall effect in an array of quantum wires. *Phys. Rev. Lett.*, 88:036401, Jan 2002.

[52] Jeffrey C. Y. Teo and C. L. Kane. From luttinger liquid to non-abelian quantum hall states. *Phys. Rev. B*, 89:085101, Feb 2014.

[53] Jelena Klinovaja and Daniel Loss. Integer and fractional quantum hall effect in a strip of stripes. *The European Physical Journal B*, 87:171, 2014.

[54] Tobias Meng, Peter Stano, Jelena Klinovaja, and Daniel Loss. Helical nuclear spin order in a strip of stripes in the quantum hall regime. *The European Physical Journal B*, 87:203, 2014.

[55] Eran Sagi, Yuval Oreg, Ady Stern, and Bertrand I. Halperin. Imprint of topological degeneracy in quasi-one-dimensional fractional quantum hall states. *Phys. Rev. B*, 91:245144, Jun 2015.

[56] Yuval Oreg, Eran Sela, and Ady Stern. Fractional helical liquids in quantum wires. *Phys. Rev. B*, 89:115402, Mar 2014.

[57] E. M. Stoudenmire, David J. Clarke, Roger S. K. Mong, and Jason Alicea. Assembling fibonacci anyons from a $\mathbb{Z}_3$ parafermion lattice model. *Phys. Rev. B*, 91:235112, Jun 2015.

[58] Tobias Meng, Titus Neupert, Martin Greiter, and Ronny Thomale. Coupled-wire construction of chiral spin liquids. *Phys. Rev. B*, 91:241106, Jun 2015.

[59] Gregory Gorohovsky, Rodrigo G. Pereira, and Eran Sela. Chiral spin liquids in arrays of spin chains. *Phys. Rev. B*, 91:245139, Jun 2015.

[60] Titus Neupert, Claudio Chamon, Christopher Mudry, and Ronny Thomale. Wire deconstructionism of two-dimensional topological phases. *Phys. Rev. B*, 90:205101, Nov 2014.

[61] Jelena Klinovaja and Yaroslav Tserkovnyak. Quantum spin hall effect in strip of stripes model. *Phys. Rev. B*, 90:115426, Sep 2014.

[62] Eran Sagi and Yuval Oreg. Non-abelian topological insulators from an array of quantum wires. *Phys. Rev. B*, 90:201102, Nov 2014.

[63] Eran Sagi and Yuval Oreg. Fractional topological insulators in three-dimensions from an array of quantum wires. *arXiv:1506.02033*, 2015.

[64] Tobias Meng and Eran Sela. Time reversal symmetry broken fractional topological phases at zero magnetic field. *Phys. Rev. B*, 90:235425, Dec 2014.

[65] Tobias Meng. Fractional topological phases in three-dimensional coupled-wire systems. *Phys. Rev. B*, 92:115152, Sep 2015.

[66] Raul A. Santos, Chia-Wei Huang, Yuval Gefen, and D. B. Gutman. Fractional topological insulators: From sliding luttinger liquids to chern-simons theory. *Phys. Rev. B*, 91:205141, May 2015.

[67] Roger S.K. Mong, David J. Clarke, Jason Alicea, Netanel H. Lindner, Paul Fendley, Chetan Nayak, Yuval Oreg, Ady Stern, Erez Berg, Kirill Shtengel, and Matthew P.A. Fisher. Universal topological quantum computation from a superconductor-abelian quantum hall heterostructure. *Phys. Rev. X*, 4:011036, Mar 2014.

[68] Inbar Seroussi, Erez Berg, and Yuval Oreg. Topological superconducting phases of weakly coupled quantum wires. *Phys. Rev. B*, 89:104523, Mar 2014.

[69] David F. Mross, Andrew Essin, and Jason Alicea. Composite dirac liquids: Parent states for symmetric surface topological order. *Phys. Rev. X*, 5:011011, Feb 2015.

[70] H.B. Nielsen and Masao Ninomiya. The adler-bell-jackiw anomaly and weyl fermions in a crystal. *Phys. Lett. B*, 130(6):389 – 396, 1983.

[71] G. E. Volovik. Quantum hall and chiral edge states in thin 3he-a film. *JETP Letters*, 55:368, 1992.

[72] N. Read and Dmitry Green. Paired states of fermions in two dimensions with breaking of parity and time-reversal symmetries and the fractional quantum hall effect. *Phys. Rev. B*, 61:10267, 2000.

[73] A. Kitaev. Anyons in an exactly solved model and beyond. *Ann. Phys.*, 321:2, 2006.

[74] Jeffrey C. Y. Teo and C. L. Kane. Topological defects and gapless modes in insulators and superconductors. *Phys. Rev. B*, 82:115120, 2010.

[75] P. Goddard, W. Nahm, and D. Olive. Symmetric spaces, sugawara's energy momentum tensor in two dimensions and free fermions. *Phys. Lett. B*, 160(13):111 – 116, 1985.

[76] C. L. Kane and Matthew P. A. Fisher. Quantized thermal transport in the fractional quantum hall effect. *Phys. Rev. B*, 55:15832–15837, Jun 1997.

[77] Andrea Cappelli, Marina Huerta, and Guillermo R. Zemba. Thermal transport in chiral conformal theories and hierarchical quantum hall states. *Nuclear Physics B*, 636(3):568 – 582, 2002.

[78] J. M. Luttinger. Theory of thermal transport coefficients. *Phys. Rev.*, 135:A1505–A1514, Sep 1964.

[79] Ian Affleck and Andreas W. W. Ludwig. Universal noninteger "ground-state degeneracy" in critical quantum systems. *Phys. Rev. Lett.*, 67:161–164, Jul 1991.

[80] Christoph Holzhey, Finn Larsen, and Frank Wilczek. Geometric and renormalized entropy in conformal field theory. *Nuclear Physics B*, 424(3):443 – 467, 1994.

[81] Pasquale Calabrese and John Cardy. Entanglement entropy and quantum field theory. *Journal of Statistical Mechanics: Theory and Experiment*, 2004(06):P06002, 2004.

[82] G. E. Volovik. *Universe in a helium droplet*. Oxford University Press, Oxford UK, 05 2003.

[83] F.A. Bais, F. Englert, A. Taormina, and P. Zizzi. Torus compactification for non-simply laced groups. *Nuclear Physics B*, 279(34):529 – 547, 1987.

[84] A. N. Schellekens and N. P. Warner. Conformal subalgebras of kac-moody algebras. *Phys. Rev. D*, 34:3092–3096, Nov 1986.

[85] F. Alexander Bais and Peter G. Bouwknegt. A classification of subgroup truncations of the bosonic string. *Nuclear Physics B*, 279(34):561 – 570, 1987.

[86] F. D. M. Haldane. Continuum dynamics of the 1-d heisenberg antiferromagnet: Identification with the o(3) nonlinear sigma model. *Physics Letters A*, 93(9):464 – 468, 1983.

[87] F. D. M. Haldane. Nonlinear field theory of large-spin heisenberg antiferromagnets: Semiclassically quantized solitons of the one-dimensional easy-axis néel state. *Phys. Rev. Lett.*, 50:1153–1156, Apr 1983.

[88] Ian Affleck, Tom Kennedy, Elliott H. Lieb, and Hal Tasaki. Rigorous results on valence-bond ground states in antiferromagnets. *Phys. Rev. Lett.*, 59:799–802, Aug 1987.

[89] Ian Affleck, Tom Kennedy, Elliott H. Lieb, and Hal Tasaki. Valence bond ground states in isotropic quantum antiferromagnets. *Comm. Math. Phys.*, 115(3):477–528, 1988.

[90] Hong-Hao Tu, Guang-Ming Zhang, and Tao Xiang. Class of exactly solvable $so(n)$ symmetric spin chains with matrix product ground states. *Phys. Rev. B*, 78:094404, Sep 2008.

[91] Hong-Hao Tu and Román Orús. Effective field theory for the SO(n) bilinear-biquadratic spin chain. *Phys. Rev. Lett.*, 107:077204, Aug 2011.

[92] F. Alet, S. Capponi, H. Nonne, P. Lecheminant, and I. P. McCulloch. Quantum criticality in the so(5) bilinear-biquadratic heisenberg chain. *Phys. Rev. B*, 83:060407, Feb 2011.

[93] S.G. Naculich, H.A. Riggs, and H.J. Schnitzer. Group-level duality in {WZW} models and chern-simons theory. *Physics Letters B*, 246(34):417 – 422, 1990.

[94] Eli J. Mlawer, Stephen G. Naculich, Harold A. Riggs, and Howard J. Schnitzer. Group-level duality of {WZW} fusion coefficients and chern-simons link observables. *Nuclear Physics B*, 352(3):863 – 896, 1991.

[95] John Cardy. *Scaling and Renormalization in Statistical Physics*. Cambridge University Press, 1996.

[96] F. D. M. Haldane. Stability of chiral luttinger liquids and abelian quantum hall states. *Phys. Rev. Lett.*, 74:2090, 1995.

[97] Paul Fendley and Hubert Saleur. Bps kinks in the gross-neveu model. *Phys. Rev. D*, 65:025001, Nov 2001.

[98] R. Jackiw and C. Rebbi. Solitons with fermion number $\frac{1}{2}$. *Phys. Rev. D*, 13:3398–3409, Jun 1976.

[99] Erik Verlinde. Fusion rules and modular transformations in 2d conformal field theory. *Nucl. Phys. B*, 300:360, 1988.

[100] Mayukh Nilay Khan, Jeffrey C. Y. Teo, and Taylor L. Hughes. to appear soon.

[101] Frank Wilczek. *Fractional Statistics and Anyon Superconductivity*. World Scientific, 1990.

[102] Xiao-Gang Wen. *Quantum Field Theory of Many Body Systems*. Oxford Univ. Press, Oxford, 2004.

[103] Xiao-Gang Wen. Vacuum degeneracy of chiral spin states in compactified space. *Phys. Rev. B*, 40:7387, 1989.

[104] Xiao-Gang Wen. Topological order in rigid states. *Int. J. Mod. Phys. B*, 04(02):239–271, 1990.

[105] Xiao-Gang Wen and Qian Niu. Ground-state degeneracy of the fractional quantum hall states in the presence of a random potential and on high-genus riemann surfaces. *Phys. Rev. B*, 41:9377, 1990.

[106] Xiao-Gang Wen. Topological orders and edge excitations in fractional quantum hall states. *Advances in Physics*, 44(5):405, 1995.

[107] N. Read and G. Moore. Nonabelions in the fractional quantum hall effect. *Nucl. Phys. B*, 360:362, 1991.

[108] N. Read and G. Moore. Fractional quantum hall effect and nonabelian statistics. *Progress of Theoretical Physics Supplement*, 107:157–166, 1992.

[109] Ian Affleck, Tom Kennedy, Elliott H. Lieb, and Hal Tasaki. Rigorous results on valence-bond ground states in antiferromagnets. *Phys. Rev. Lett.*, 59:799, 1987.

[110] F. A. Bais and J. K. Slingerland. Condensate-induced transitions between topologically ordered phases. *Phys. Rev. B*, 79:045316, Jan 2009.

[111] Mayukh Nilay Khan, Jeffrey C. Y. Teo, and Taylor L. Hughes. Anyonic symmetries and topological defects in abelian topological phases: An application to the *ade* classification. *Phys. Rev. B*, 90:235149, Dec 2014.

[112] Jeffrey C.Y. Teo, Taylor L. Hughes, and Eduardo Fradkin. Theory of twist liquids: Gauging an anyonic symmetry. *Annals of Physics*, 360(0):349 – 445, 2015.

[113] Chong Wang, Andrew C. Potter, and T. Senthil. Classification of interacting electronic topological insulators in three dimensions. *Science*, 343(6171):629–631, 2014.

[114] B. Swingle, M. Barkeshli, J. McGreevy, and T. Senthil. Correlated topological insulators and the fractional magnetoelectric effect. *Phys. Rev. B*, 83:195139, 2011.

[115] Joseph Maciejko, Xiao-Liang Qi, Andreas Karch, and Shou-Cheng Zhang. Models of three-dimensional fractional topological insulators. *Phys. Rev. B*, 86:235128, Dec 2012.

[116] Peng Ye, Taylor L. Hughes, Joseph Maciejko, and Eduardo Fradkin. Composite particle theory of three-dimensional gapped fermionic phases: Fractional topological insulators and charge-loop excitation symmetry. *Phys. Rev. B*, 94:115104, Sep 2016.

[117] Joseph Maciejko and Gregory A. Fiete. Fractionalized topological insulators. *Nature Physics*, 11:385 EP –, 04 2015.

[118] Ady Stern. Fractional topological insulators: A pedagogical review. *Annual Review of Condensed Matter Physics*, 7(1):349–368, 2016.

[119] Peng Ye, Meng Cheng, and Eduardo Fradkin. Fractional s-duality, classification of fractional topological insulators, and surface topological order. *Phys. Rev. B*, 96:085125, Aug 2017.

[120] E. Witten. Dyons of charge e/2. *Physics Letters B*, 86:283, 1979.

[121] Liang Fu and C. L. Kane. Probing neutral majorana fermion edge modes with charge transport. *Phys. Rev. Lett.*, 102:216403, 2009.

[122] Xiao-Liang Qi, Edward Witten, and Shou-Cheng Zhang. Axion topological field theory of topological superconductors. *Phys. Rev. B*, 87:134519, Apr 2013.

[123] F. D. M. Haldane. Model for a quantum hall effect without landau levels: Condensed-matter realization of the "parity anomaly". *Phys. Rev. Lett.*, 61:2015–2018, Oct 1988.

[124] Chao-Xing Liu, Shou-Cheng Zhang, and Xiao-Liang Qi. The quantum anomalous hall effect: Theory and experiment. *Annual Review of Condensed Matter Physics*, 7:301–321, 2016.

[125] N. Regnault and B. Andrei Bernevig. Fractional chern insulator. *Phys. Rev. X*, 1:021014, 2011.

[126] Titus Neupert, Luiz Santos, Claudio Chamon, and Christopher Mudry. Fractional quantum hall states at zero magnetic field. *Phys. Rev. Lett.*, 106:236804, 2011.

[127] Evelyn Tang, Jia-Wei Mei, and Xiao-Gang Wen. High-temperature fractional quantum hall states. *Phys. Rev. Lett.*, 106:236802, 2011.

[128] D. N. Sheng, Zheng-Cheng Gu, Kai Sun, and L. Sheng. Fractional quantum hall effect in the absence of landau levels. *Nat. Comm.*, 2:389, 2011.

[129] Marvin E Cage, Kv Klitzing, AM Chang, F Duncan, M Haldane, RB Laughlin, AMM Pruisken, DJ Thouless, Richard E Prange, and Steven M Girvin. *The quantum Hall effect*. Springer Science & Business Media, 2012.

[130] R. B. Laughlin. Quantized hall conductivity in two dimensions. *Phys. Rev. B*, 23:5632–5633, May 1981.

[131] B. I. Halperin. Quantized hall conductance, current-carrying edge states, and the existence of extended states in a two-dimensional disordered potential. *Phys. Rev. B*, 25:2185–2190, Feb 1982.

[132] Yasuhiro Hatsugai. Chern number and edge states in the integer quantum hall effect. *Phys. Rev. Lett.*, 71:3697–3700, Nov 1993.

[133] Hermann Schulz-Baldes, Johannes Kellendonk, and Thomas Richter. Simultaneous quantization of edge and bulk hall conductivity. *Journal of Physics A: Mathematical and General*, 33(2):L27, 2000.

[134] Gregory Moore and Nathan Seiberg. Classical and quantum conformal field theory. *Comm. Math. Phys.*, 123:177, 1989.

[135] Parsa H. Bonderson. *Non-Abelian Anyons and Interferometry.* PhD thesis, California Institute of Technology, 2007.

[136] Michael Levin. Protected edge modes without symmetry. *Phys. Rev. X*, 3:021009, 2013.

[137] Liang Fu and C. L. Kane. Superconducting proximity effect and majorana fermions at the surface of a topological insulator. *Phys. Rev. Lett.*, 100:096407, 2008.

[138] Chenjie Wang and Michael Levin. Anomaly indicators for time-reversal symmetric topological orders. *Phys. Rev. Lett.*, 119:136801, Sep 2017.

[139] Yuji Tachikawa and Kazuya Yonekura. Derivation of the time-reversal anomaly for $(2+1)$-dimensional topological phases. *Phys. Rev. Lett.*, 119:111603, Sep 2017.

[140] Gil Young Cho, Jeffrey C. Y. Teo, and Eduardo Fradkin. Symmetric-gapped surface states of fractional topological insulators. *Phys. Rev. B*, 96:161109, Oct 2017.

[141] Liang Kong. Anyon condensation and tensor categories. *Nucl. Phys. B*, 886:436, 2014.

[142] Titus Neupert, Huan He, Curt von Keyserlingk, Germán Sierra, and B. Andrei Bernevig. Boson condensation in topologically ordered quantum liquids. *Phys. Rev. B*, 93:115103, Mar 2016.

[143] Dam Thanh Son. Is the composite fermion a dirac particle? *Phys. Rev. X*, 5:031027, Sep 2015.

[144] Maissam Barkeshli, Michael Mulligan, and Matthew P. A. Fisher. Particle-hole symmetry and the composite fermi liquid. *Phys. Rev. B*, 92:165125, Oct 2015.

[145] Chong Wang and T. Senthil. Composite fermi liquids in the lowest landau level. *Phys. Rev. B*, 94:245107, Dec 2016.

[146] H. Blaine Lawson and Marie-Louise Michelsohn. *Spin Geometry*. Princeton University Press, 1990.